

HUNGARIAN UNIVERSITY OF AGRICULTURE AND LIFE SCIENCES DOCTORAL (PhD) DISSERTATION

CHEMICAL CLASSIFICATION OF TANZANIAN SODA-SALINE WATERS (EASTERN RIFT VALLEY)

DOI: 10.54598/005930

A Dissertation Submitted for the degree of Doctor of Philosophy at the Doctoral School of Environmental Sciences, Hungarian University of Agriculture and Life Sciences

 \mathbf{BY}

AZARIA STEPHANO LAMECK

GÖDÖLLŐ, HUNGARY

Title: Chemical Classification of Tanzanian Soda-Saline Waters (Eastern Rift Valley).		
Discipline: E	nvironmental Sciences	
Name of Doct	toral School: Environmental Scien	nces
Head:	Csákiné Dr. Michéli Erika	
	Professor, DSc.	
Doctoral Scho	ool of Environmental Sciences	
Supervisors:	Dr. Emil Boros	
	Senior research fellow, PhD	
	Institute of Aquatic Ecology, HU	N-REN, Centre for Ecological Research,
	Karolina str. 29. Budapest, 1113,	Hungary
	Ákos Pető, PhD	
	associate professor, head of depar	rtment
	Department of Nature Conservati	on and Landscape Management
	Institute of Wildlife Management	and Nature Conservation
	Hungarian University of Agricult	ure and Life Sciences
Approval		
•••••		•••••
Approval of the	ne School Leader	Approval of the Supervisor(s)

DECLARATION

university. Replication of any portion of this dissertation is prohibited without the author's and the
Hungarian University of Agriculture and Life Sciences' consent.
Data
Date:
DECLARATION BY SUPERVISORS
This dissertation has been submitted with our approval as supervisors.
Date:
Dr. Emil Boros
Senior research fellow, PhD
Institute of Aquatic Ecology, HUN-REN, Centre for Ecological Research, Karolina str. 29.
Budapest, 1113, Hungary
Ákos Pető, PhD
Associate professor, head of department
Department of Nature Conservation and Landscape Management
Institute of Wildlife Management and Nature Conservation

This dissertation is my original work and has not been submitted for a degree at any other

Hungarian University of Agriculture and Life Sciences

DEDICATION

This work is dedicated to my wife, **Eva James Mwachese**, and my children (**Eliazary, Adriely**, and **Ariana**), for their everlasting love, understanding, and patience throughout my absence, which has provided enormous emotional support and constant encouragement through the highs and lows of my academic journey.

TABLE OF CONTENTS

DI	ECLA	RAT	TIONii		
DI	EDIC	ATIO	ATIONiii		
Ta	ble of	f Cor	ntentsiv		
Lis	st of I	Figur	esix		
Lis	st of a	ıbbre	viations and acronymsxi		
1.	Intr	oduc	etion1		
	1.1	Bac	kground	1	
	1.2	Pro	blem Statement and Justification	2	
	1.3	Res	search Objectives and Questions	3	
	1.4	Sig	nificance of Study	4	
	1.5	Lin	nitations of Study	5	
2.	LIT	TER A	ATURE REVIEW6		
	2.1	Occ	currence of IASW	<i>6</i>	
	2.2	Fur	ndamentals Processes Controlling IASW Chemistry	8	
	2.2	.1	Dissolution	8	
	2.2	.2	Evaporative Concentrations	9	
	2.2	.3	Chemical Weathering	. 10	
	2.2	.4	Mineral Precipitation	. 11	
	2.2	.5	Ion Exchange	. 12	
	2.2	.6	Inflow and outflow of water and solutes	. 12	
	2.2	.7	Atmospheric Inputs	. 13	
	2.2	.8	Magmatic and Hydrothermal Inputs	. 13	
	2.2	.9	Reduction of sulfate	. 14	
	2.2	10	Geochemical Evolution	15	

2.3 Gl	obal Geographical Distribution of IASW	17
2.4 W	ater Chemical Type Classification	20
3. MATE	RIALS AND METHODS	22
3.1 St	udy Area	22
3.1.1	Description of the study area	22
3.2 Da	ata acquisition and analysis	24
3.2.1	Chemical Properties of IASW in EARV	24
3.2.2	Water chemical types classification and carbonate estimation	25
3.2.3	GIS and Statistical Methods	26
3.3 W	ater sampling and sample analysis	27
3.3.1	Geochemical speciation, statistical analysis	28
3.4 Te	emperature and precipitatation	28
3.4.1	Drought monitoring and analysis	29
3.5 Gl	S-based soil type classification	29
3.6 Gl	S-based Geological Features	30
3.7 La	and use land cover (LULC) changes	30
3.7.1	Remote sensing dataset and processing	30
3.7.2	Image processing and classification	31
4. RESUI	LTS	33
4.1 Re	eview of chemical properties of the IASW of EARV	33
4.1.1	Spearman Correlations	36
4.1.2	Water chemical type classification	37
4.1.3	Moran's I spatial autocorrelation analysis of Na ⁺ , Cl ⁻ , CO ₃ ²⁻ , and TD	S in EARV 40
4.1.4	The model for Spatial autocorrelation of (Cl ⁻ , SO ₄ ²⁻ , HCO ₃ ⁻ + CO ₃ ²⁻) to geological
types (USGS) and soil types (DSMW)	41

4.1.5	The spatial patterns of the Na ⁺ , Cl ⁻ , $HCO_3^- + CO_3^{2-}$, and TDS in EARV	45
4.2 TI	he chemical composition, classification, and geographical distributions of se	oda-
saline la	kes in ETRV.	47
4.2.1	Physiochemical Properties	47
4.2.2	Major Ions Compositions	48
4.2.3	Spearman Correlations	51
4.2.4	Saturation Indices (SI)	52
4.2.5	Hydrochemical Characteristics	53
4.2.6	Water chemical type of the investigated lakes	54
4.2.7	Geographical distributions of the IASW in ETRV	55
4.3 In	fluence of environmental variables and anthropogenic activities on soda-sa	line
lake che	mistry in Northern Tanzania: A Remote Sensing and GIS-based approach	57
4.3.1	Validation of CHIRPS and MERRA-2 data	57
4.3.2	Climate Variability	58
4.3.3	Drought Analysis	59
4.3.4	Soil Types Classification	61
4.3.5	Geological and Hydrogeological Features	64
4.3.6	Land Use and Land Cover (LULC) Changes	67
5. Discus	sion	71
5.1 R	eview of chemical properties of the IASW of EARV	71
5.1.1	Spatial distributions of the IASW in EARV	72
5.2 TI	ne chemical composition, classification, and geographical distributions of soda-	-saline
lakes in l	ETRV	75
5.2.1	Physiochemical properties of the ETRV	75
5.2.2	The major ions chemistry of the ETRV	75
5.2.3	Chemical Classification of IASW of the ETRV	78

5	.3 Inf	luence of environmental variables and anthropogenic activities on soda-sal	line lake
c	hemistry	in Northern Tanzania: A Remote Sensing and GIS-based approach	79
	5.3.1	Climate Variability and Drought Analysis	79
	5.3.2	Influence of Soil Type	80
	5.3.3	Influence of Geological Features	80
	5.3.4	Land use and Land Cover changes	81
6.	Conclus	sions and Recommendations	83
6	.1 Co	nclusions	83
6	.2 Red	commendations	84
7.	KEY SO	CIENTIFIC FINDINGS AND IMPORTANT OUTPUT	85
8.	Summa	ry	85
9.	ACKNO	DWLEDGEMENTS	87
10.	Relate	ed publications	88
11.	Appe	ndices	89
12.	Refer	ence	92

LIST OF TABLES

Table 1: The assessed major ion concentrations in the EASL (Concentrations are in mg/l exception)	ρt
for alkalinity $(HCO_3^- + CO_3^{2^-})$ which is in meq/l) and estimated salinity (TDS) in g/l	. 34
Table 2: The statistical summary of the investigated major ion concentrations	. 35
Table 3: The Spearman Correlations of the IASW (significant correlations are red coloured)	. 37
Table 4: Percentage equivalent, dominant ions, water chemical type, and ion balance of assess	ed
data in the EASL	. 38
Table 5: Regional number of the classified lakes by country	. 39
Table 6: The statistical results of spatial autocorrelation with the inverse Euclidean distance	
method by using chemical variables	. 41
Table 7:The Linear Mixed Effects Model for $HCO_3^- + CO_3^{2-}$. 42
Table 8: The Linear Mixed Effects Model for $\mathrm{SO_4}^{2^-}$. 43
Table 9: The Linear Mixed Effects Model Cl ⁻	. 44
Table 10: The Spearman correlations of the physiochemical variables of the investigated lakes	i
(** represent significant correlation at $p < 0.01$, * represent significant correlation at $p < 0.05$)	52
Table 11: The calculated equivalent percentages of the investigated lakes	. 55
Table 12: The dominance trend of the ionic concentrations and water chemical types of the	
ETRV lakes.	. 55
Table 13: The key characteristics of the soil groups in the study area (Northern Tanzania)	. 63
Table 14: The geological features and key chemical constituents in the study area (Northern	
Tanzania)	. 66
Table 15: Accuracy Assessment	. 67
Table 16: LULC areas and percentages for 2000, 2014 and 2023	. 68
Table 17: Individual Lakes statistics for 2000, 2014 and 2023 in the study area	. 68
Table 18: LULC changes between the study years	. 70
Table 19: Changes in individual Lake area coverage between the study years	. 70

LIST OF FIGURES

Figure 1: Schematic diagrams illustrating the types of water bodies of Lake basins. (a) Open la	ake
$basin(P>E).\ (b)\ Closed\ lake\ basin(P$	
(Lewis, 2016)	7
Figure 2: The impact of Hydraulic discharge of groundwater (gravity-driven flow) in an	
unconfined drainage basin on water anion faces (modified from (Tóth, 1980))	7
Figure 3: The Global distribution of the regions characterized by hydrologically closed lakes	
adopted from Deocampo & Jones, (2014).	8
Figure 4: Microbial-redox process of the sulfate in the soda lakes (Sorokin et al., 2014)	. 15
Figure 5: The probable evaporation paths of natural water modified from (Drever, 1982; Hardi	ie
& Eugster, 1970). Lake water under investigation likely evolves along I–IB	. 17
Figure 6: Worldwide distribution of IASW. The areas with active Volcanoes are symbolized b	y
triangles, soda lakes by circles, arid and semiarid regions (light grey and dark grey areas	
respectively), and endorheic zones by light grey shaded areas (Pecoraino et al., 2015)	. 19
Figure 7: The important hotspots of IASW in Eurasia (Boros & Kolpakova, 2018)	. 19
Figure 8: The regions with major seismic occurrences and active volcanoes in EARS are in the	e
interior of the African Plate (Scoon, 2020).	. 20
Figure 9: Locations and spatial distributions of the investigated inland saline waters in East	
Africa by countries	. 23
Figure 10: Locations of the investigated lakes along eastern Tanzania Rift Valley	. 24
Figure 11: The general ternary scatter plot of the chemical ion composition of the investigated	l
EASL (each point represents a lake)	. 36
Figure 12: The water chemical type of the IASW of the EARV	. 40
Figure 13: Sodium (Na ⁺) spatial distribution in the EASL based on assessed data	. 45
Figure 14: The spatial distributions of Cl ⁻ in the EARV based on assessed data	. 46
Figure 15: The spatial distributions of the estimated carbonates (HCO ₃ ⁻ +CO ₃ ²⁻) in the EASL	
based on assessed data	. 46
Figure 16: The spatial distributions of the estimated salinity (TDS) in the EASL are based on	
assessed data.	. 47
Figure 17: Concentrations and distributions of Physiochemical properties	. 48
Figure 18: The composition of cations and distributions in the investigated lakes	50

Figure 19: The composition of anions and distributions in the investigated lakes 51
Figure 20: The plots of the mineral saturation indices (anhydrite, calcite, gypsum, aragonite,
dolomite and halite) against (a) TDS, (b) pH, (c) salinity, and (d) alkalinity53
Figure 21: The Piper diagram showing the evolutional hydrochemical types of the investigated
lake
Figure 22: The geographical distributions of the Soda-saline lakes in ETRV 56
Figure 23:The geological features surrounding the IASW in the ETRV 57
Figure 24: (a) Station temperature versus MERRA-2 temperature data (b) observed precipitation
versus CHIRPS data
Figure 25: The average monthly precipitation (mm) and temperatures (°C) for Lake Manyara (a
and b), Lake Eyasi (c and d), and Lake Natron (e and f), respectively
Figure 26: The evolution of the SPEI for 3, 6, and 12-month timescale in Lake Manyara, Lake
Natron, and Lake Eyasi basin showing the variation in the duration, severity, and intensity of dry
and wet events
Figure 27: The reference soil groups of the study area extracted from the DSMW (Note, Entisol
(USDA Taxonomy)/Regosol (FAO), Inceptisols (USDA Taxonomy)/Cambisol (FAO)) 63
Figure 28:The geological map of the study area generated from the World Geological Map
USGS database
Figure 29: Map showing the spatial distribution of the various LULC classes over the study
period
Figure 30: Maps showing the spatio-temporal dynamics of the three lakes in the study area 69

LIST OF ABBREVIATIONS AND ACRONYMS

ASTM Advanced Speciation Methods

CHIRPS Climate Hazards Group Infrared Precipitation with Station

CRS Coordinate Reference System

DSMW Digital Soil Map of the World

EARS East African Rift System

EARV East African Rift Valley

EASL East African Soda Lake

EC Electrical Conductivity

ETRV Eastern Tanzania Rift Valley

FAO Food and Agriculture Organization

GEE Google Earth Engine

ICP-MS Inductive Coupled- Mass Spectrometry

LULC Land Use Land Cover

IASW Inland alkaline soda waters

NASA POWER National Aeronautics and Space Administration of Worldwide Energy Resources

NDBI Normalized Difference Built-up Index

NDMI Normalized Difference Moisture Index

NDVI Normalized Difference Vegetation Index

NTU Nephelometric Unit

OLI Operational Land Imagery

OMPs Organic Micropollutants

QGIS Quantum Geographical Information System

RF Random Forest

SPEI Standardized Precipitation Evapotranspiration Index

SPI Standardized Precipitation Index

SRB Sulfate-Reducing Bacteria

TDS Total Dissolved Solids

TM Thematic Mapper

USDA United States Department of Agriculture

USGS United States Geological Survey

1. Introduction

1.1 Background

Inland alkaline soda waters (IASW) are characterized by a permanent pH exciding 9 (pH>9), enriched with dissolved Na⁺, HCO₃⁻ + CO₃²⁻, and sometimes higher dissolved Cl⁻, and SO₄²⁻ and having a low or almost insignificant amount of alkaline earth metals ions (Ca²⁺ and Mg²⁺) (Boros & Kolpakova, 2018; Deocampo & Renaut, 2016; Eugster & Jones, 1979; Jones & Deocampo, 2003). IASW (including all types of surface waters e.g. lakes, pans, playas, wetlands etc.) are commonly found in arid and semi-arid regions globally, including the East African Rift Valley (EARV), the Great Basin in the United States, Central Europe, China, and Russia (Boros & Kolpakova, 2018; Deocampo & Renaut, 2016; Kempe & Kazmierczak, 2002; Sorokin et al., 2014). They develop in hydrologically closed basins (without the outlet) and evaporation surpasses the drainage water inputs from the surrounding escarpments (Deocampo & Renaut, 2016; Eugster & Jones, 1979; Eugster, 1980; Pecoraino et al., 2015).

In contrast to other saline lakes, IASW are distinguished by their higher alkalinity with very dilute inflow originating from the surrounding volcanic terrain (Deocampo & Renaut, 2016; Pecoraino et al., 2015). Evaporations of water with high Na⁺, Cl⁻, and HCO₃⁻/CO₃²⁻ concentrations, create an alkaline brine that alters the CO₂ / HCO₃⁻ // CO₃²⁻ equilibrium towards CO₃²⁻, creating a soda (Na₂CO₃) lake with pH values of 10–11, sometimes exceeding 12 (Grant & Yu, 2011). The sodarich lava flow from active volcanic activity contributes to the lake basin's higher carbonate and bicarbonate mineral content (Deocampo, & Jones, 2014; Grant & Yu, 2011; Kempe & Kazmierczak, 2007). The surrounding geology of the lake basin is characterized by high Na⁺ and low Mg²⁺/Ca²⁺ silicates (Grant & Yu, 2011). The leaching of volcanic minerals from surrounding rocks and soils creates higher alkalinity in the lake basin. Geological, hydrological, and climatic conditions (Deocampo & Renaut, 2016; Eugster, 1980; Pecoraino et al., 2015) are the primary environmental variables that contribute to the unique chemical compositions of soda lakes.

IASW in East Africa are situated in the EARV and are associated with active tectonic and volcanic activity (Deocampo & Renaut, 2016; Grant & Jones, 2016; Grant, 2006; Pecoraino et al., 2015; Scoon, 2020). The EARV is divided into the eastern and western rift. The eastern rift runs from Ethiopia passes across Kenya and Tanzania and extends to Mozambique. The western rift begins in Uganda, passing through Rwanda and Burundi, and extends to Tanzania where it

intersects with the eastern rift at the triple junction in the Mbeya district of Tanzania (Scoon, 2020). The eastern arm of the rift valley hosts more soda lakes than the western rift. Among the countries that are located in the eastern rift, Tanzania has the highest number of soda lakes (20), followed by Ethiopia (9), Kenya (8), and Uganda (4) (Lameck et al., 2023).

IASW are biodiversity hotspots and highly productive, despite the harsh environmental conditions. Soda lakes are the habitats of diverse microbial communities, such as phytoplankton, algae, archaea, bacteria, and cyanobacteria, which thrive in environments with elevated alkalinity and salinity (Ali et al., 2022; Grant & Jones, 2016; Grant, 2004; Jeilu et al., 2022; Jones et al.,1998). The unique chemistry and ecology of IASW interest scientists studying extremophiles (organisms adapted to extreme environments), biogeochemistry, and astrobiology. Furthermore, these ecosystems host scientific research into biodiversity conservation, biotechnology, and industry applications. Microbes can be utilized for synthesizing enzymes, pharmacological bioactive chemicals (antibiotics, pigments), Arthrospira cultivation, methanogenesis (CO₂ sequestration), and bioremediate environmental pollutants (Antony et al., 2013; Nyakeri et al., 2018; Sorokin et al., 2014; Yaiche & Saadi, 2023).

The IASW are a renowned tourist destination known for its abundant natural resources, particularly for hosting migrating water birds. For example, Momella's lakes and Lake Natron host approximately 75% of the world's Lesser Flamingo population (*Phoeniconaias minor*), making them the most prolific aquatic ecosystems on the planet (Lihepanyama et al., 2022; Mgimwa et al., 2021). IASW watersheds also offer other ecological services, including water for household use, livestock and wildlife, salt extraction, climate regulation, the purification of water, nitrogen cycling, and recreational opportunities.

1.2 Problem Statement and Justification

Regardless of the several ecological functions offered by Tanzania's IASW, human activities, regional and global climate change, and inadequate monitoring and waste management measures are jeopardizing their chemical composition (Tebbs et al., 2013; Yona et al., 2022). A recent investigation by Zhao et al., (2022) pointed out the presence of harmful organic micropollutants (OMPs) in Tanzanian IASW. These OMPs are believed to have emerged from human activities and may thus endanger these ecosystems. Although Lake Natron has been extensively studied

(Fritz et al., 1987; Mgimwa et al., 2021; Robinson, 2015; Tebbs et al., 2013; Yona et al., 2022; Zaitsev & Keller, 2006), a comprehensive up-to-date study on the chemical compositions of other IASW in the region is still lacking despite their much scientific attention. The only chemical data for lakes Balangida, Balangida Lalu, Mikuyu, Singida, Kindai, and Sulunga are from the 1970s (Hecky & Kilham, 1973). To gain a better understanding of these IASW, a more current and comprehensive investigation is required. Furthermore, the classification of the region's IASW into the respective water chemical types and their geographical distributions has not been done. In this study, we adopted Boros & Kolpakova, (2018) classification criteria to classify the IASW in eastern Tanzania into their distinctive water chemical type. This classification criterion is straightforward and precise for categorizing inland soda saline water based on terms like "soda," "soda-saline," and "saline". The study aimed to (i) review the chemical properties of IASW in the EARV, (ii) investigate the chemical compositions of IASW in the Eastern Tanzania Rift Valley (ETRV), (iii) classify the lakes into distinct water chemical types, (iv) evaluate the geographical distribution of the identified water chemical types (v) To examine the influence of environmental variables and anthropogenic activities on the chemistry of IASW using remote sensing and a GISbased approach. The findings will offer an overview of the chemical composition of IASW across East Africa, the present status of the chemical composition, the distinctive chemical type of their water, and detail the geographical distributions of IASW in the eastern Tanzania rift valley. They will also set a baseline for lakes that haven't been extensively studied. The most up-to-date information on the chemical composition of these lakes is essential for scientists and government agencies to monitor and manage these important ecosystems.

1.3 Research Objectives and Questions

Objective 1: To review the chemical properties of IASW in the EARV

- 1.1. What is the status of the chemical properties of IASW in the EARV?
- 1.2. How are the IASW water classes of each country distributed in the EARV?
- 1.3. How do Na⁺, Cl⁻, CO₃²⁻, and TDS spatially distributed in the EARV?

Objective 2: To classify the IASW in the ETRV into their distinctive water chemical types

2.1. How many lakes are classified as "soda", "soda-saline" or "saline" in the ETRV?

- **Objective 3:** To assess the spatial distribution of the determined chemical types in ETRV
 - 3.1. How are the IASW water chemical types spatially distributed in the ETRV?
- **Objective 4:** To examine the key environmental elements influencing the chemistry of soda-saline lake waters using Remote sensing and a GIS-based approach
 - 4.1. How do the key environmental drivers (Climate, soil types, geological features and anthropogenic activity), influence the water chemistry of IASW in the ETRV?

1.4 Significance of Study

- 1. Classification of Water Chemical Types: The study categorizes the lakes into distinct chemical water types, offering a precise framework for future investigations. This classification approach is being applied for the first time in the region, although it has been previously used in Eurasian regions. By adopting this classification, the study helps clarify the chemical diversity and provides a distinction between the various chemical profiles.
- 2. Comprehensive Chemical Analysis: This research provides an extensive and updated evaluation of the chemical properties of IASW in the ETRV. Given the limited studies in this region, this comprehensive analysis offers valuable new insights into the chemistry of these lakes, which have not been thoroughly explored in recent studies.
- 3. Spatial distribution of different water chemical types: The research explores and maps the spatial distribution of different water chemical types across the ETRV. This mapping is significant because it enhances our understanding of the regional variability of soda-saline lakes, a facet that has been previously underexplored in terms of its geographical patterns.
- 4. Integrating Climate, Soil, Geology, and Land Use/Land Cover (LULC) Patterns as Environmental Drivers and Anthropogenic Influences on IASW Chemistry: This approach is innovative for the region because it considers the interconnectedness of multiple environmental and anthropogenic factors (climate, soil, geology, and LULC) to understand their collective influence on the chemical composition of IASW lakes.
- 5. Establishing a Baseline for Future Research: This study establishes a contemporary reference point for the chemical compositions of the IASW lakes, providing up-to-date data on lakes that have not been widely studied. As many of these lakes remain underexplored, this baseline is crucial for future monitoring efforts and comparative studies.

6. Contributing to Scientific Knowledge: This research contributes significantly to the scientific literature on soda lakes and their distinctive ecosystems. The study deepens our understanding of the chemical diversity (water chemical classes) and their spatial distribution across the EARV. It also highlights the interconnectedness of climate, soil, geology, and LULC and their collective influence on the lake's water chemistry.

1.5 Limitations of Study

- 2. Budget constraints: The insufficient financial assistance for this study necessitated the student to utilize his financial resources to facilitate the fieldwork. This led to the collection of a limited number of samples, which may not accurately reflect the representative of the sample and hence impact the validity of the findings.
- 3. Chemical Data Reliance: In reviewing the chemical properties of the EARV soda lakes we used chemical data from previously published papers, thus we cannot guarantee its correctness although we controlled the ion data with the ion balance formula. This reliance on outdated data may not accurately reflect the current chemical compositions.
- 4. Geographical constraints: Our field investigation was hindered by the restricted access to lakes within the national parks. As a consequence, the current comprehensive chemical analysis of other IASW in the region is lacking.
- 5. Missing hydrogeological analysis and thorough interpretation due to a lack of groundwater chemistry data has led to an insufficient understanding of the impact of groundwater intrusion on IASW and how it influences lake water chemistry.
- 6. Technological Limitations: The use of remote sensing and GIS-based methods partially can be an alternative to field data. However, these methods may have inherent limitations in accurately recording and analysing complex climate, soil data, and geological features, as the accuracy of these methods needs to be validated by comparing them with field data thereby compromising their correctness.
- 7. Biodiversity Considerations: The study focuses primarily on the chemical properties of soda lakes, their classification and geographical distributions. However, this study did not thoroughly examine the impacts of chemical alterations on various microbial populations and other organisms, which are crucial for comprehending ecosystem health and functionality.

2. LITERATURE REVIEW

2.1 Occurrence of IASW

Soda lakes, also known as inland alkaline endorheic waters (IASW), are distinctive water bodies in hydrologically closed basins, without any external outlet to drain their discharges into rivers or oceans. In contrast to open lakes, IASW are closed lakes (Figure 1) with no external outlet (Lewis, 2016). The IASW basins are not connected to the discharge rivers; most have semistatic or astatic water balance. The occurrence of the IASW is influenced by a variety of variables such as climatic (precipitation and evaporation), geological (nature of the underlying rocks), and geochemical processes (gas-water-rock interaction) (Deocampo & Renaut, 2016; Pecoraino et al., 2015). Due to their endorheic nature; IASW are prevalent in regions where evaporation significantly exceeds precipitation, and the main means for water loss are through evaporation, seepage, or underground drainage (Rosen, 1994; Schagerl & Robin, 2016). Geographically, IASW predominantly occurs in dry or semi-arid regions, particularly within tectonically or volcanically active areas, such as caldera basins that facilitate the formation of carbonate-rich soda lakes (Deocampo & Jones, 2014). IASW observed globally are linked to modern or old volcanic activity (Pecoraino et al., 2015). The existence of regional tectonic or volcano-tectonic structures can lead to the inflow of thermal water containing endogenous carbon dioxide, which is crucial for the development of alkaline lakes (Pecoraino et al., 2015). For forming an IASW brines, the following basic characteristics must be satisfied, showing a delicate balance within these ecosystems. (1) an underfilled tectonic basin in which down warping surpasses the rate of sedimentation, (2) a closed hydrological basin in which evaporation exceeds outflow, (3) evolution of solutes in the lake waters that lead to high Na/(Ca + Mg) and (HCO₃ + CO₃)/(SO₄ + Cl) ratios, that is alkaline brine, (4)There needs to be a steady-state body of rich nutrients waters, (5) a warm climate favouring high primary productivity by microbes and algae, and (6) a high rate of bacterial sulphate reduction (Deocampo & Renaut, 2016; Warren, 2006). Furthermore, groundwater recharge and gravity-flow systems (Local discharge, Intermediate discharge, and Regional discharge) owing to the Hydraulic Head (Driving Force), as depicted in Figure 2 (Tóth, 1999), also impact the ion facies of the IASW. Tóth, (1999), reported that gravity-flow systems facilitated systematic change in the water anion facies from HCO₃⁻, SO₄²⁻, and Cl⁻ (Figure 2). These changes in water anion facies influence the creation of distinctive water chemical types (soda, soda-saline, and saline lakes). The IASW hydrological

closed basins are distributed across various parts of the world (Figure 3), including the Pacific Northwest, the EARV, Central Asia, and the central and southern Andes in South America (Deocampo & Renaut, 2016).

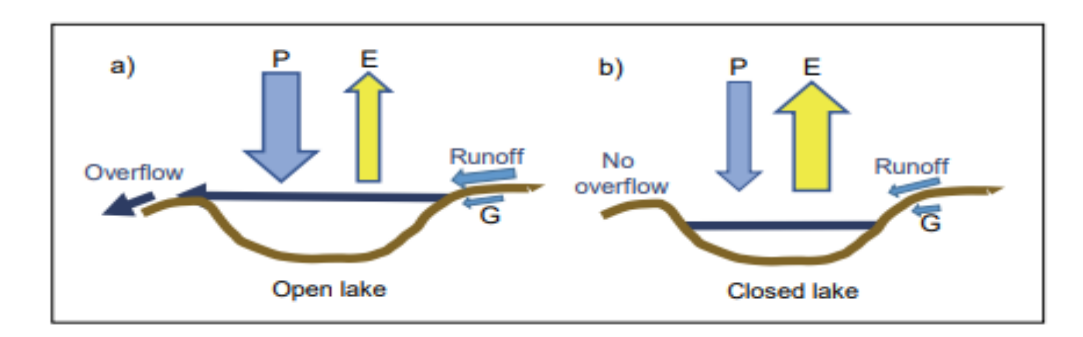


Figure 1: Schematic diagrams illustrating the types of water bodies of Lake basins. (a) Open lake basin(P>E). (b) Closed lake basin(P<E), P = precipitation, E = evaporation, G = groundwater. (Lewis, 2016)

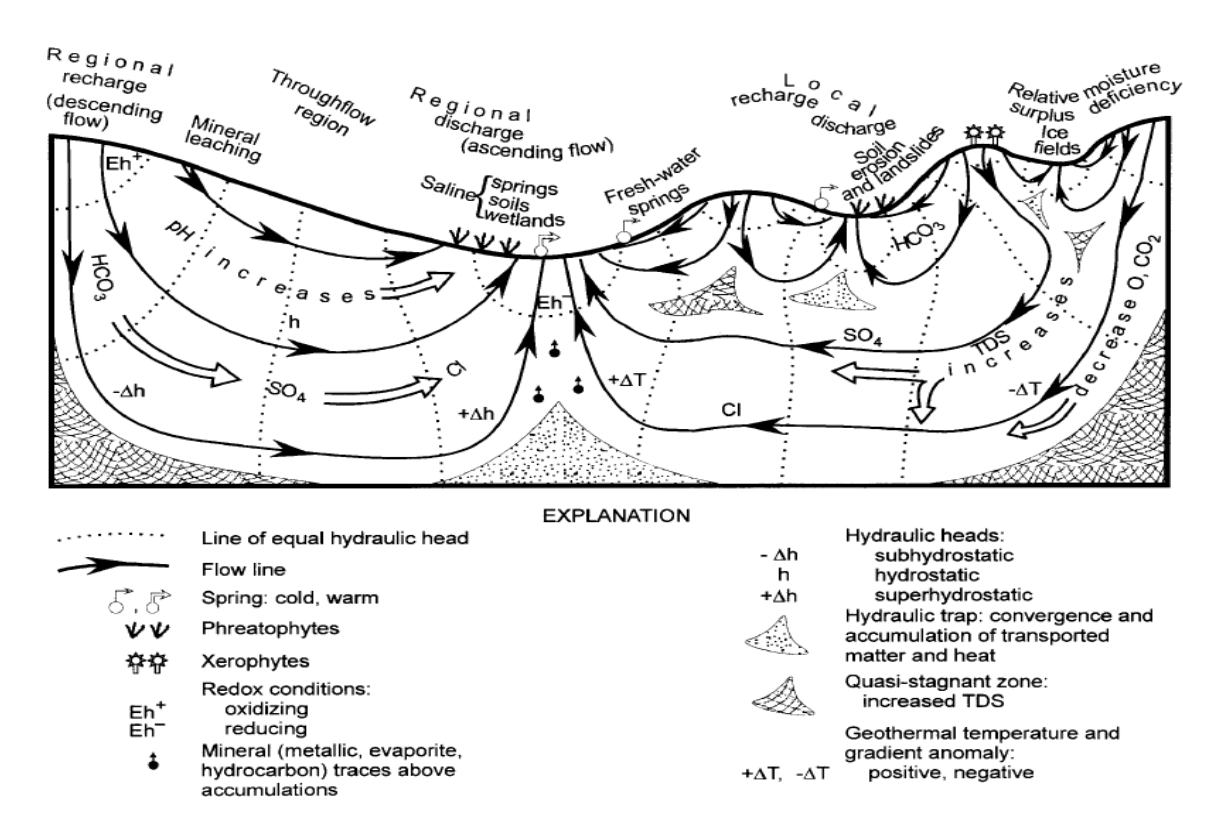


Figure 2: The impact of Hydraulic discharge of groundwater (gravity-driven flow) in an unconfined drainage basin on water anion faces (modified from (Tóth, 1980)).

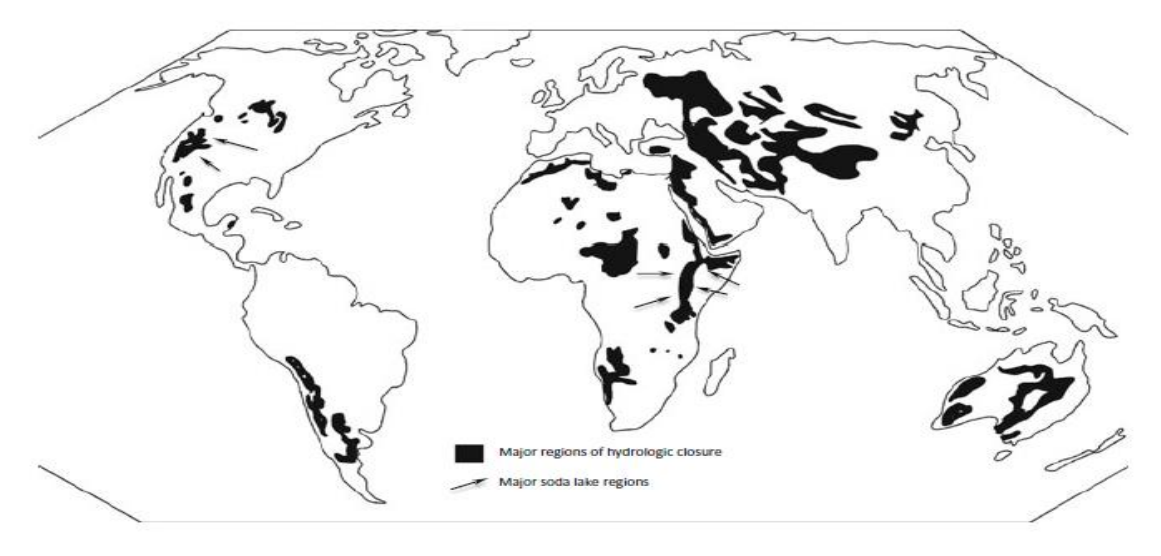


Figure 3: The Global distribution of the regions characterized by hydrologically closed lakes adopted from Deocampo & Jones, (2014).

2.2 Fundamentals Processes Controlling IASW Chemistry

The geochemistry of IASW is primarily influenced by the chemical composition of rocks and soils (weathering reactions) in the drainage basins, geology (water interaction with surrounding minerals), groundwater interaction, geothermal spring, surface water (transport and mineral accumulation), dissolved CO₂, and mineral precipitation-dissolution (Deocampo & Renaut, 2016; Tóth, 1999; Pecoraino et al., 2015). These factors dictate whether the final composition of the evaporating lake waters becomes enriched with carbonate-rich ("soda") or remains neutral or acidic. In modern soda lakes, the trona-forming brine is usually an alkaline solution, often with a pH over 9 (Eugster & Hardie, 1978).

2.2.1 Dissolution

Dissolution is an essential process and is considered the first step in the geochemical evolution of the lake's water. The interaction and dissolution of gases like N₂, Ar, O₂, H₂, He, CO₂, NH₃, CH₄, and H₂S contribute to the formation of either acidic or alkaline water (Jozsef Toth, 1999; Symonds et al., 2001). The dissolution of the soluble weathered minerals, including halite (NaCl) sylvite

(KCl), limestone (CaCO₃), dolomite (CaMgCO₃), and gypsum (CaSO₄), is the primary source of Ca²⁺, Mg²⁺, Na⁺, K⁺, HCO₃⁻, CO₃²⁻, SO₄²⁻, and Cl⁻ in lake water (Deocampo & Renaut, 2016; Tóth, 1999). The dissolution of basaltic rocks (relatively rich in calcium), alkaline rocks (sodiumrich silicate minerals), and K-feldspar minerals enrich the cations in lake water (Makoba & Muzuka, 2019). For instance, limestone dissolution can generate dilute fluids with Ca²⁺ > HCO₃⁻. The dissolution of plagioclase feldspar minerals (sodium-rich) absorbs hydrogen ions from a solution and releases alkali cations, as described by (Eq 1) and eventually raises pH and increases alkalinity in the lake basin (Deocampo & Renaut, 2016). The composition of minerals in the rocks surrounding basins significantly impacts the chemical properties of water. However, the dissolution of silicates and other insoluble rocks to some extent releases minor or trace constituents of major ions into lake water.

$$2NaAlSi_{3}O_{8(s)} + 2H^{+}_{(aq)} + 9H_{2}O_{(l)} \rightarrow Al_{2}Si_{2}O_{5}(OH)_{4(s)} + 2Na^{+}_{(aq)} + 4H_{2}SiO_{4(aq)}$$
 (Eq 1) (Na-feldspar) (kaolinite)

2.2.2 Evaporative Concentrations

Evaporative Concentration is another key mechanism that influences hydrochemistry and geochemical evolution. The initial concentration of dilute water during evaporation determines the final composition of the brines (Deocampo & Renaut, 2016; Garrels & Mackenzie, 1967; Pecoraino et al., 2015; Yechieli & Wood, 2002). The evaporation rate in regions with soda lakes exceeds water input (Pecoraino et al., 2015) from precipitation, river basin discharge, or groundwater, resulting in highly concentrated dissolved ions in the lake water. As water evaporates, it concentrates dissolved ions (Na⁺, HCO₃⁻, CO₃²⁻, and Cl⁻), raising alkalinity and pH (9 to 12) (Eugster & Jones, 1979; Garrels & Mackenzie, 1967; Hardie & Eugster, 1970; Pecoraino et al., 2015). The concentration of carbonate species increases as the basin's waters become more concentrated through evaporation (Deocampo & Renaut, 2016). Despite the notable rise in alkalinity due to evaporative concentration, Deocampo, (2004) surprisingly noted a decline in the percentage of anion charge from carbonate species, dropping from 95% in the incoming water to approximately 73% in Lake Makat. The decrease in carbonate proportion correlates to a corresponding decrease in Ca²⁺ and Mg²⁺ concentrations resulting in extremely low levels of alkaline earth carbonates in developed brines. The dissolving ions gradually accumulate until the

brine reaches a saturation point of the respective solid mineral phase (Tosca & Tutolo, 2023). Once the particular solid mineral phase reaches its saturation point, the precipitated mineral is removed from the solution and the solute concentration continues to increase (Deocampo & Jones, 2014; Peter Kilham, 1990).

2.2.3 Chemical Weathering

The chemical weathering of volcanic rock minerals from the nearby escarpments releases various ions into the lake waters. The weathering of various volcanic rocks (basaltic, trachytic, phonolite, and carbonatite ashes) leads to the influx of carbonate and bicarbonate ions into the lake, increasing its alkalinity (Deocampo & Renaut, 2016; Gizaw, 1996; Jones et al., 1977). A study by Zaitsev & Keller, (2006) reported that the weathered volcanic rocks of the Oldonyo Lengai in northern Tanzania contribute to forming various soluble secondary minerals. These minerals include nahcolite (NaHCO₃), trona (Na₃H(CO₃)₂·2H₂O, thermonatrite (Na₂CO₃·H₂O), pirssonite (CaCO₃·Na₂CO₃·2H₂O), gaylussite (CaCO₃·Na₂CO₃·5H₂O) and calcite (CaCO₃) and results into the release of alkali and carbonate into the lake water. The mineral composition of the rift valley is quite impressive, featuring nephelinite with nepheline, augite, anorthoclase, and albite (Ghiglieri et al., 2012; Makoba & Muzuka, 2019). These minerals release a substantial amount of Na+ and K+ ions during weathering. Hydrolysis facilitates the weathering of silicate minerals, producing HCO₃⁻ and cations (Eq 2 and Eq 3) (Pecoraino et al., 2015). Basaltic rocks contain significant calcium, whereas alkaline rocks are known for their sodium-rich silicate minerals and abundant K-feldspar (Deocampo & Renaut, 2016). However, the majority of the volcanic rocks lack quartz minerals. Chemical weathering intensifies and accelerates in high-rainfall areas, such as rift edges and core volcanoes. Areas with rain shadow effects, like rift floors and semi-arid regions with gentle terrain, have the lowest rates.

$$CO_2 + H_2O + rhyolite$$
 (K-feldspar, quartz, and Na-plagioclase) \rightarrow clay minerals + Na⁺ + K⁺ + HCO₃⁻ (Eq 2)

$$CO_2 + H_2O$$
 + basalt (plagioclase, olivine, pyroxene) \rightarrow carbonate minerals (calcite, magnesite, and serpentine) + clay mineral $+ HCO_3^-$ (Eq 3)

Some weathering events release ions into the water, but cannot increase alkalinity, however, it can contribute to the acidity of the lake water. This process includes the oxidation of sulfide minerals, such as pyrite (FeS2), which results in the oxidation of both ferrous iron and sulfide (Eq 4 and Eq 5). This reaction occurs in two steps.

$$4FeS_{2(s)} + 14O_{2(g)} + 4H_2O_{(l)} \rightarrow 4Fe^{2+}_{(aq)} + 8SO_4^{2-}_{(aq)} + 8H^+_{(aq)}$$
 (Eq 4)

Ferrous iron quickly oxidizes in oxygen-rich environments due to its instability

$$4Fe^{2+}_{(aq)} + O_{2(g)} + 4H^{+}_{(aq)} \rightarrow 4Fe^{3+}_{(aq)} + 8H_2O_{(aq)}$$
 (Eq 5)

2.2.4 Mineral Precipitation

Mineral precipitation occurs when the concentration of particular ions reaches saturation. The saturation of the particular ions and mineral precipitates depends on their water solubility, which is influenced by temperature, pH, water activity, and pCO₂ (Getenet et al., 2023; Getenet, Manuel, et al., 2022). In the soda lakes of the EARV particularly in Lake Magadi, Nasikie Engid a (southern Kenya), and Natron (north Tanzania) and its tributaries sodium carbonates/bicarbonat es as well as halite are major precipitating minerals (Getenet et al., 2023). The pH-dependent fraction of CO₃ / HCO₃ determines the Na-carbonate precipitation sequence. The higher pH and HCO₃⁻ and CO₃²⁻ lead to the precipitation of the Ca-Mg carbonate minerals (calcite and sepiolite) resulting in significant depletion of Ca²⁺ and Mg²⁺ ions (Svetlana V Borzenko & Shvartsev, 2019). In a recent study conducted by Getenet et al., (2023), it was found that trona is the first mineral to precipitate in lake brines when the CO₃ / HCO₃ >1. In contrast, nahcolite precipitates rather than trona, which forms afterwards due to the incomplete decomposition of nahcolite in the hot springs with a CO₃/HCO₃ >1. The precipitation of thermonatrite started once trona reached equilibrium with the remaining brines, as there was no additional CO₂ being introduced (Getenet et al., 2023). Following the trona precipitation, the residual brine becomes depleted with HCO₃⁻, resulting in the sequential precipitation of halite/villiaumite, thermonatrite, and sylvite (Getenet et al., 2023). The sequential mineral precipitations imply that the evolution of hyperalkaline, saline, and SiO₂rich brines is primarily driven by evaporation and mineral precipitation (Svetlana V Borzenko & Shvartsev, 2019; Getenet et al., 2023).

2.2.5 Ion Exchange

Ion Exchange occurs when the lake water interacts with surrounding sediment leading to the exchange of cations and anions in the water with those adsorbed on the surface of the clay or other minerals in the sediment (Tóth, 1999; Kharaka et al., 1984). Clay minerals (e.g., kaolinite, montmorillonite, illite, chlorite, vermiculite, zeolite), ferric oxide, and organic matter are the most effective ion exchangers due to their large surface area (Tóth, 1999). The most common type of ion exchange is exchanging Na⁺ with Ca²⁺ and/or Mg²⁺ in bentonite, which softens water by enriching it with Na⁺ (Tóth, 1999). The reverse ion exchange process, which involves elemental combinations with clay minerals, also regulates the water chemistry of the soda lake (Garrels & Mackenzie, 1967; Mackenzie et al., 1995). Clay minerals in reverse ion exchanges ser ve as the precursor for the elemental combinations, resulting in the removal of ions as a new clay mineral form. A typical reverse ion exchange involves the conversion of kaolinite into illite and smectite, while simultaneously removing K⁺, Na⁺, Mg²⁺, and HCO₃⁻ from the solution (Mackenzie et al., 1995).

2.2.6 Inflow and outflow of water and solutes

Various solutes can enter the lake basin via nearby escarpments' surface runoff and groundwater. The chemical composition of the inflow rivers plays a crucial role in determining the chemical evolution of the soda saline lakes (Hardie & Eugster, 1970; Jones & Deocampo, 2003; Yechieli & Wood, 2002). The initial chemistry of inflow is influenced by the lithology and distribution of weatherable rocks and sediments, as well as groundwater residence time (Jones et al., 2009). The runoff of the inflow from the surrounding hills and slopes carries various weathered volcanic rocks, surface soils, and sediments into the lake basin, contributing to the lake water's chemical composition (Jones & Deocampo, 2003; Jones et al., 2009). The seasonal rivers and streams originating from the adjacent escarpments have a crucial impact on the chemical composition of the lake water by transporting dissolved solute into the lake basins. Aquifers in the drainage basins are replenished by underground waters by gravity flow, which then discharge their contents into the lake below the surface via springs and seeps (Tóth, 1999; Pecoraino et al., 2015). Due to various geological and hydrological circumstances, the influence of the underground springs on

water and solute influx into the lake varies and is hard to quantify. Since alkaline soda lakes are often found in the hydrological closed basins, water outputs occur by (1) evaporation without solute loss, (2) groundwater infiltration by gravity flow, and (3) mineral precipitation after saturation, which is the primary solute loss(Jones & Deocampo, 2003).

2.2.7 Atmospheric Inputs

Most precipitation in East Africa is mostly influenced by the monsoonal winds originating from the Indian Ocean and the Intertropical Convergence Zone (ITCZ) migrates north-south seasonal (Johnson & Odada, 1996). The chemical analysis of the rains in East Africa revealed that the chemical composition of the rains reflects the airborne dust dissolution (originating locally or regionally), and marine aerosols and atmospheric gas dissolution (mostly CO₂) (Kanuga, 1982).

$$CO_2 + H_2O = H_2CO_3 \leftrightarrow HCO_3^- + H^+$$
 (Eq 6)

Dissolving atmospheric carbon dioxide in rainwater produces carbonic acid dissociating into bicarbonate and hydrogen ions (Eq 7).

The ionic ratios of the East African rainfall as shown in Table 4.2 by (Deocampo & Renaut, 2016) closely resemble those in saltwater, suggesting that marine aerosols are responsible for a significant portion of the ions present. Excess calcium and bicarbonate levels suggest carbonate dust dissolution. Rainfall also contributes significantly to chloride levels in soda lakes, highlighting how atmospheric processes impact lake chemistry (Deocampo & Renaut, 2016). Lake flats in dry basins frequently have efflorescent trona and halite (NaCl) crusts (Nielsen, 1999). Weathering and mobilization of trona and halite by wind (e.g., "dust devils") can cause redeposition in local water bodies, significantly the chemistry of the dissolved fraction.

2.2.8 Magmatic and Hydrothermal Inputs

The magmatic-hydrothermal springs have been recognized as potential sources of solutes in soda saline lakes, notably in volcanic rift zones and saline crater lakes (Pecoraino et al., 2015; Robin W. Renaut et al., 2021a). Thermal spring water plays a significant role in introducing solutes to

streams within the drainage basin (Renaut et al., 2021a). Hot springs and volcanic gases (CO2 and SO₂) influence the alkalinity of Kenya, Ethiopia, and northern Tanzanian rift lakes (Renaut & Jones, 2011). The CO₂-rich springs interact with the bedrock through hydrolytic neutralization reactions, producing water containing Na⁺ and HCO₃⁻ (Nicholson, 1993; Renaut & Jones, 2011). The precipitation of nahcolite and trona from the perennial hot spring inflow waters of Kenya's Lake Nasikie Engida highlights their contributions to the lake's water alkalinity (Getenet et al., 2023; Renaut et al., 2021). Furthermore, lakes can develop alkalinity from directly discharging magmatic CO₂ (Benvenuti et al., 2013) into the lake basin by neighbouring erupting volcanic mountains.

2.2.9 Reduction of sulfate

Microbial activity in soda lakes degrades organic matter, converting sulfate ions to sulfide and removing sulfates from lake water (Tóth, 1999; Sorokin et al., 2014, 2015). The generated H₂S is released into the atmosphere, and metal sulfide precipitates out of the water, causing the lake to become more permanently alkaline (Dunnette et al., 1985; Kilham, 1984; Kilham & Cloke, 1990; Sorokin et al., 2014, 2015). In soda lakes sulfate-reducing bacteria (SRB) (*Desulfonatronum*, *Desulfonatronovibrio*, and *Desulfonatronospira*) play a crucial role in the conversion of sulphate to sulphide (Sorokin et al., 2010, 2014). SRB can use diverse energy sources and electron acceptors to proliferate. This entails utilizing organic matter (short chain), hydrogen, or formate as electron donors, and sulfate, thiosulfate, or sulfite as electron acceptors (Sorokin et al., 2010, 2008). Alternatively, they can obtain energy through thiosulfate or sulfite disproportionation Figure 4 (Sorokin et al., 2010, 2008). The reduction of the sulfate to sulfide by SRB regulates the sulfate concentrations in soda lakes.

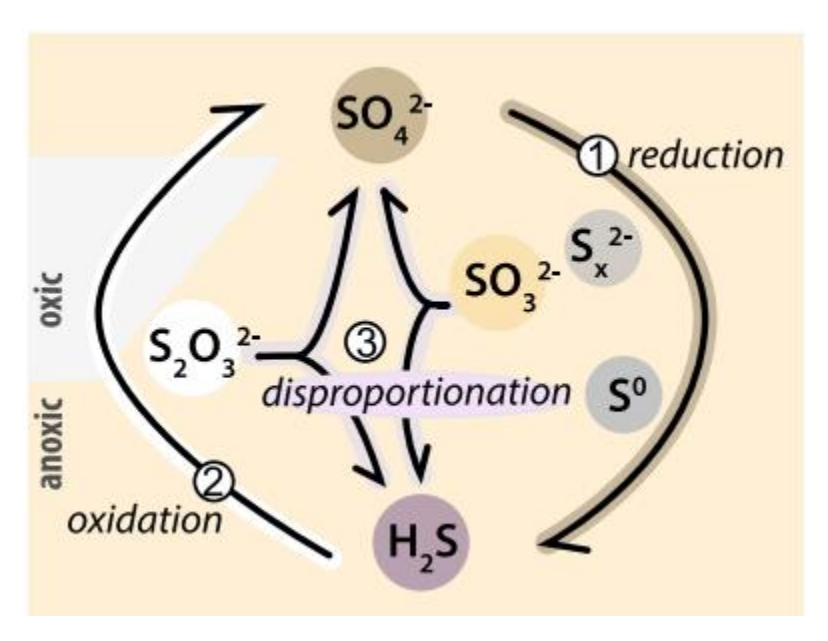


Figure 4: Microbial-redox process of the sulfate in the soda lakes (Sorokin et al., 2014).

2.2.10 Geochemical Evolution

The geochemical evolution of soda lakes is closely linked to the chemical composition of their inflow waters (Deocampo & Renaut, 2016; Hardie & Eugster, 1970; Pecoraino et al., 2015), which are primarily influenced by atmospheric inputs and chemical weathering processes. In the East African Rift's soda lakes, the water influx, mainly derived from neighbouring volcanic areas, is characterized by a dominance of Na⁺ or Ca²⁺ cations, complemented by K⁺ as a subsidiary cation and a notably scant presence of Mg²⁺ cations (Deocampo & Jones, 2014; Renaut et al., 2013). This composition suggests the hydrolysis of parent bedrock abundant in feldspars and volcanic glass, highlighting the significant role of silicate mineral dissolution in shaping the lake's ion content. Among the anions, carbonate species are prevalent, accompanied by high chloride levels and variable sulfate concentrations, which together contribute to the unique ionic signature of these lakes. The rock types, their reactivity with dilute natural waters, and the resulting interaction with the main cations and anions dictate the geochemical evolution pathway of soda saline lake (Jones & Deocampo, 2003).

The geochemical evolution of these lakes during the evaporative concentration is well framed by the chemical divide model (Drever, 1982; Hardie & Eugster, 1970), a concept that elucidates how the brine evolves as water evaporates. The chemical divide model was formerly known as

"fractionation by mineral precipitation" (Eugster, 1980) or "the principle of chemical divide" (Drever, 1982). However, in recent years, it has been often known as the "chemical divide" (Babel & Schreiber, 2014). According to the chemical divide model, the molar ratio of precipitated brine ions fluctuates unless it remains unaltered from the original solution throughout the evaporation process. As water evaporates, the remaining brine becomes more concentrated with dissolved ions until saturated with a solid phase (Tosca & Tutolo, 2023). When certain minerals reach a saturation point, the brine solution becomes depleted with cations and anions due to mineral precipitation, resulting in a chemical divide.

In the context of soda saline lakes in the eastern Tanzania rift valley, the brine solutions are saturated with dolomite, calcite, sepiolite, goethite, hematite, hydroxyapatite, manganite, aragonite and undersaturated with anhydrite, chalcedony, celestite, gypsum, halite, siderite, sylvite, and vivianite minerals (Lameck et al., 2024). The precipitation events, particularly calcite and sepiolite, lead to the sequestration of calcium, magnesium, and carbonate ions from the lake water, marking distinct stages or 'chemical divides' in the geochemical evolution of the lake brine. The analyses by Lameck et al., (2024), indicate that the brines in these Tanzanian lakes have higher bicarbonate levels relative to calcium and magnesium, adhering to the m HCO $_3$ ⁻ > 2m Ca $_2$ ⁺ and m HCO $_3$ ⁻ > 2m Mg $_2$ ⁺ ratios. Continuous calcite precipitation (first chemical divide) and sepiolite (second chemical divide) in brine water with Na-CO $_3$ -SO $_4$ -Cl. This sequential precipitation underpins the pathways I and I-B Figure 5 of geochemical evolution delineating a clear trajectory of mineralogical and chemical changes driven by evaporation and solute concentration processes in these unique soda saline lake environments.

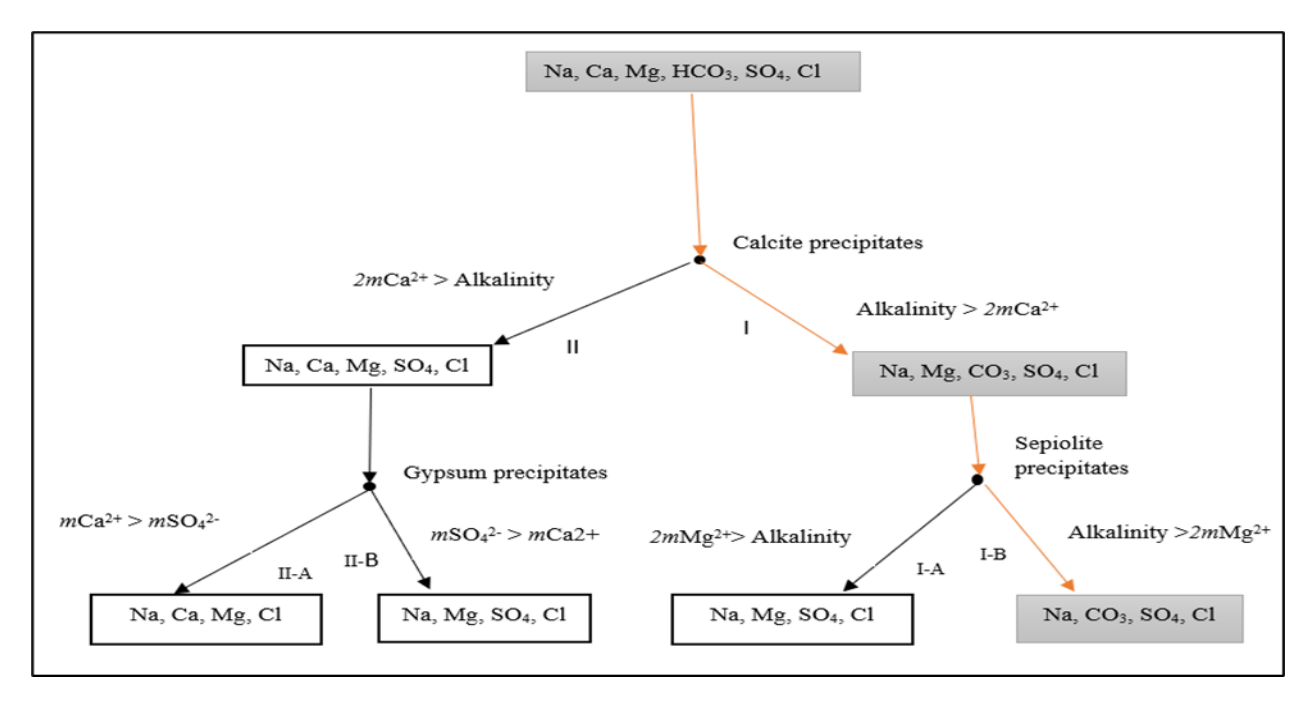


Figure 5: The probable evaporation paths of natural water modified from (Drever, 1982; Hardie & Eugster, 1970). Lake water under investigation likely evolves along I–IB.

2.3 Global Geographical Distribution of IASW

IASW predominantly occur in arid and semi-arid regions across the globe, where evaporation rates surpass precipitation and inflow, resulting in a higher concentration of salts and minerals (Deocampo & Renaut, 2016; Pecoraino et al., 2015). IASW are distributed globally (Figure 6), including prominent locations in the Rift Valley in East Africa (Figure 8), North America, South America, and Central Asia.

The EARV hosts several IASW, due to the intense tectonic and volcanic activity in the region (Deocampo & Renaut, 2016; Grant & Jones, 2016; Grant, 2006; Pecoraino et al., 2015; Scoon, 2020). East African Rift System (EARS) is linked to active volcanoes and major seismic occurrences in the interior of the African Plate (Scoon, 2020) as demonstrated in (Figure 8). The East African region is home to several alkaline lakes as described in Table 4 by Lameck et al., (2023), however, the eastern Rift Valley hosts more soda lakes than the western Rift. According to the recent review by Lameck et al., (2023), Tanzania has the most soda lakes (20), followed by Ethiopia (9), Kenya (8), and Uganda (4). Despite being near the equator, precipitations in the East

African region are scarce owing to the rain-shadow effect (Pecoraino et al., 2015). Lower precipitation and higher evaporation led to the formation of IASW.

Apart from the EARV, the IASW are prominent in various regions on the globe, with notable examples in both North and South America, situated along the active volcanic belt encircling the Pacific Ocean. In the United States, Lake Mono and Lake Albert, along with Mexico's Lake Atlacoya and Bolivia's Laguna Cachi, exemplify this phenomenon, reflecting the interconnectedness of alkaline lake formation with volcanic activity (Alcocer, 1998; Baesman et al., 2009; Sahajpal et al., 2011; Wurtsbaugh et al., 2017). Similarly, Asia's central region, spanning from the Caspian Sea to Tibet and Qinghai in China, offers favourable conditions for alkaline lakes, attributed to its specific climate and hydrogeology (Boros & Kolpakova, 2018; Borzenko & Shvartsev, 2019; Zheng & Liu, 2009). The correlations that exist between the presence of alkaline lakes and recent volcanic eruptions in the region particularly in China are highlighted by (Mianping et al., 1993). Additionally, the Carpathian Basin in Central Europe (Austria, Hungary, Serbia, and Turkey) Figure 7 is known for its shallow soda pans, formed during the late Pleistocene and early Holocene due to unique regional factors (Boros et al., 2014; Boros et al., 2017; Boros & Kolpakova, 2018; Felföldi, 2020; Stenger-Kovács et al., 2014). This low depth is one of the most distinguishing characteristics of these pans. Contrastingly, Australia's semi-arid basins host saline lakes with varying pH levels (1.7 to 8.6), formed predominantly by the interaction of regionally acidic saline groundwaters into the lakes, rather than volcanic influences (Bowen & Benison, 2009). The oxidation of sulfide and Fe substantially influences the formation of acid. In addition, Antarctica also hosts saline lakes (Green & Lyons, 2009) with high pH levels as high as 10, however, the continent's surface is dominated by a permanent ice glacier that covers approximately 99 % of its total area. Regardless of the saline lakes' existence in Antarctica, there is no proven evidence directly linking these lakes to volcanic activity or magmatic materials, underscoring the diverse origins and characteristics of alkaline lakes across different global contexts.

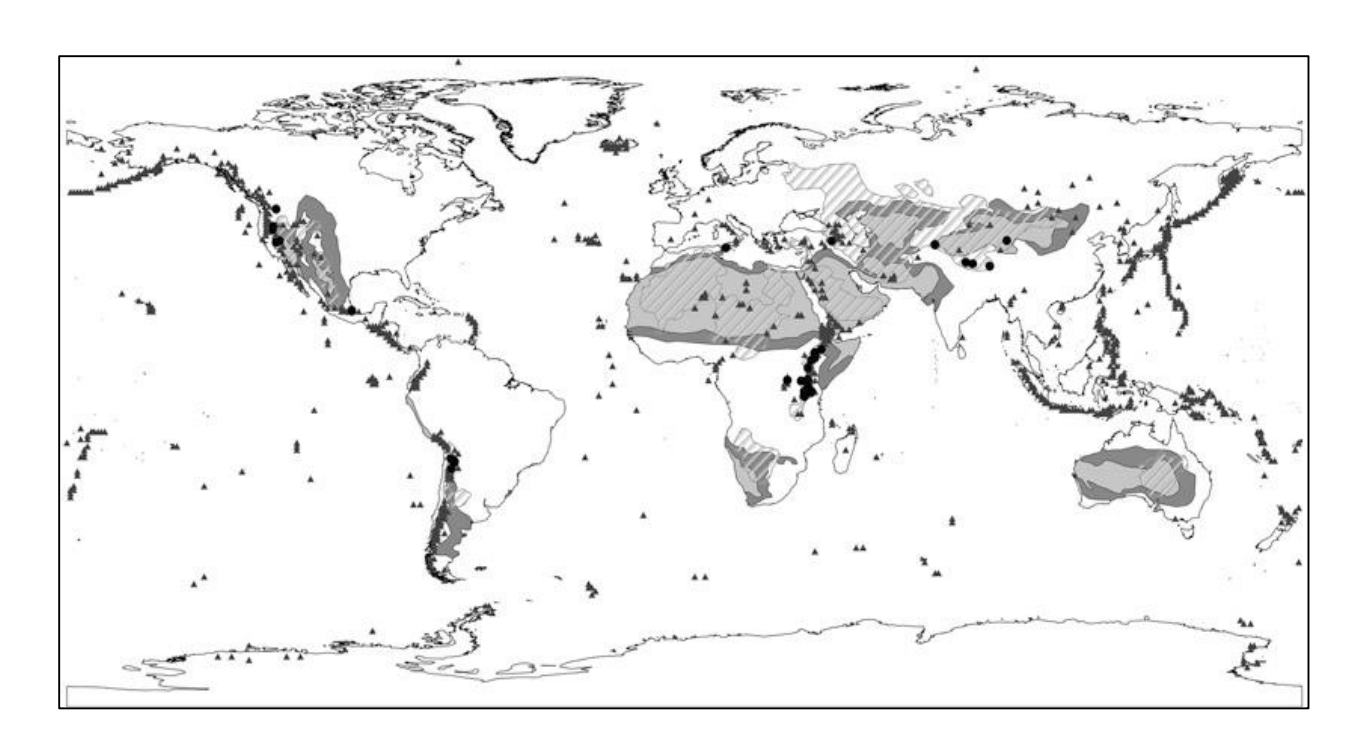


Figure 6: Worldwide distribution of IASW. The areas with active Volcanoes are symbolized by triangles, soda lakes by circles, arid and semiarid regions (light grey and dark grey areas respectively), and endorheic zones by light grey shaded areas (Pecoraino et al., 2015).

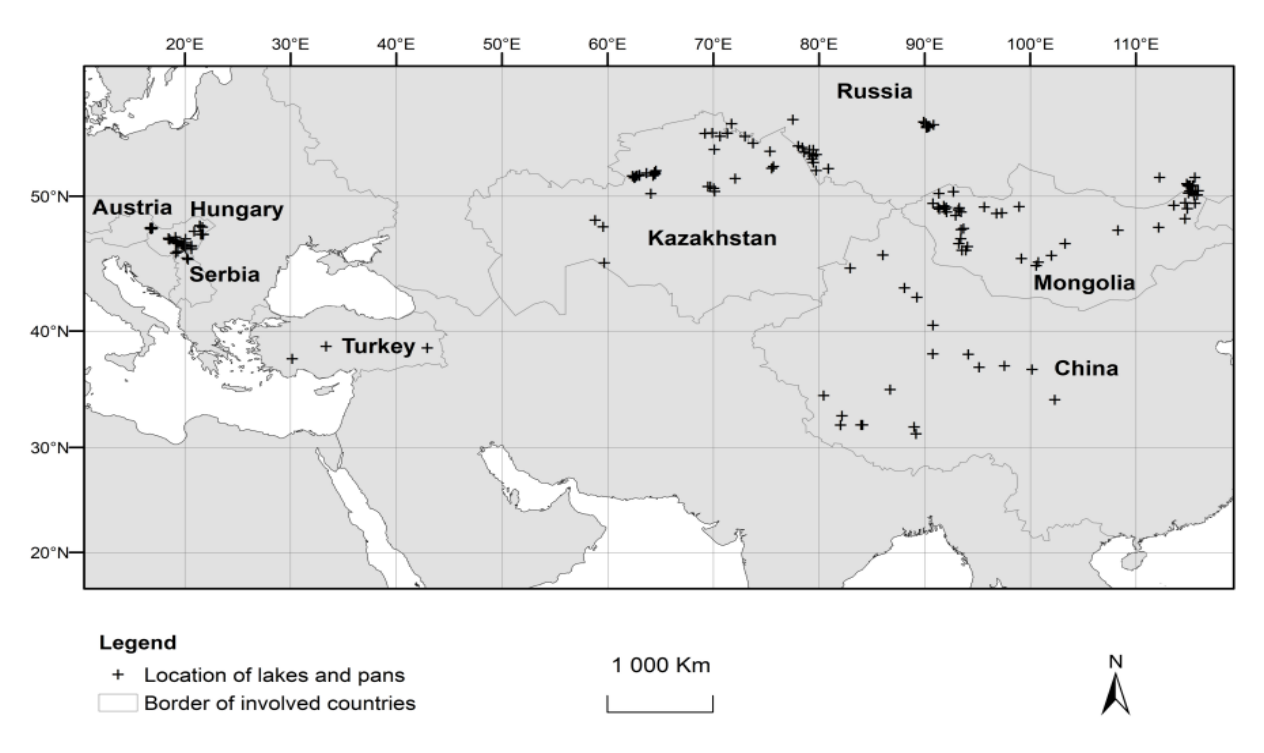


Figure 7: The important hotspots of IASW in Eurasia (Boros & Kolpakova, 2018)

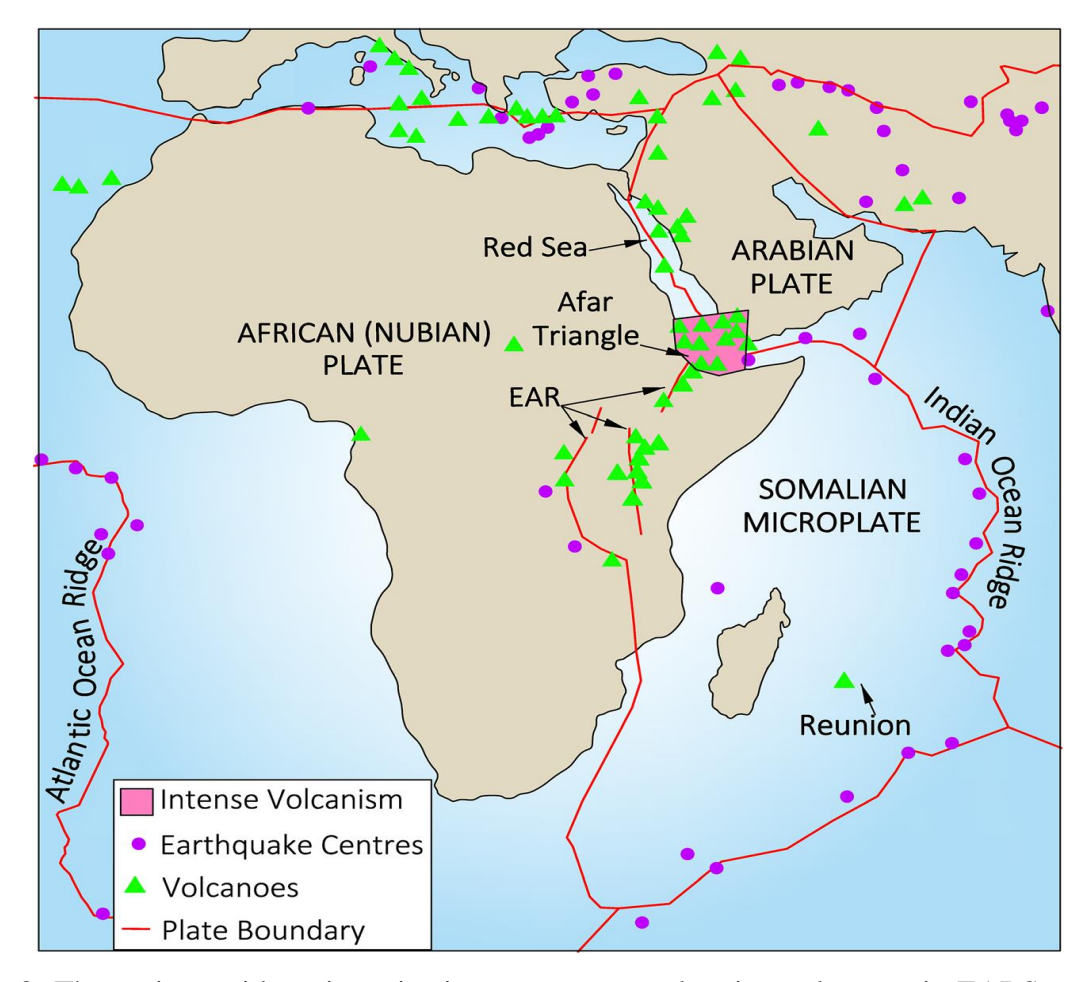


Figure 8: The regions with major seismic occurrences and active volcanoes in EARS are in the interior of the African Plate (Scoon, 2020).

2.4 Water Chemical Type Classification

Understanding the chemical composition of inland soda saline lakes is essential for distinguishing the different water chemical types. The proportions of ionic components (cations and anions) in inland lake water determine the chemical type of water. Several researchers have illustrated various methods for classifying distinct water chemical types of inland lakes. Based on the prevalence of anions and various subtypes mixed with key cations including sodium (Na⁺), calcium (Ca²⁺), and magnesium (Mg²⁺), Hammer (1978) classified saline waters into carbonate, chloride, and sulphate water types. Nevertheless, the inaccurate categorization of inland soda saline lakes might occur due to imprecise usage of chemical terminologies, particularly when pH is the

primary variable considered (Boros & Kolpakova, 2018). Using pH as the criterion for water chemical type classification, the study by Namsaraev et al., (2010) incorrectly identified Lake Khilganta (Southeastern Transbaikalia) as a soda lake. The inland reservoir waters were classified into carbonate, sulphate (sodium or magnesium), or chloride categories using a method called the "metamorphic coefficient" developed by MG Valyashko. According to Boros & Kolpakova, (2018), the Valyashko approach can serve as an indicator for classifying soda brine chemicals. However, relying solely on this method is inadequate for categorizing inland waters. The Valyashko approach is inadequate for classifying water chemical types based only on the CO₃⁻ + HCO₃⁻ and Mg²⁺ + Ca²⁺ species ratios. Furthermore, (Litchfield, 2011) and (Timms et al., 1986) classified inland saline water by ranking the primary ions with >25% equivalent, which aids in determining the water chemical type from diverse ion combinations in saltwater. Boros & Kolpakova, 2018) developed a simple and accurate classification criterion for defining the inland soda saline water type by utilizing terms such as "soda," "soda-saline," and "saline" for various forms of saline water. The criteria for this classification are as follows.

Soda type

• Na⁺ > 25 e % and first in the cation's dominance sequence and $HCO_3^- + CO_3^{2-} > 25$ e % and first in the anion's dominance sequence.

Soda-saline type

• Na⁺ > 25 e % and first in the cation's dominance sequence and $HCO_3^- + CO_3^{2-} > 25$ e % and but not first in the anion's dominance sequence ($HCO_3^- + CO_3^{2-} < than Cl^- \text{ or } SO_4^{2-} = \%$).

Saline type

• Na⁺ > 25 e % and first in the cation's dominance sequence (Na⁺ > than any other cation) and $HCO_3^- + CO_3^{2-} < 25$ e % and Cl^- or SO_4^{2-} is first in the anion's dominance sequence.

This term-based classification reduces confusion between interdisciplinary studies and provides a more comprehensive understanding of the chemical features of soda and alkaline water.

3. MATERIALS AND METHODS

3.1 Study Area

3.1.1 Description of the study area

This dissertation covers the chemistry of the IASW of the EARV Figure 9, with a specific emphasis on the eastern Tanzania rift valley (Figure 10). These endorheic lakes in the EARV system are not linked to rivers; they acquire water from streams that flow down from the elevated marginal escarpments of the neighbouring hills during the rainy season (Ebinger et al., 1993; Olaka et al., 2010). The EARS is characterised by unique geological and hydrological phenomena, including ongoing volcanic activity, plate tectonic movements, earthquake occurrence and geothermal activities (Dawson, 2008b; Scoon, 2020). The EARS is characterized by high escarpments, volcanic peaks, and shallow basins (Scoon, 2018). The region's geology is diverse, with sedimentary rocks, clay-like soil, and volcanic rocks like basaltic lava prevalent in the area (Owen et al., 2018; Scoon, 2018). Additionally, minerals such as nephelinite with nepheline (Na₃Kal₄Si₄O₁₆), augite, anorthoclase, and albite are commonly found in the EARV (Scoon, 2018). The natural vegetation exhibits the characteristics of a savannah ecosystem, with a predominant presence of grassland covering a significant portion of the region, complemented by bushland in the hilly areas.

The ETRV encounters its most intense precipitation from November to May, followed by an extended period of drought from July to October. The area is characterised by an arid and semi-arid climate, with temperatures often dropping to approximately 2°C in June or July and regularly reaching highs of 35°C in February, September, and October (Catherine et al., 2015; Mwabumba et al., 2022). This arid and semi-arid climate is ideal for inducing high evaporation rates causing higher water loss exceeding the amount of precipitation (Olaka et al., 2010). The geology of the ETRV especially in northern Tanzania is defined by active tectonics, volcanism, sedimentary basins, and faulting, shaping its distinct landscape and hydrology. The ETRV features prominent volcanic structures, including calderas, large volcanic cones, and stratovolcanoes, as documented by Scoon (2018). Evidence of volcanic dominance in northern Tanzania is clearly illustrated in the Ngorongoro Volcanic Complex, an overlapping group of eight volcanoes displayed in Figures 5.5 and 5.7 by Scoon (2018). The complex is dominated by alkaline basalt and phonolite magmas (Mollel et al., 2008). The highland volcanoes are underlain by Proterozoic metamorphic rocks, rich

in alkaline minerals like basalts, nephelinites, nephelinite—phonolite, and carbonates (Dawson, 2008b, 2010; Scoon, 2018, 2020). Volcanic debris from Oldoinyo Sambu, Mosonik, Oldoinyo Lengai, and Kerimasi mountains deposits consolidated clays, sands, volcanic ash, and volcaniclastics into the lake basins. The ETRV exhibits significant geothermal activity, especially concentrated in northern Tanzania around Lake Eyasi, Ngorongoro, Lake Natron, Ol Doinyo Lengai volcano, and the Arusha area (Omenda, 2010). Additionally, low-temperature geothermal activity is notably present in central and southeastern Tanzania, particularly within the Singida and Rufiji regions, as illustrated in Figure 11 by Omenda, (2010).

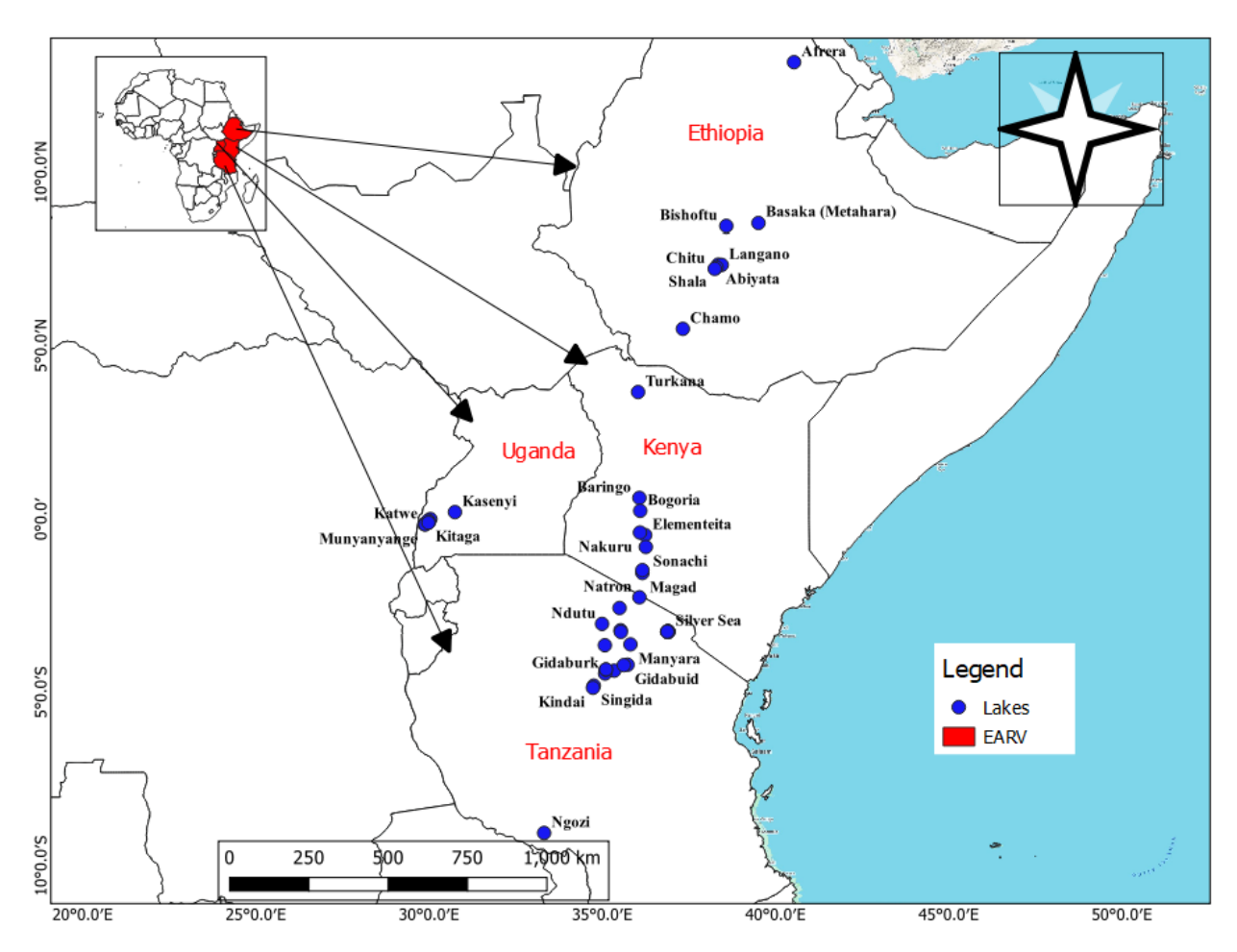


Figure 9: Locations and spatial distributions of the investigated inland saline waters in East Africa by countries

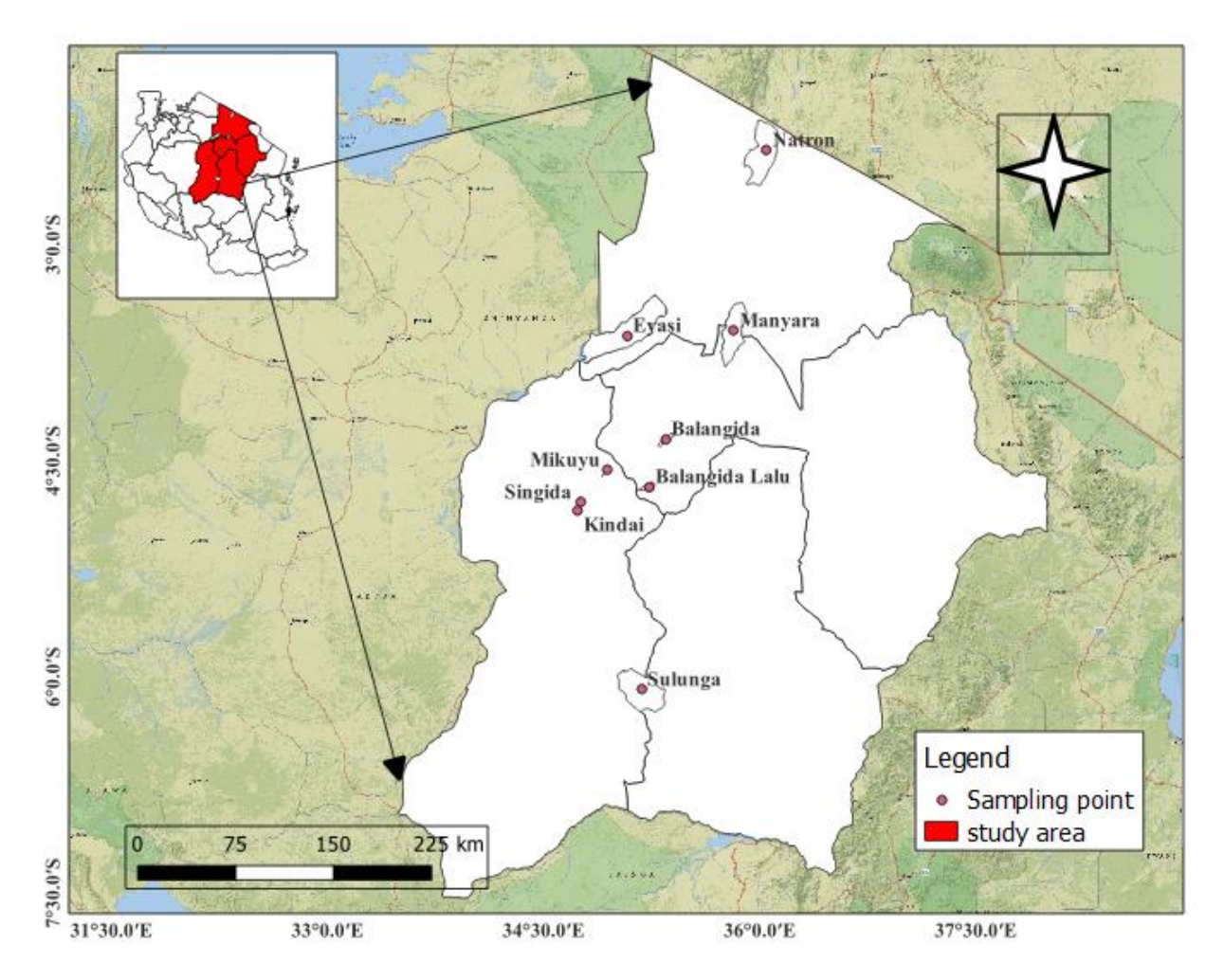


Figure 10: Locations of the investigated lakes along eastern Tanzania Rift Valley

3.2 Data acquisition and analysis

3.2.1 Chemical Properties of IASW in EARV

The chemistry (Na⁺, Ca²⁺, Mg²⁺, K⁺, HCO₃⁻, CO₃²⁻, Cl⁻, and SO₄²⁻) and pH (if available with ion data) of the EASL were reviewed using data from published studies published between 1965 and 2022. The lake with a minimum total dissolved solids (TDS) concentration of 1 g/l was considered in this study. We used academic literature databases such as Scopus, CAB Direct, and Web of Science, as well as the Google Scholar search engine and specialised websites, to conduct a comprehensive search for potential and relevant scientific peer-reviewed articles on the chemistry of soda-saline lakes. The chemistry data of the EARV were gathered across the IASW in the

EARV area, including Ethiopia, Kenya, Tanzania, and Uganda. The mean values were employed when various chemical data series were accessible in the same lake, such as different depths, periods, and seasons (seasonal variations). The data was sourced exclusively from publicly available studies, hence its correctness and repeatability may vary. Nevertheless, the methods employed in examining the chemical data vary as detailed in the method section of each article.

3.2.2 Water chemical types classification and carbonate estimation

The water chemical types of EASL were classified using the concentrations of the prominent ions. We adopted a classification criterion proposed by Boros & Kolpakova, (2018), which is based on a total quantity of cations or anions that exceeded 25 equivalent percentages (> 25e %). The dominant orders for cations and anions were determined independently (Eugster & Hardie, 1978; Hammer, 1978). Ensuring accuracy in the estimation of carbonates, all the input ion concentration data was carefully controlled and selected using a conventional ion balance percentage calculation. The calculation was based on Eq 7 (Freexe & Cherry, 1979), and was performed with a 10% error limit (Singhal & Gupta, 1999). Any value exceeding this limit is considered unacceptable.

The HCO₃⁻ Concentration was determined using the Advanced Speciation Method (ASTM) in waters where only the total alkalinity (methyl-orange) was known from the reference calculation. The computation was performed using the sample pH and total alkalinity, following known theoretical correlations in Eq 8 (Rounds, 2012).

$$[HCO_3] = \frac{Alk_o - K_w \times 10^{pH} + \frac{10^{-pH}}{y}}{1 + 2K_2 \times 10^{pH}}$$
(Eq 8)

Where

Alk₀: total alkalinity (meq/L)

K_w: acid dissociation constant for water (1E-14)

K₂: second acid dissociation constant for H₂CO₃⁻ (5.6E-11)
pH: pH of the sample
γ: activity coefficient for HCO₃⁻ (0.5) after (Pytkowicx, 1975)

The ASTM can also estimate the concentration of carbonate (CO₃²⁻) using yet another specific function. However, the calculation of carbonate [CO₃²⁻] was not trustworthy using this approach (Rounds, 2012). This is because acid/base characteristics (such as phosphate, silicate, ammonia, and so on) must be present in considerable proportions in these severely alkaline lake waters (Boros et al., 2017). Consequently, the carbonate content was determined using a mathematical equation (Eq 9) that relates bicarbonate and carbonate. This equation was applied to a dataset from the Carpathian Basin, specifically Austria, Hungary, and Serbia, which includes various soda lakes and pans that are representative of the region (Boros et al., 2014). The precise amounts of carbonates [HCO₃⁻, CO₃²⁻] were determined using a regional dataset of alkalinity titrations (ASTM 2320 B) with methyl red/bromocresol and phenolphthalein indicators published by Boros (2023):

$$[CO_3^{2^-}] = -2.878E - 7 \pm 5.438E - 8 \times [HCO_3^-] 2 + 0.069 \pm 0.003 \times [HCO_3^-]...$$
 (Eq 9)
N=200; df=198; r2=0.901; p<0.0001

3.2.3 GIS and Statistical Methods

Spatial autocorrelation was assessed by analyzing feature locations and attribute values using the Global Moran's I statistic, with an inverse distance squared conceptualization and the Manhattan distance method. Due to significant spatial autocorrelation (p < 0.05), further GIS analyses applied mixed models with spatial random factors. Linear Mixed Models (LMM) were then used to examine relationships among anion concentrations (Cl⁻, SO₄²⁻, HCO₃⁻, CO₃²⁻) as dependent variables and six independent environmental predictors, including, From the centre of the lakes: (Distance of Holocene volcanoes, Elevation of Holocene volcanoes, Distance of Pleistocene volcanoes, Elevation of Pleistocene volcanoes), with the intersection of the lakes: (Surface geology (World Geological Map USGS database), Soil types (DSMW)). Pleistocene volcanoes

erupted during the Ice Ages over 2.5 million years ago, and Holocene volcanoes have been active in a warmer and more stable climate from 11,700 years ago to the present (*Global Volcanism Pr ogram, 2013.https://doi.org/10.5479/si.GVP.VOTW4-2013*). Spatial data were processed using ESRI ArcMap 10.4.1 GIS software, where spatial environmental predictors were linked to lake polygons through spatial join tools. The extracted data was then analyzed statistically in OriginPro 2024 (OriginLab, Northampton, MA, http://www.originlab.com), with significance levels at p < 0.05*, p < 0.005**, and p < 0.0005***. The normality of variables and residuals was assessed using the Kolmogorov-Smirnov test, and log transformation was applied to the raw data to enhance model fit and normalize residuals.

3.3 Water sampling and sample analysis

From September 12 to September 18, 2022, we conducted a fieldwork expedition in the eastern Tanzania Rift Valley. During this expedition, we collected water samples from nine (9) inland soda-saline lakes, as shown in Figure 10. To guarantee reliable sampling and analytical data, we took grab samples using the acid-sterilized plastic bottle (100 ml). We collected three composite samples from each lake, except for Lake Balangida, where we took one sample because it was nearly entirely dry during the fieldwork expedition. Following the collection of samples at the sampling locations, we employed a multi-parameter (Oakton 600 Series Waterproof Portable Metre Kit) to measure the pH, temperature, electrical conductivity (EC), salinity (TDS), and dissolved oxygen (DO) at the sampling site. This was done to acquire accurate readings as some parameters do change with time therefore it is necessary to take the readings immediately after sample collection. In addition, a turbidimeter was employed to quantify turbidity level. For the analysis of major cations (Na⁺, K⁺, Ca²⁺ and Mg²⁺), the water sample was carefully filtered using a filter with a pore diameter of 0.45 µm. To ensure accuracy in measurements, the filtered sample was then acidified with pure HNO₃ until it reached a pH of 2. On the other hand, the samples for the analysis of anions (HCO₃⁻, CO₃²⁻, Cl⁻, and SO₄²⁻) were not acidified. Both samples for cations and anions analysis were stored in an ice bath and transported to the laboratory for analysis.

The inductive coupled plasma-mass spectrometry (ICP-MS) technique was used to examine the cations (Na $^+$, K $^+$, Ca $^{2+}$, and Mg $^{2+}$) concentrations. We used the pH and total alkalinity

titrimetric approach to determine the concentrations of HCO_3^- and CO_3^{2-} . The argentometric method, which involves titration of water samples with silver nitrate was used to determine the concentrations of Cl^- and the turbidimetric method was used to determine the concentration of SO_4^{2-} by using barium sulfate.

3.3.1 Geochemical speciation, statistical analysis

The PHREEQC software version 3 (Parkhurst & Appelo, 2013) was used to compute the chemical speciation and mineral-saturation indices using Eq (10).

$$SI = Log (IAP / Ksp)$$
 (Eq 10)

Where Ksp represents the solubility constant at a specific temperature, and IAP represents the ion activity of the solution. The saturation index quantifies the process of mineral dissolution or precipitation in lake water. Positive SI values (SI>0) indicate mineral oversaturation, whereas negative SI values (SI<0) imply mineral dissolution. A non-parametric Spearman correlation matrix was used in the present study to determine the degree of correlation that exists between the variables as well as the nature of the relationship that exists between them (Chen et al., 2021).

3.4 Temperature and precipitatation

This study used satellite-based rainfall and temperature data collected from predetermined locations within the catchment area of each lake. Satellite-based climatic data over historical data from the catchment area meteorological station was used due to data limitations and unequal geographical coverage (Mwabumba et al., 2022). However, the satellite-based climate data underwent quality control and was validated using weather station data from the Arusha Meteorological Authority. The monthly satellite-derived precipitation data were sourced from the Climate Hazards Group Infrared Precipitation with Station (CHIRPS) datasets (Funk et al., 2015). The CHIRPS dataset is a product of a collaborative partnership between the United States Geological Survey (USGS) and the University of California Santa Barbara (UCSB). The dataset offers information on rainfall with a spatial resolution of 0.05° (Funk et al., 2015) and daily temporal resolution. We retrieved satellite-derived temperature data from MERRA-2, which is a

part of the National Aeronautics and Space Administration of Worldwide Energy Resource (NASA POWER) project, at a spatial resolution of 0.5° (Westberg et al., 2013). We retrieved satellite-derived climatic data (daily precipitation and temperature data) for the period spanning from 1981 to 2022.

3.4.1 Drought monitoring and analysis

We evaluated and monitored the incidence of drought in Northern Tanzania between 1981 and 2022 using the daily precipitation and temperature data acquired from the CHIRPS and NASA POWER projects. We adopted the Standardised Precipitation Evapotranspiration Index (SPEI) invented by Vicente-Serrano et al., (2010), to assess the frequency and intensity of droughts in the region. SPEI is a contemporary drought indicator that considers the impact of both precipitation and temperature on the evaluation of drought conditions. It is an extension of the Standardised Precipitation Index (SPI), which takes into account solely precipitation in drought assessment. Thus, SPEI offers a deeper understanding of the occurrence and severity of droughts in the region, potentially impacting the chemical makeup of the soda-saline lakes in northern Tanzania. The detailed descriptions of the computational approaches for SPEI are thoroughly documented in the publications of (Vicente-Serrano et al., 2010) and (Beguería et al., 2014).

3.5 GIS-based soil type classification

The soil information for the region surrounding the soda-saline lake in northern Tanzania was retrieved from the FAO Digital Soil Map of the World (DSMW) using GIS techniques. The FAO Digital Soil Map of the World (DSMW) is a digital representation of the FAO-UNESCO Soil Map of the World, which was prepared on paper with a scale of 1:5 million (FAO/UNESCO, 2003). The DSMW offers comprehensive data on soil type classes and characteristics, including texture, pH levels, and soil organic matter content (FAO/UNESCO, 2003). We downloaded the FAO DSMW shapefile and imported it into the QGIS software (version 3.22.10) using the "add layer" feature. We clipped the imported shapefile with the study area using the "clip" function in QGIS. The clip function helps to integrate the soil information from the FAO DSMW with our study area

for further soil classification. To have more comprehensive information on the soil type within the study region, the clipped soil map was then classified into several soil classes according to the FAO-UNESCO Legend. Using this extensive information, we analysed the geographical distribution of different soil types in the study region and explored the relationships between specific soil types and the chemistry of the soda-saline lakes.

3.6 GIS-based Geological Features

Using world geological maps from the United States Geological Survey (USGS) database, we retrieved the fundamental geological information for the study region that encompassed the sodasaline lakes in northern Tanzania. We retrieved the QGIS-compatible shapefiles of the world's geological maps from the USGS database. The downloaded geological map shapefile underwent significant data cleaning to ensure correctness, which included converting all files to a compatible Coordinate Reference System (CRS). The downloaded world geological map was then imported into the QGIS project via the "add layer" feature. Subsequently, the downloaded world geological map shapefile was integrated with the study area shapefile using the "clip" function. After finishing the integration procedure, we classified the geological characteristics of the study area. The geological units were precisely classified, with unique colours, patterns, and symbols allocated to ensure visual distinction on the map.

3.7 Land use land cover (LULC) changes

3.7.1 Remote sensing dataset and processing

LULC changes in Northern Tanzania over the 23-year were examined using Landsat images from 2000, 2014, and 2023. The selection of these particular years was based on the need for assessing changes and patterns over both short and long periods, taking into account the availability of cloud-free images with cloud cover of less than 5%. We used images from the Landsat-5 Thematic Mapper (TM) and the Landsat-8 Operational Land Imagery (OLI) archives accessible on the Google Earth Engine (GEE) platform. The images were processed using the GEE platform to classify LULC classes across the study region. GEE offers a substantial collection of geospatial

data, particularly satellite images, that allows for large-scale analysis. The spectral bands (Blue, Red, Near Infrared, and Shortwave Infrared) were processed, and several indices were derived, including the Normalized Difference Moisture Index (NDMI), Normalized Difference Built-up Index (NDBI), and Normalized Difference Vegetation Index (NDVI). Subsequently, the supervised classification procedure employed these spectral bands and indices as input characteristics. The spatial resolution of the bands was thirty (30) metres. To ensure consistency and minimize the impacts of moisture and phenological variations (Tilahun *et al.*, 2024), satellite images were retrieved within the same season of the year selected. We selected images taken between June and September, which corresponds to the time with the least amount of rainfall in the study area. This was done to reduce the effects of cloud cover and ensure the coverage and quality of the images were consistent.

3.7.2 Image processing and classification

We processed Landsat images on GEE and subsequently exported them to QGIS version 3.28.6 for classification and generating LULC change maps. We identified six LULC categories: water bodies, forests, shrubs/grasses, bareland, agricultural land, and built-up areas. To classify each image, a minimum of 330 samples were chosen by sketching polygons. Afterwards, the samples were randomly divided into two groups of equal size, 50% of the samples were used for training, while the other 50% were used for validating the overall classification accuracy (Ahmed et al 2024). Furthermore, the visualization was improved by employing different-colour composites of the satellite images. The Dzetsaka plugin in QGIS was used to do supervised classification, encompassing a range of machine-learning algorithms. Extra dependencies were installed to make use of Dzetsaka's methods, including the Scikit-learn 1.0.1 Python package, which is a commonly used library for machine learning (Karasiak, 2020; Pedregosa et al., 2011). The Random Forest (RF) classifier was used to categorise the three Landsat images because of its ability to accurately identify distinct LULC classes in varied environmental areas (Rodriguez-Galiano et al., 2012; Thonfeld et al., 2020) well as proven excellent accuracy. The RF algorithm was trained using reference information obtained via a combination of fieldwork, existing base maps (topographical maps), and feature digitization from Google Earth employing interpretation components such as

size, texture, tone, and shapes. The study area's accuracy assessment relied on the confusion (error) matrix obtained from the classified LULC data. The LULC classification is deemed incomplete until the accuracy achieves the acceptable threshold as indicated by the criteria established by Congalton and Green, (2019). The analysis used Kappa statistics and overall accuracy to assess the classification outcomes.

4. **RESULTS**

4.1 Review of chemical properties of the IASW of EARV

The ion chemical data (Na⁺, K⁺, Ca²⁺, Mg²⁺, Cl⁻, SO₄²⁻, HCO₃⁻, and CO₃²⁻) of the EASL compiled from the original published articles, and their details are tabulated in Table 1. The descriptive statistical summary of the ion chemical data is presented in Table 2. The pH ranged from 8.3 to 10.5 with the highest pH (10.5) recorded in Lake Ghama in Tanzania and the lowest pH of 8.3 in Lake Kindai in Tanzania. The Na⁺ concentrations in IASW varied between 351 and 138,000 mg/l as seen in Table 1. Lake Katwe in Uganda has the highest recorded concentration of 138,000 mg/l, while Lake Chamo, in Ethiopia, has the lowest recorded concentration of 351 mg/l. The potassium (K⁺) ion was moderately higher after Na⁺, ranging from 0–29,000 mg/l. The data presented in Tables 1 and 3 indicate that Na⁺ was the dominant dissolved cation in all lakes within the Rift Valley. The ternary scatterplot (Figure 11a) shows that Na⁺ is the most common dissolved cation in all lakes, accounting for more than 60% equivalent percentage. Ca2+ concentration in EASL ranged from 0-61mg/l, with Lake Kindai Tanzania having the highest concentration of 61 mg/l. Mg²⁺ ion concentrations in EASL ranged from 0-145 mg/l, with the highest values of 145 mg/l in Lake Gidabuid in Tanzania. IASW, like other inland waters globally, has a low concentration of divalent alkaline earth metals. The percentages of Ca²⁺ and Mg²⁺ equivalents were below 25% in all lakes, except for Lake Afrera which had 27% of Ca²⁺ equivalents and Lake Bishoftu, which had exactly 25% of Mg²⁺ equivalents, as shown in Table 4 and Figure 11b. The HCO₃⁻ varied from 134.2 to 131179 mg/l, while CO₃²⁻ ranged from 11 to 83100 mg/l. Lakes Natron and Murumuri have the greatest estimated amounts of HCO₃⁻ and CO₃²⁻, reaching 131,179 mg/l and 83,100 mg/l, respectively. Lake Kindai in Tanzania has the lowest estimated HCO₃⁻ and CO₃²⁻, at 159 mg/l and 11 mg/l, respectively. The HCO₃⁻ + CO₃²⁻ ions were the most dominant anion (Figure 11b) in EASL and most of the lakes had more than 25% e except lakes Ngozi, Kindai, Singida, Afrera, Kikorongo, and Katanga with equivalent percentages below 25% as indicated by Table 4. The Cl⁻ ion concentrations varied between 69 and 137,200 mg/l, with the lowest concentration seen in Lake Silver Sea (69 mg/l) and the highest concentration observed in Lake Kasenyi (137,200 mg/l). The Cl⁻ in the Rift Valley lakes is the second dominant ion among anions, with a mean of 14596.9 mg/l and contributing around 35.5% of the total anions (Lameck et al., 2023). The SO_4^{2-} in the IASW of the Rift Valley is the least in

the anion dominance sequence, accounting for 18.6% of the total anions (Lameck et al., 2023). The anion dominance sequence of the IASW was found to be $HCO_3^- + CO_3^{2-} > Cl^- > SO_4^{2-}$.

Table 1: The assessed major ion concentrations in the EASL (Concentrations are in mg/l except for alkalinity ($HCO_3^- + CO_3^{2-}$) which is in meq/l) and estimated salinity (TDS) in g/l.

													Salinity	
Country	Lake	alk (meq/l)	pН	Na ⁺	K ⁺	Ca ²⁺	Mg^{2+}	Cl ⁻	SO ₄ ²⁻	HCO ₃ ⁻	CO ₃ ²⁻	Salinity	classes	References
Kenya	Elementeita	107	9.4	3793	274	0	0	1985	144	6544	440	13.18	4	(Melack&Kilham,1974)
Kenya	Baringo	13	8.6	356	23	12	2	113	110	796	55	1.46	2	(Oduor et al., 2003)
Tanzania	Eyasi	38	9.55	2713	0	4	10	2244	279	2342	160	7.752	3	(Deocampo, 2005)
Tanzania	Natron	2150	9.63	67821	649	3	3	36514	2613	131179	4116	242.89	5	(Fritz et al., 1987)
Tanzania	Balangida	925.6	9.7	43600	1000	8	0	29970	8780	56496	2987	142.84	5	(Hecky & Kilham, 1973)
Tanzania	El Kekhotoito	42.1	9.7	1150	154	3	2	109	390	2602	178	4.588	3	(Hecky & Kilham, 1973)
Tanzania	Embagai	183.3	10.1	3900	600	4	2	325	0	11267	742	16.84	4	(Hecky & Kilham, 1973)
Tanzania	Ghama	163.3	10.5	5850	69	6	16	3300	580	10177	674	20.67	4	(Hecky & Kilham, 1973)
Tanzania	Gidaburk	87.4	9	3700	174	9	80	1970	1500	5338	361	13.13	4	(Hecky & Kilham, 1973)
Tanzania	Kindai	2.58	8.3	865	20	61	74	1640	18	159	11	2.84	2	(Hecky & Kilham, 1973)
Tanzania	Kusare	38.7	9.3	910	113	3	3	75	149	2374	163	3.78	3	(Hecky & Kilham, 1973)
Tanzania	Lekandiro	50.6	10.1	1350	130	3	5	175	331	3173	216	5.383	3	(Hecky & Kilham, 1973)
Tanzania	Lgarya (Ndutu		9.8	18000	284	0	0	5920	2730	33837	2010	62.78	5	(Hecky & Kilham, 1973)
Tanzania	Ngorongoro	80.8	9.2	2230	244	18	12	396	720	4940	334	8.89	3	(Hecky & Kilham, 1973)
	Hippo													• • • • • • • • • • • • • • • • • • • •
Tanzania	Silver Sea	14	9.1	385	74	3	2	69	150	863	59	1.60	2	(Hecky & Kilham, 1973)
Tanzania	Singida	5.66	8.6	1240	10	56	69	1890	140	348	24	3.77	3	(Hecky & Kilham, 1973)
Tanzania	Small Momela	46.7	9.8	1230	188	1	2	117	285	2892	198	4.91	3	(Hecky & Kilham, 1973)
Tanzania	Gidabugarak	45.2	8.9	2239	45	45	34	1744	744	2763	189	7.80	3	(Kilham & Cloke, 1990)
Tanzania	Gidabuid	27.4	8.5	1881	83	28	145	2109	764	1674	115	6.79	3	(Kilham & Cloke, 1990)
Tanzania	Gidamuniud	182.9	9.5	10598	414	28	72	10086	941	11179	737	34.05	4	(Kilham & Cloke, 1990)
Tanzania	Gidamur	70	9.4	2099	53	11	22	939	135	4287	291	7.83	3	(Kilham & Cloke, 1990)
Tanzania	Laja	85.2	9.4	3609	13	9	41	2049	701	5214	353	11.99	4	(Kilham & Cloke, 1990)
Tanzania	Ndanakid	30.2	8.9	1899	54	12	44	1599	528	1848	127	6.11	3	(Kilham & Cloke, 1990)
Tanzania	Ndobot	144	9.5	7449	131	3	59	6665	514	8806	586	24.21	4	(Kilham & Cloke, 1990)
Tanzania	Magad	84	10.2	2644	469	2	0	993	768	5232	354	10.46	4	(Melack &Kilham, 1974)
Tanzania	Manyara	78	9.2	2506	0	1	1	1170	240	4769	323	9.01	3	(Melack &Kilham, 1974)
Ethiopia	Aranguadi	51.4	10.3	1540	317	13	0	780	34	3272	223	6.17	3	(Prosser et al., 1968)
Ethiopia	Bishoftu	20	9.2	368	59	7	70	142	17	1231	85	1.97	2	(Wood & Talling, 1988)
Ethiopia	Chitu	400	10.1	20500	1200	0	0	12337	188	24486	1520	60.23	5	(Ogato et al., 2014)
Ethiopia	Kilotes (Kilole	63.4	9.6	1621	176	14	0	482	19	3895	265	6.47	3	(Prosser et al.,1968)
Kenya	Turkana	20	9.2	753	20	5	2	446	40	1231	85	2.58	2	(Yuretich & Cerling,1983)
Tanzania	Big Momela		9.8	5400	840	3	5	620	1023	3875	5200	16.96	4	(Nanyaro et al., 1984)
Tanzania	Tulusia	188.8	10.4	5600	790	2	5	565	665	4150	5950	17.72	4	(Nanyaro et al., 1984)

Tanzania	Reshitani	199	10.1	4100	590	1	1	430	300	3550	3660	12.63	4	(Nanyaro et al., 1984)
Tanzania	Chamo		8.93	315	17	10	10	94	7	839	58	1.35	2	(Gizaw, 1996)
Ethiopia	Bogoria		10	24970	393	5	0	5535	135	35860	13445	80.34	5	(Jirsa et al., 2013)
Kenya	Nakuru		10.1	27525	732	3	0	6585	613	30295	11360	77.11	5	(Jirsa et al., 2013)
Kenya	Magadi		9.8	12850	228.5	4.5	12	5250	100.5	9600	6100	188.98	5	(Getenet, et al., 2022)
Kenya	Sonachi		9.7	3005.3	382.2	3.7	2.15	303.6	109.4	3258.2	1307.2	15.40	4	(Fazi et al., 2021)
Kenya	Nasikie Engida		9.5	47622	1444	2	0	30054	752	20567	39850	140.29	5	(Renaut et al., 2021b)
Kenya	Kasenyi			136000	6800	0	140	137200	56300	11600	33200	381.24	5	(Arad & Morton, 1969)
Uganda	Katwe			138000	29000	0	10	133000	67000	7000	42000	416.01	5	(Arad & Morton, 1969)
Uganda	Kikorongo			11100	2200	0	0	5100	1900	3150	11850	35.3	5	(Arad & Morton, 1969)
Uganda	Kitaga			69000	3500	0	0	20200	85600	5800	19600	203.7	5	(Arad & Morton, 1969)
Uganda	Mahiga			84000	16400	0	120	72300	71000	3100	8900	255.82	5	(Arad & Morton, 1969)
Uganda	Munyanyange			37000	7700	0	0	15700	4400	11200	34000	110	5	(Arad & Morton, 1969)
Uganda	Murumuri			137000	11200	0	0	46900	71100	13900	83100	363.2	5	(Arad & Morton, 1969)
Uganda	Nyamunuka			61300	5600	0	0	32100	21000	10600	51800	182.4	5	(Arad & Morton, 1969)
Ethiopia	Abiyata		9.59	9900	374	1	0	4219	480	19276	1226	35.476	5	(Gizaw, 1996)
Ethiopia	Langano		9.05	445	23	8	3	180	17	945	65	1.68	2	(Gizaw, 1996)
Ethiopia	Basaka		9.4	1900	60	1	0	572	540	3447	235	6.755	3	(Gizaw, 1996)
Ethiopia	(Metahara)Shala		9.27	6700	216	2	0	3174	205	13115	857	24.27	4	(Gizaw, 1996)

Note, Aquatic bodies salinity classes according to (Saccò et al., 2021), (1) freshwater (0.02–1.0 g/l), (2) moderately saline (1.1–3 g/l), (3) brackish (3.1–10 g/l), (4) saline (10.1–35 g/l), (5) hypersaline (>35 g/l)

Table 2: The statistical summary of the investigated major ion concentrations

Ions (mg/l)	Min-Max	Mean	Median	25th Perc	75th Perc
Na ⁺	315-138000	21333	3847	1560	23853
K^+	0-29000	1848.34	258.85	62.25	827.50
Ca^{2+}	0.0-15430.8	293.44	3.193	0.925	9.10
Mg^{2+}	0.0-911.25	36.6574	2.1500	0.08	20.49
Cl ⁻	68.5-137200.0	14596.9	1930.0	487.1	9230.3
$\mathrm{SO_4}^{2-}$	0.0-85600.0	7599.1	521.1	145.3	1120.3
HCO_3^-	134.2-131179.1	10588.8	4528.0	2431.3	11033.9
CO_3^{2-}	11-83100.00	8177.32	400.45	166.37	4928.99

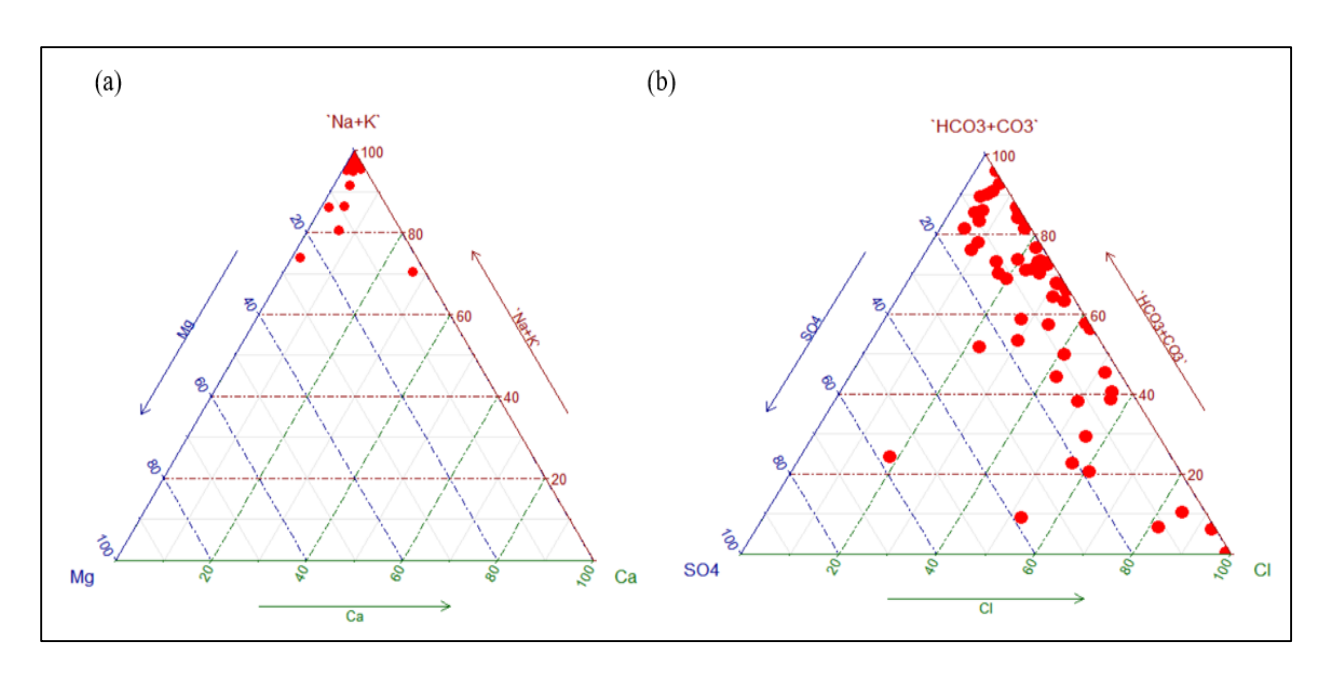


Figure 11: The general ternary scatter plot of the chemical ion composition of the investigated EASL (each point represents a lake).

4.1.1 Spearman Correlations

The Spearman correlation coefficients between major ions and TDS are summarized in Table 3. The analysis showed significant positive correlations between TDS and the monovalent ions Na+ and K+. In contrast, a significant negative correlation was observed between TDS and Ca²⁺, while no significant correlation was found between TDS and Mg²⁺. Furthermore, there was a significant positive correlation between TDS and the major anions HCO₃⁻, CO₃²⁻, Cl⁻, and SO₄²⁻ in the IASW.Most of the correlations are significant, because of ion interactions.

Table 3: The Spearman Correlations of the IASW (significant correlations are red coloured)

			S	pearman Co	rrelations				
	Na ⁺	K ⁺	Ca ²⁺	Mg^{2+}	Cl-	SO ₄ ²⁻	HCO ₃ -	CO3 ²⁻	TDS
Na ⁺	1	0.8276	-0.5571	-0.2375	0.8889	0.752	0.7483	0.8692	0.9955
K^+	0.8276	1	-0.5936	-0.3411	0.6239	0.6518	0.573	0.8052	0.837
Ca^{2+}	-0.5571	-0.5936	1	0.5367	-0.3561	-0.4302	-0.4772	-0.6966	-0.551
Mg^{2+}	-0.2375	-0.3411	0.5367	1	-0.0805	-0.0182	-0.4698	-0.4387	-0.2358
Cl^-	0.8889	0.6239	-0.3561	-0.0805	1	0.7182	0.5739	0.6335	0.8775
SO_4^{2-}	0.752	0.6518	-0.4302	-0.0182	0.7182	1	0.4168	0.6228	0.7489
HCO_3^-	0.7483	0.573	-0.4772	-0.4698	0.5739	0.4168	1	0.8131	0.7662
$\mathrm{CO_3}^{2-}$	0.8692	0.8052	-0.6966	-0.4387	0.6335	0.6228	0.8131	1	0.8682
TDS	0.9955	0.837	-0.551	-0.2358	0.8775	0.7489	0.7662	0.8682	1

4.1.2 Water chemical type classification

The ion equivalent percentages, predominant cations and anions, and water chemical type of the EARV lakes, according to the classification criteria established by Boros & Kolpakova, (2018) are detailed in Table 4. The regional breakdown of classified lakes by country is provided in Table 5 and presented in Figure 12. The result revealed that soda water chemical type is more dominant in the region, contributing 73.2% of the total number of lakes investigated. The majority of the sodatype lakes in the region were found in Tanzania (46.7%), followed by Ethiopia (22%), Kenya (19.5%), and Uganda (9.8%). Furthermore, 12.5% of the lakes fall into the soda-saline category and were most prevalent in Tanzania, accounting for 100% of the lakes investigated. In addition, our study revealed that 14.3% of the investigated lakes fall under saline water chemical type. The majority of the saline water chemical types were identified in Uganda (50%), Tanzania (37.5%), and Ethiopia (12.5%).

Table 4: Percentage equivalent, dominant ions, water chemical type, and ion balance of assessed data in the EASL

		g	ee%					Domi	nant ions		
Lakes	Na ⁺	K ⁺	Ca ²⁺	Mg^{2+}	Cl ⁻	SO ₄ ²⁻	HCO ₃ -+CO ₃ ² -	Cation	Anion	Water chemical type	Ion balance
Elementeita	96	4	0	0	31	2	67	Na ⁺	$HCO_3^- + CO_3^{2-}$	Soda	-3
Baringo	92	3	4	1	16	11	73	Na^+	$HCO_3^- + CO_3^{2-}$	Soda	-9
Ngozi	93	7	0	0	82	12	7	Na^+	Cl ⁻	Saline	-5
Eyasi	99	0	0	1	56	5	39	Na^+	Cl ⁻	Soda-saline	3
Natron	99	1	0	0	31	2	68	Na^+	$HCO_3^- + CO_3^{2-}$	Soda	-6
Balangida	99	1	0	0	41	9	50	Na^+	$HCO_3^- + CO_3^{2-}$	Soda	-3
El Kekhotoito	92	7	0	0	5	14	81	Na^+	$HCO_3^- + CO_3^{2-}$	Soda	-5
Embagai	92	8	0	0	4	0	96	Na^+	$HCO_3^- + CO_3^{2-}$	Soda	-8
Ghama	99	1	0	1	32	4	64	Na^+	$HCO_3^- + CO_3^{2-}$	Soda	-7
Gidaburk	93	3	0	4	30	17	53	Na^+	$HCO_3^- + CO_3^{2-}$	Soda	-4
Kindai	80	1	6	13	93	1	6	Na^+	Cl ⁻	Saline	-2
Kusare	92	7	0	1	4	6	89	Na^+	$HCO_3^- + CO_3^{2-}$	Soda	-7
Lekandiro	94	5	0	1	7	10	83	Na^+	$HCO_3^- + CO_3^{2-}$	Soda	-6
Lgarya (Ndutu)	99	1	0	0	20	7	74	Na^+	$HCO_3^- + CO_3^{2-}$	Soda	-3
Ngorongoro Hippo	92	6	1	1	9	13	78	Na^+	$HCO_3^- + CO_3^{2-}$	Soda	-6
Silver Sea	88	10	1	1	9	15	76	Na ⁺	$HCO_3^- + CO_3^{2-}$	Soda	-6
Singida	86	0	4	9	85	5	10	Na ⁺	Cl-	Saline	0
Small Momela	91	8	0	0	5	9	85	Na ⁺	$HCO_3^- + CO_3^{2-}$	Soda	-4
Gidabugarak	94	1	2	3	42	13	44	Na ⁺	$HCO_3^- + CO_3^{2-}$	Soda-saline	-6
Gidabuid	84	2	1	12	56	15	29	Na ⁺	Cl ⁻	Soda-saline	-5
Gidamuniud	96	2	0	1	56	4	41	Na ⁺	Cl ⁻	Soda-saline	-3
Gidamur	96	1	1	2	24	3	73	Na ⁺	$HCO_3^- + CO_3^{2-}$	Soda	-7
Laja	97	0	0	2	34	9	57	Na ⁺	$HCO_3^- + CO_3^{2-}$	Soda	-3
Ndanakid	94	2	1	4	50	12	38	Na ⁺	Cl ⁻	Soda-saline	-1
Ndobot	97	1	0	1	52	3	45	Na ⁺	Cl ⁻	Soda-saline	-4
Magad	90	9	0	0	20	11	69	Na ⁺	$HCO_3^- + CO_3^{2-}$	Soda	-5
Manyara	100	0	0	0	26	4	70	Na ⁺	$HCO_3^- + CO_3^{2-}$	Soda	-8
Afrera	68	2	27	3	99	1	0	Na ⁺	$HCO_3^- + CO_3^{2-}$	Soda	3
Aranguadi	88	11	1	0	26	1	73	Na ⁺	Cl ⁻	Saline	-5
Bishoftu	68	6	2	25	15	1	84	Na ⁺	$HCO_3^- + CO_3^{2-}$	Soda	-7
Chitu	97	3	0	0	43	0	56	Na ⁺	$HCO_3^- + CO_3^{2-}$	Soda	7
Kilotes (Kilole)	93	6	1	0	16	0	84	Na ⁺	$HCO_3^- + CO_3^{2-}$	Soda	-7
Turkana	97	2	1	1	35	2	63	Na ⁺	$HCO_3^- + CO_3^{2-}$	Soda	-4
Big Momela	91	8	0	0	6	8	86	Na ⁺	$HCO_3^- + CO_3^{2-}$	Soda	-4
Tulusia	92	8	0	0	5	5	90	Na ⁺	$HCO_3^- + CO_3^{2-}$	Soda	-6
Reshitani	92	8	0	0	6	3	91	Na ⁺	$HCO_3^- + CO_3^{2-}$	Soda	-1
Chamo	89	3	3	5	14	1	85	Na ⁺	$HCO_3^- + CO_3^{2-}$ $HCO_3^- + CO_3^{2-}$	Soda	-9
Bogoria	99	1	0	0	13	0	87	Na ⁺	11003 1 003	Soda	-4

Nakuru	98	2	0	0	17	1	82	Na^+	$HCO_3^- + CO_3^{2-}$	Soda	6
Magadi	99	1	0	0	42	1	58	Na^+	$HCO_3^- + CO_3^{2-}$	Soda	-1
Sonachi	93	7	0	0	7	1	93	Na^+	$HCO_3^- + CO_3^{2-}$	Soda	3
Nasikie Engida	98	2	0	0	34	1	66	Na^+	$HCO_3^- + CO_3^{2-}$	Soda	-9
Kasenyi	97	3	0	0	61	18	20	Na^+	$HCO_3^- + CO_3^{2-}$	Soda	-2
Katwe	89	11	0	0	56	21	23	Na^+	$HCO_3^- + CO_3^{2-}$	Saline	1
Kikorongo	90	10	0	0	23	6	71	Na^+	Cl^-	Saline	-8
Kitaga	97	3	0	0	18	57	24	Na^+	Cl^-	Soda	0
Mahiga	89	10	0	0	53	38	9	Na^+	$HCO_3^- + CO_3^{2-}$	Saline	3
Munyanyange	89	11	0	0	24	5	71	Na^+	$\mathrm{SO_4}^{2^-}$	Saline	-1
Murumuri	95	5	0	0	23	26	52	Na^+	Cl^-	Soda	4
Nyamunuka	95	5	0	0	28	13	59	Na^+	$HCO_3^- + CO_3^{2-}$	Soda	-7
Abiyata	98	2	0	0	25	2	73	Na^+	$HCO_3^- + CO_3^{2-}$	Soda	-5
Langano	94	3	2	1	22	2	76	Na^+	$HCO_3^- + CO_3^{2-}$	Soda	-6
Basaka (Metahara)	98	2	0	0	18	12	70	Na^+	$HCO_3^- + CO_3^{2-}$	Soda	-4
Shala	98	2	0	0	27	1	72	Na^+	$HCO_3^- + CO_3^{2-}$	Soda	-6
									$HCO_3^- + CO_3^{2-}$		

Table 5: Regional number of the classified lakes by country

Country	Soda	Soda-saline	Saline	Total
Tanzania	20	7	3	30
Kenya	8	0	0	8
Ethiopia	9	0	1	10
Uganda	4	0	4	9
Total	41	7	8	56

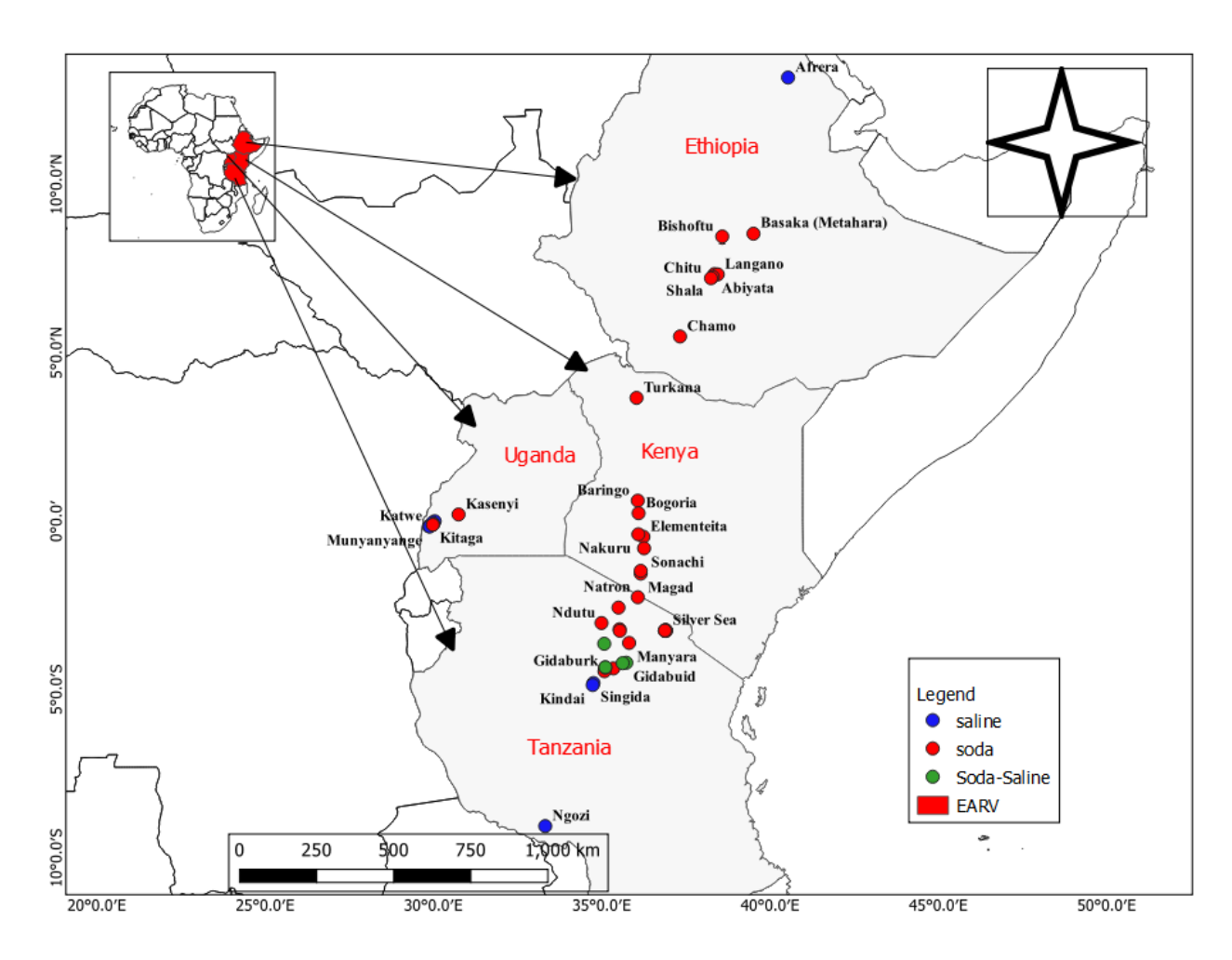


Figure 12: The water chemical type of the IASW of the EARV

4.1.3 Moran's I spatial autocorrelation analysis of Na+, Cl-, CO32-, and TDS in EARV

The Moran's I spatial autocorrelation analysis reveals that the distribution of Na⁺, Cl⁻, SO₄²⁻, HCO₃⁻ + CO₃²⁻, and TDS across the EARV shows significant spatial autocorrelation (p < 0.0001), as presented in Table 6. Na⁺, Cl⁻, and SO₄²⁻ exhibit strong clustering patterns, whereas bicarbonate/carbonate shows weaker clustering. These clustering patterns indicate non-random spatial distributions for all ions and TDS across the EARV.

Table 6: The statistical results of spatial autocorrelation with the inverse Euclidean distance method by using chemical variables

Autocorrelation	Na ⁺	Cl ⁻	$\mathrm{SO_4}^{2-}$	HCO ₃ ⁻ + CO ₃ ²⁻	TDS
Moran's Index:	0.392495	0.437955	0.470169	0.280613	0.389283
z-score:	4.714042	5.239139	5.701369	3.460942	4.675865
p-value:	p<0.0001****	p<0.0001****	p<0.0001****	0.000538***	p<0.0001****

4.1.4 The model for Spatial autocorrelation of (Cl $^-$, SO $_4^{2-}$, HCO $_3^-$ + CO $_3^{2-}$) to geological types (USGS) and soil types (DSMW).

Three valid models were obtained to explore spatial autocorrelation of anions (Cl $^-$, SO₄ $^{2-}$, HCO₃ $^{2-}$ + CO₃ $^-$) as dependent variables with geological types (USGS) and soil types (DSMW), and the results are summarized in Table 7, Table 8 and Table 9. The concentration of carbonates (HCO₃ $^{2-}$ + CO₃ $^-$) showed the most significant fixed effects in the Linear Mixed Model (LMM), with a high overall model correlation ($r^2 = 0.637$). Key predictors included a negative predictor value for distance to Pleistocene volcanoes and a positive predictor value for elevation of Holocene volcanoes. Additionally, positive predictor values were observed for categorical variables such as Chromic Cambisols, Humic Gleysols, Inceptisols, Ochric Andosols, Haplic Xerosols, and Calcic Xerosols. However, no significant fixed effects were found for geological classes. The model for SO₄ $^{2-}$ concentration was simpler, with significant fixed effects in the LMM only for the Tertiary geological class (positive predictor value) and Chromic Cambisols (negative predictor value), yielding a high overall model correlation ($r^2 = 0.805$). In the concentration of Cl $^-$, the only significant fixed effect was the distance to Holocene volcanoes, with a positive predictor value and an overall model correlation of $r^2 = 0.746$.

Table 7:The Linear Mixed Effects Model for $HCO_3^- + CO_3^{2-}$

Linear Mixed Effects Model for (HCO ₃ ⁻ + CO ₃ ²⁻)											
		Standard									
Fixed Effect Parameters	Value	Error	t-Value	Prob> t	Significance						
Intercept	-2.73006	4.12524	-0.66179	0.51498							
Elevation of Holocene volcanoes	1.97018	0.70584	2.79126	0.01064	*						
Elevation of Holocene volcanoes	0.08464	0.16139	0.52444	0.60522							
Distance of Pleistocene volcanoes	-1.42531	0.47129	-3.02429	0.00623	**						
Elevation of Pleistocene volcanoes	-0.88504	0.4492	-1.97023	0.06153							
USGSgeol=Waterbody (H2O)	-0.01601	0.75258	-0.02128	0.98321							
USGSgeol=Quaternary (Q)	-1.12546	0.91699	-1.22735	0.23266							
USGSgeol=Holocene and Pleistocene (QT)	0.44314	0.51654	0.8579	0.4002							
USGSgeol=Quaternary eolian (Qe)	0.40149	0.82698	0.48549	0.63213							
USGSgeol=Quaternary Volcanic (Qv)	-0.22248	0.59417	-0.37444	0.71166							
USGSgeol=Tertiary (T)	0.72013	0.38193	1.88549	0.07264							
USGSgeol=Tertiary Intrusive (Ti)	-1.08877	0.64308	-1.69305	0.10456							
DSMW=Chromic Cambisols (Bc)	1.26775	0.58205	2.1781	0.0404	*						
DSMW=Humic Gleysols (Gh)	1.93894	0.85629	2.26435	0.03375	*						
DSMW=Inceptsol (I)	1.45896	0.63106	2.31192	0.03053	*						
DSMW=Eutric Nitosols (Ne)	0.02106	0.54382	0.03872	0.96946							
DSMW=Humic Nitosols (Nh)	0.37503	0.82747	0.45323	0.65482							
DSMW=Dystric Regosols (Rd)	-1.35842	0.78884	-1.72206	0.09909							
DSMW=Mollic Andosols (Tm)	0.50815	0.48843	1.04037	0.30947							
DSMW=Ochric Andosol (To)	2.37727	0.98541	2.41246	0.02463	*						
DSMW=Inland water or ocean (WR)	0.72097	0.72225	0.99823	0.32902							
DSMW=Haplic Xerosols (Xh)	2.36228	0.89008	2.65402	0.0145	*						
DSMW=Calcic Xerosols (Xk)	2.13599	0.98812	2.16166	0.04179	*						
DSMW=Orthic Solonchaks (Zo)	-2.53659	1.7005	-1.49167	0.14999							
Statistics											
Number of Points	48										
Degrees of Freedom	22										
Reduced Chi-Sqr	0.20708										
Residual Sum of Squares	4.55582										
R-Value	0.91112										
Adj. R-Square	0.63711										
Intraclass Correlation	0.94969										

Table 8: The Linear Mixed Effects Model for SO_4^{2-}

Linear N	Mixed Effects		42-		
Fig. 1 Figs D	X 7 1	Standard	. 77.1	75 1 1.1	G1 101
Fixed Effect Parameters	Value	Error	t-Value	Prob> t	Significance
Intercept	-2.16722	4.27111	-0.50741	0.61691	
Elevation of Holocene volcanoes	1.15686	0.73214	1.58011	0.12835	
Elevation of Holocene volcanoes	-0.0945	0.16504	-0.57255	0.57275	
Distance of Pleistocene volcanoes	-0.38357	0.48558	-0.78991	0.43801	
Elevation of Pleistocene volcanoes	-0.44524	0.46606	-0.95534	0.34979	
USGSgeol=Waterbody (H2O)	0.03211	0.77077	0.04166	0.96715	
USGSgeol=Quaternary (Q)	-0.02585	0.9378	-0.02757	0.97826	
USGSgeol=Holocene and Pleistocene (QT)	-0.70968	0.52853	-1.34275	0.19304	
USGSgeol=Quaternary eolian (Qe)	0.10644	0.84798	0.12552	0.90125	
USGSgeol=Quaternary Volcanic (Qv)	0.1114	0.60902	0.18292	0.85653	
USGSgeol=Tertiary (T)	0.86484	0.39045	2.21501	0.03742	*
USGSgeol=Tertiary Intrusive (Ti)	0.3038	0.66123	0.45944	0.65042	
DSMW=Chromic Cambisols (Bc)	-2.06868	0.5949	-3.47733	0.00214	**
DSMW=Humic Gleysols (Gh)	1.16126	0.88034	1.3191	0.2007	
DSMW=Inceptsol (I)	1.03058	0.64745	1.59174	0.12571	
DSMW=Eutric Nitosols (Ne)	0.20963	0.55784	0.37579	0.71067	
DSMW=Humic Nitosols (Nh)	0.06852	0.84585	0.081	0.93617	
DSMW=Dystric Regosols (Rd)	-0.07034	0.80701	-0.08716	0.93133	
DSMW=Mollic Andosols (Tm)	-0.09681	0.49994	-0.19363	0.84824	
DSMW=Ochric Andosol (To)	0.47939	1.01041	0.47445	0.63985	
DSMW=Inland water or ocean (WR)	0.46622	0.74163	0.62865	0.53605	
DSMW=Haplic Xerosols (Xh)	1.15333	0.91254	1.26387	0.2195	
DSMW=Calcic Xerosols (Xk)	1.49585	1.0117	1.47856	0.15343	
DSMW=Orthic Solonchaks (Zo)	1.13448	1.76056	0.64439	0.52599	
Statistics					
Number of Points	48				
Degrees of Freedom	22				
Reduced Chi-Sqr	0.21573				
Residual Sum of Squares	4.74614				
R Value	0.95327				
Adj. R-Square	0.805				
Intraclass Correlation	0.96032				

Table 9: The Linear Mixed Effects Model Cl

Linea	Linear Mixed Effects Model for Cl-											
		Standard										
Fixed Effect Parameters	Value	Error	t-Value	Prob> t	Significance							
Intercept	-0.57164	5.01052	-0.11409	0.9102								
Elevation of Holocene volcanoes	0.76318	0.74144	1.02932	0.31451								
Elevation of Holocene volcanoes	0.37242	0.17048	2.18452	0.03987	*							
Distance of Pleistocene volcanoes	-0.43993	0.49639	-0.88625	0.38507								
Elevation of Pleistocene volcanoes	-0.2177	0.47182	-0.46141	0.64904								
USGSgeol=Waterbody (H2O)	-0.54974	0.79454	-0.6919	0.49624								
USGSgeol=Quaternary (Q)	-1.72407	0.96865	-1.77987	0.08892								
USGSgeol=Holocene and Pleistocene (QT)	-0.48575	0.54553	-0.89043	0.38287								
USGSgeol=Quaternary eolian (Qe)	-0.18033	0.87265	-0.20665	0.83819								
USGSgeol=Quaternary Volcanic (Qv)	-0.29269	0.6271	-0.46674	0.64527								
USGSgeol=Tertiary (T)	-2.99216	1.75968	-1.7004	0.10315								
USGSgeol=Tertiary Intrusive (Ti)	-0.61187	0.67788	-0.90262	0.37651								
DSMW=Ferric Acrisols (Af)	-3.20328	1.78765	-1.7919	0.08692								
DSMW=Chromic Cambisols (Bc)	-3.29145	1.85772	-1.77177	0.09028								
DSMW=Humic Gleysols (Gh)	-1.68625	2.2628	-0.74521	0.46404								
DSMW=Inceptsol (I)	-1.67521	2.01696	-0.83056	0.41514								
DSMW=Eutric Nitosols (Ne)	-2.74778	1.5744	-1.74529	0.09489								
DSMW=Humic Nitosols (Nh)	-2.76595	1.89435	-1.46011	0.15839								
DSMW=Dystric Regosols (Rd)	-2.38381	1.72233	-1.38406	0.18022								
DSMW=Mollic Andosols (Tm)	-2.98672	1.81871	-1.64222	0.11476								
DSMW=Ochric Andosol (To)	-1.95774	2.07979	-0.94131	0.35677								
DSMW=Inland water or ocean (WR)	-1.96801	1.42505	-1.38102	0.18114								
DSMW=Haplic Xerosols (Xh)	-0.35421	1.76603	-0.20057	0.84288								
DSMW=Calcic Xerosols (Xk)	-0.84512	1.961	-0.43096	0.67069								
Statistics												
Number of Points	48											
Degrees of Freedom	22											
Reduced Chi-Sqr	0.23143											
Residual Sum of Squares	5.09151											
R-Value	0.93854											
Adj. R-Square	0.74546											
Intraclass Correlation	0.94543											

4.1.5 The spatial patterns of the Na⁺, Cl⁻, HCO₃⁻ + CO₃²⁻, and TDS in EARV

Na⁺, Cl⁻, HCO₃⁻ + CO₃²⁻, and TDS concentrations in the Eastern Rift Valley exhibit a north-to-south increasing gradient, with the northernmost Afrera lake in Ethiopia and Uganda (a western branch of the Rift Valley) as exceptions Figure 13Figure 14Figure 15 Figure 16. The concentration gradient is particularly evident in lakes across northern Tanzania and southern Kenya.

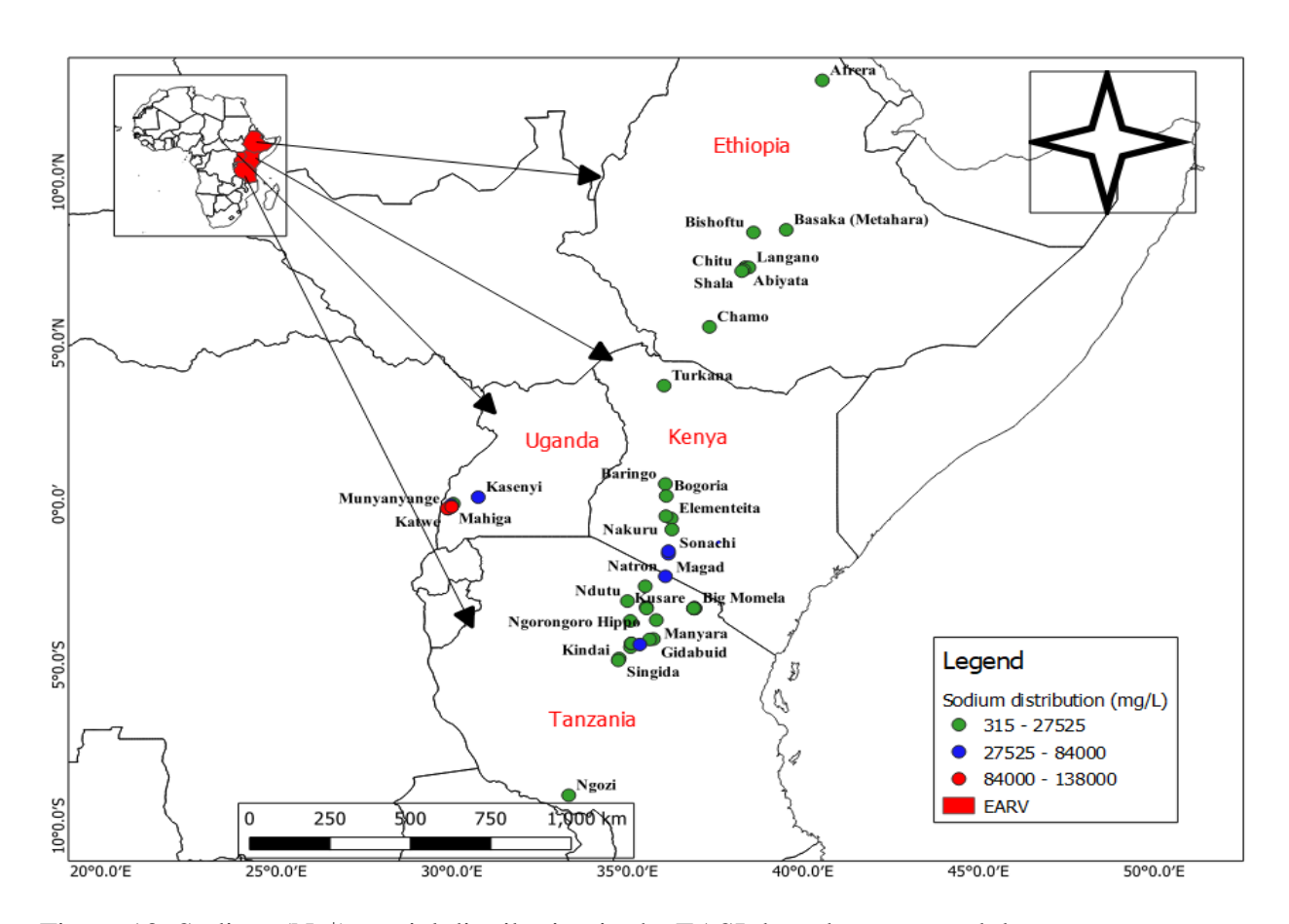


Figure 13: Sodium (Na⁺) spatial distribution in the EASL based on assessed data

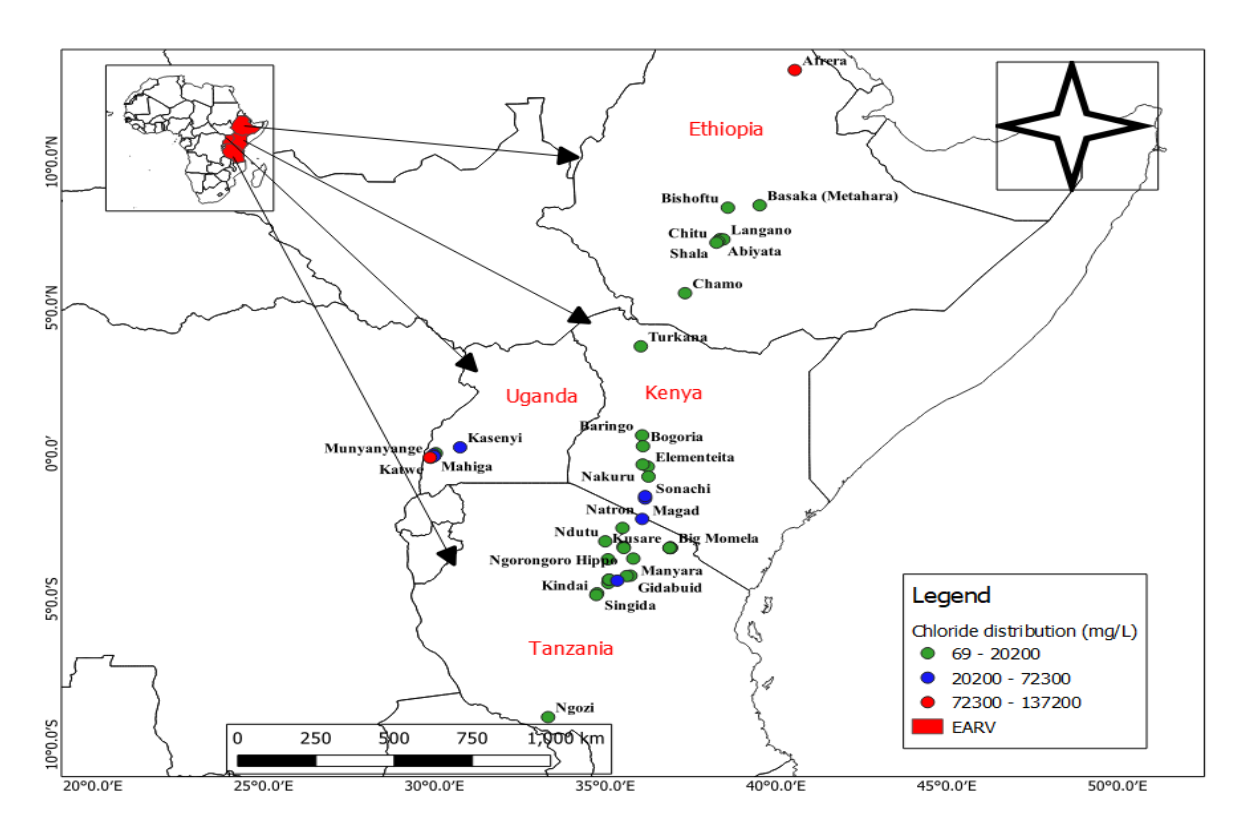


Figure 14: The spatial distributions of Cl⁻ in the EARV based on assessed data

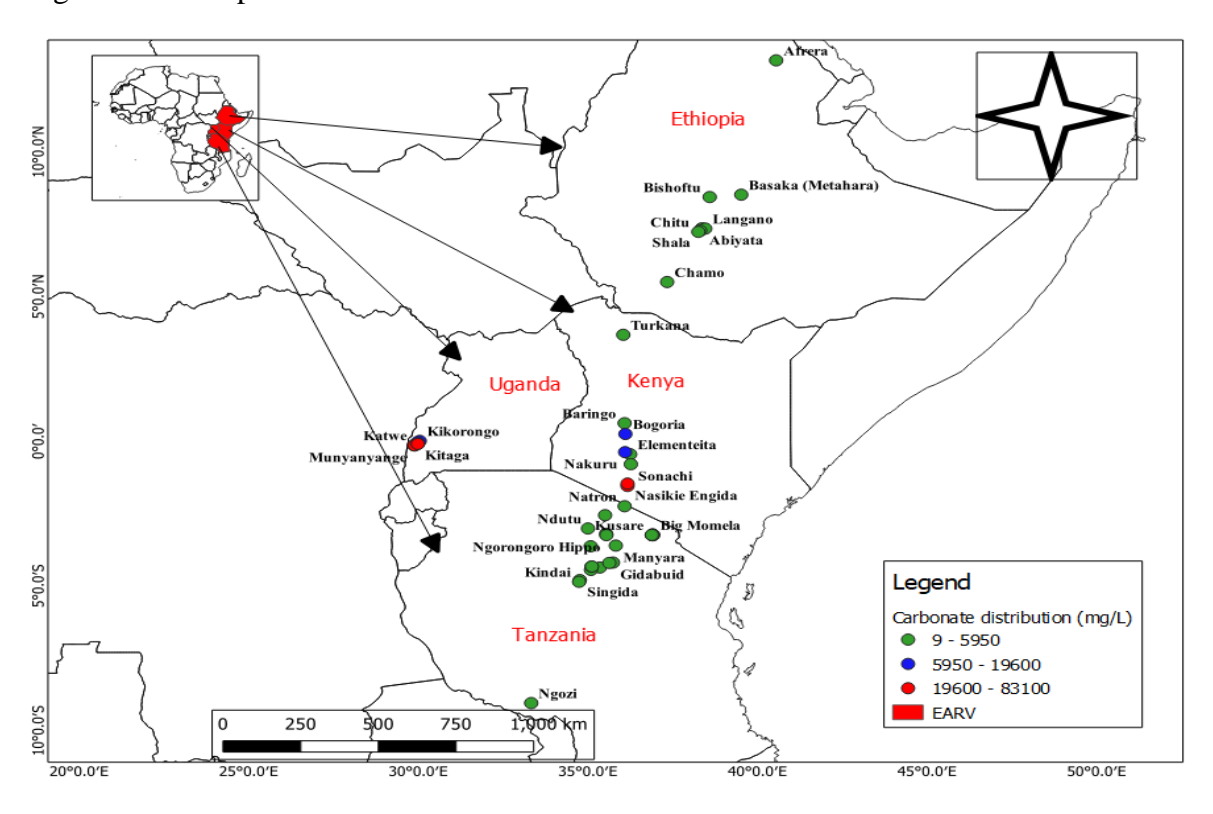


Figure 15: The spatial distributions of the estimated carbonates ($HCO_3^-+CO_3^{2-}$) in the EASL based on assessed data

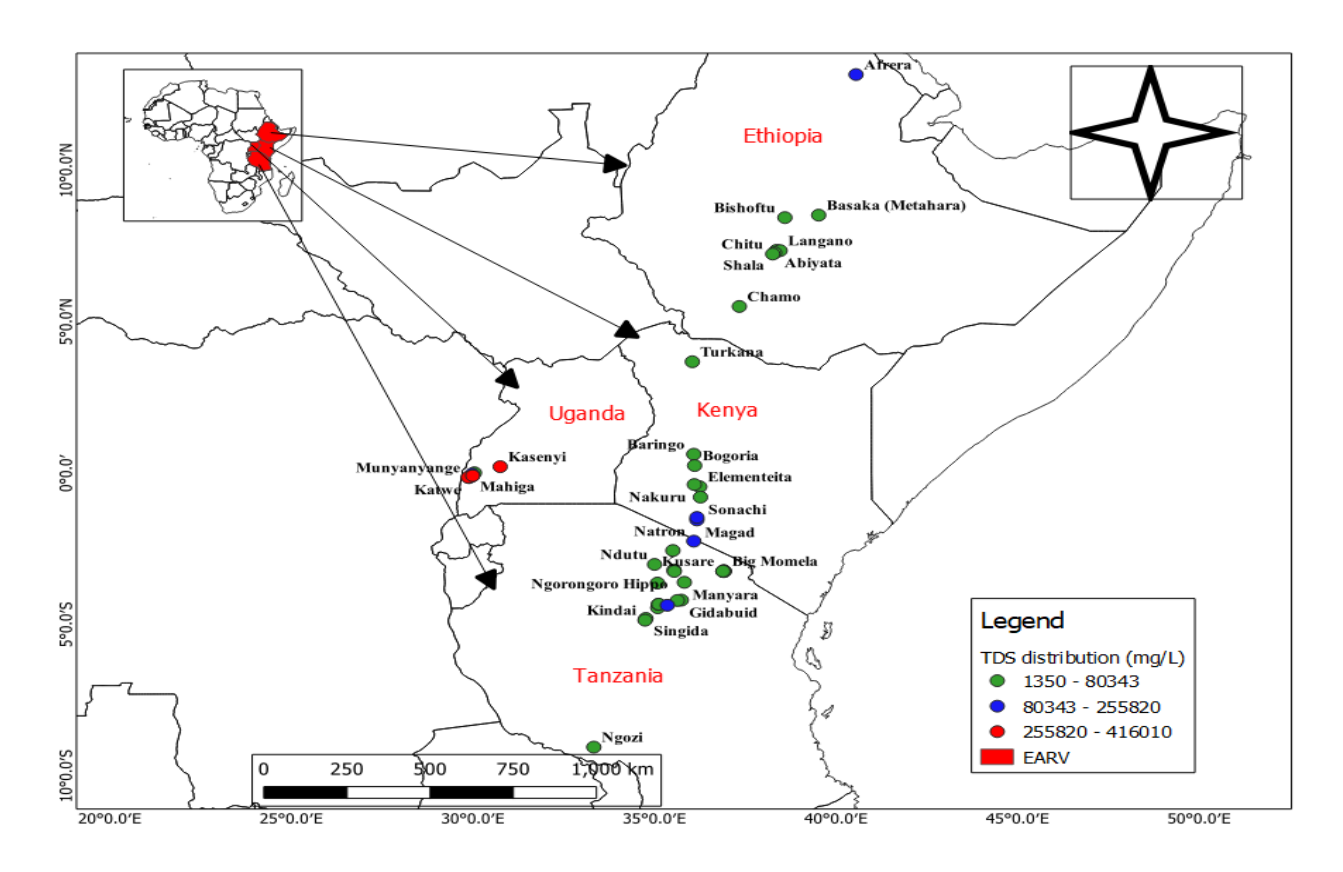


Figure 16: The spatial distributions of the estimated salinity (TDS) in the EASL are based on assessed data.

4.2 The chemical composition, classification, and geographical distributions of sodasaline lakes in ETRV.

4.2.1 Physiochemical Properties

The physiochemical properties of the examined lakes are depicted in Figure 17, and their details are given in the supplemental material (Table S1). The pH values ranged from 9.0 to 10.2, with Lake Eyasi, Natron, and Balangida having the highest pH (9.7–10.2), while Lake Kindai, Singida, Mikuyu, and Sulunga had the lowest (9.0–9.3). EC values varied between 2843 and 109,800 μ S/cm, with Lake Natron, Balangida, and Balangida Lelu having the highest EC (8032–109,800 μ S/cm), and Lake Eyasi, Mikuyu, and Sulunga having the lowest (2843–554 μ S/cm). Salinity levels ranged from 1750 to 99,400 mg/l, with Lake Eyasi, Balangida, and Balangida Lelu showing the highest values (9190–99,400 mg/l), while Lake Mikuyu, Manyara, and Sulunga had the lowest

(1750–3748 mg/l). Turbidity levels varied, with Lake Manyara having the highest (597.66 NTU), followed by Lake Sulunga (463 NTU), and Lake Kindai having the lowest (11.73 NTU). DO levels ranged from 3.44 to 7.26 mg/l, with Lake Singida having the highest (7.26 mg/l) and Lake Balangida the lowest (3.44 mg/l). Water temperature fluctuated between 26.5 and 33.7°C.

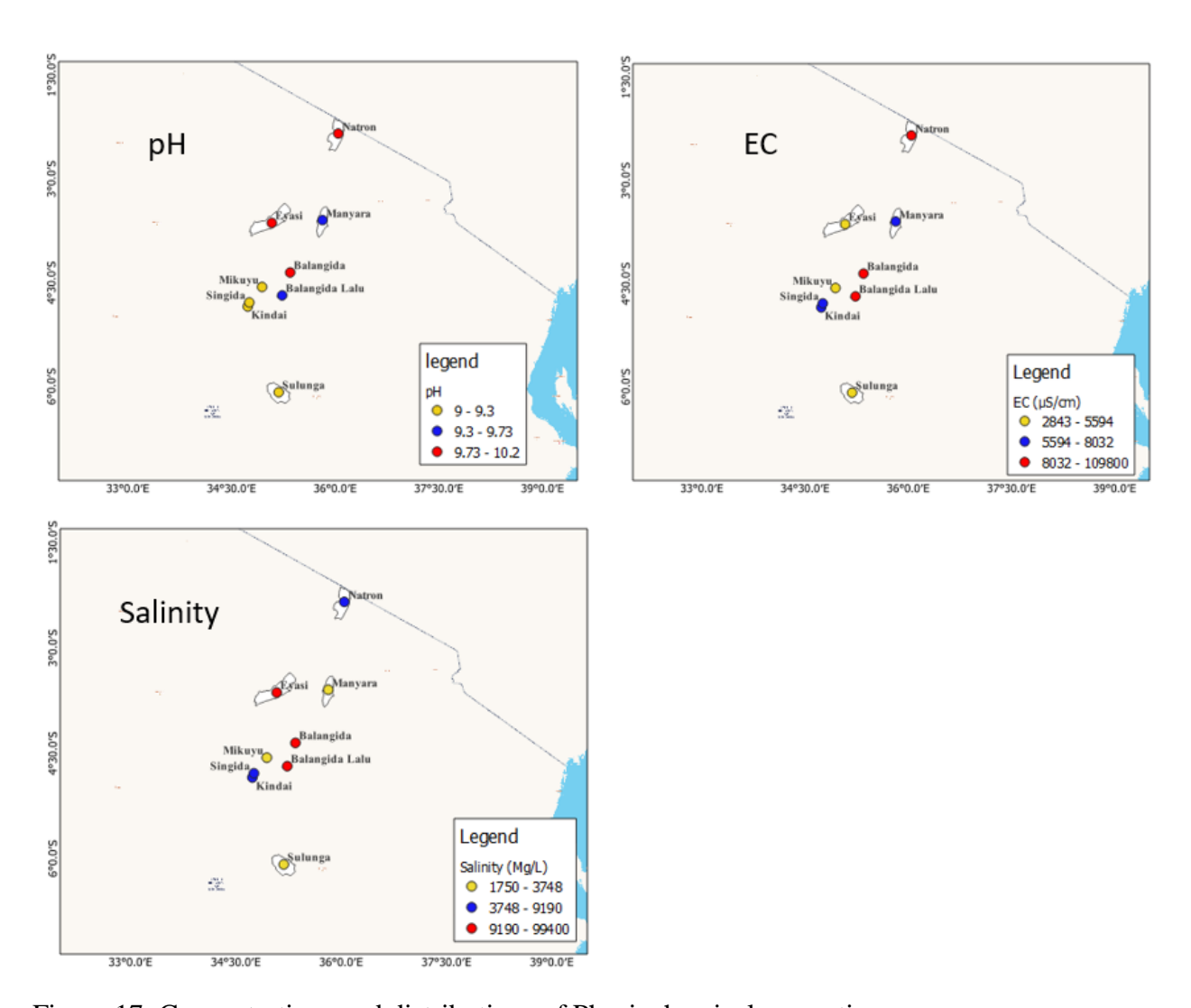


Figure 17: Concentrations and distributions of Physiochemical properties

4.2.2 Major Ions Compositions

Table S1 provides comprehensive details of the major ion concentrations, while Figure 18 and Figure 19 visually depict their corresponding distributions. Na⁺ concentrations ranged from 911 to

52,209 mg/l, with the highest values found in Lakes Balangida, Balangida Lelu, and Eyasi (6,332 to 52,209 mg/l) and the lowest in Sulunga and Mikuyu (911 to 1,780 mg/l). K⁺ concentrations ranged from 9 to 3,343 mg/l, with the highest levels in Balangida (3,343 mg/l), Balangida Lelu (1,523.3 mg/l), and Natron (215 mg/l), while Sulunga, Mikuyu, and Eyasi had the lowest (9.02-22.4 mg/l). Ca²⁺ concentrations ranged from 0.3 to 68.2 mg/l, with the highest in Kindai, Singida, and Sulunga (24.24–68.2 mg/l) and the lowest in Balangida, Balangida Lelu, Eyasi, and Natron (0.26-5.86 mg/l). Mg²⁺ concentrations ranged from 0.7 to 80.5 mg/l, with the highest values in Kindai, Singida, and Balangida Lelu (42.91–80.48 mg/l), and the lowest in Natron, Eyasi, and Balangida (0.65–5.1 mg/l). HCO₃⁻ concentrations ranged from 399 to 45,021 mg/l, with the highest values in Balangida, Balangida Lelu, and Eyasi (4,232–45,021 mg/l), and lowest values in Singida, Kindai, and Sulunga (299–564 mg/l). CO₃²⁻ concentrations ranged from 6.1 to 15,618.5 mg/l, with the highest levels in Balangida, Balangida Lelu, and Natron (1,213.1–25,618.4 mg/l), and lowest in Singida, Kindai, and Sulunga (6.1–14.1 mg/l). Cl⁻ concentrations ranged from 996 to 34,738 mg/l, with the highest in Balangida, Balangida Lelu, and Evasi (4,118–34,738 mg/l), and lowest in Sulunga, Manyara, and Mikuyu (996–2,044 mg/l). SO_4^{2-} concentrations ranged from 82 to 247,917 mg/l, with highest levels in Balangida, Balangida Lelu, and Eyasi (1,861–247,917 mg/l), and lowest in Kindai, Singida, and Sulunga (82–149 mg/l).

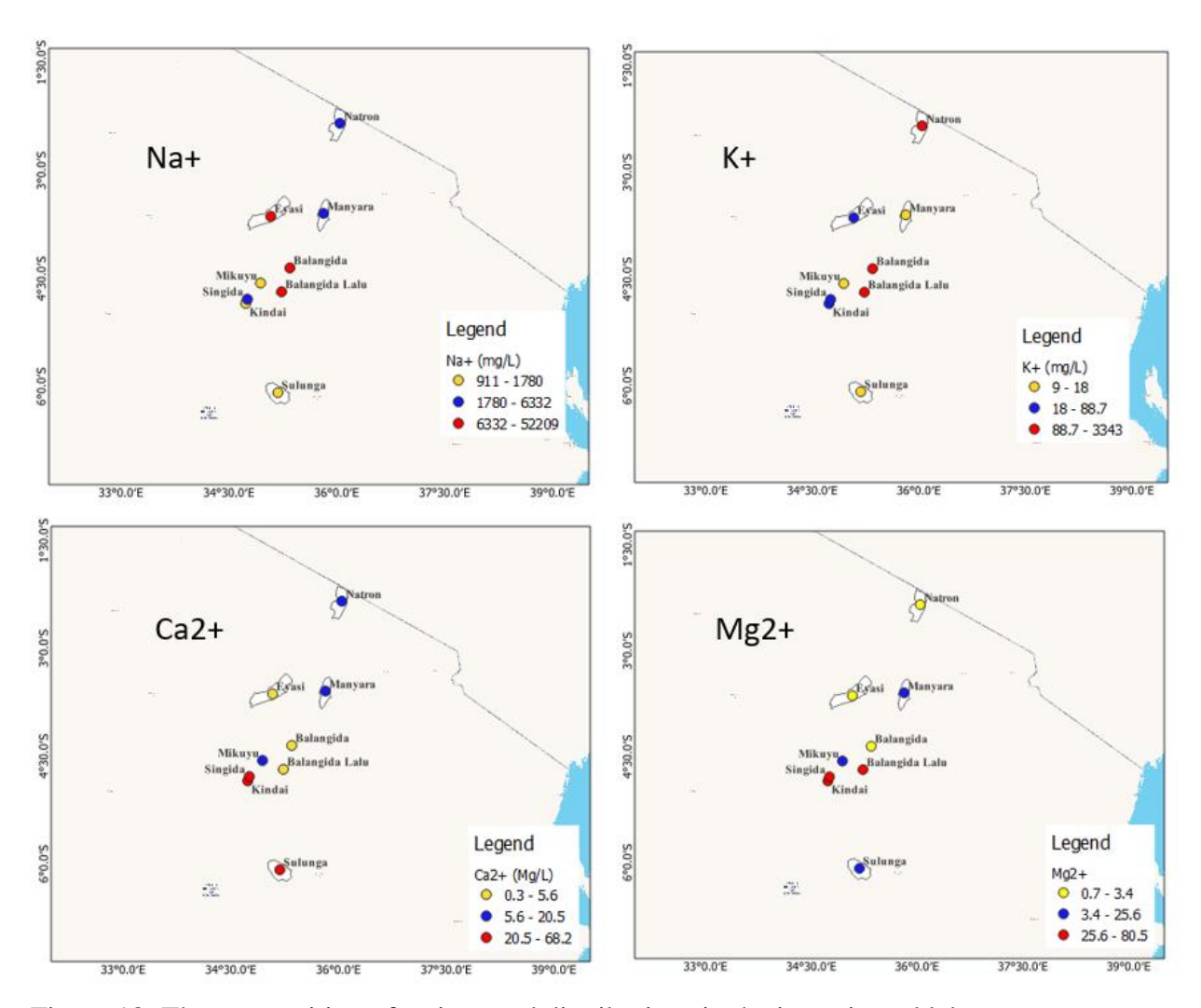


Figure 18: The composition of cations and distributions in the investigated lakes

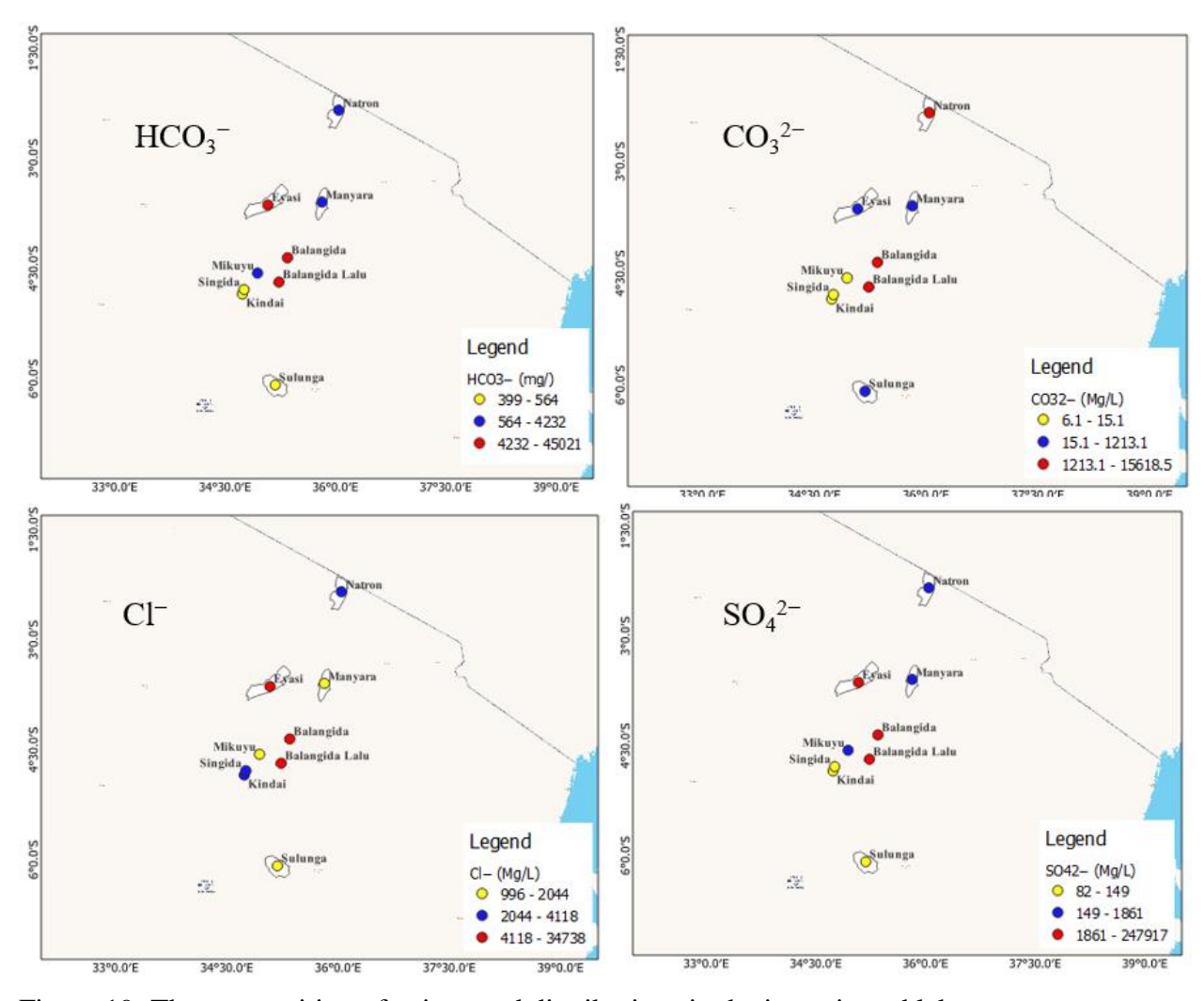


Figure 19: The composition of anions and distributions in the investigated lakes

4.2.3 Spearman Correlations

Table 10 presents the Spearman correlation results of the ETRV lake. A significant positive correlation was found between pH and both salinity (r = 0.69) and TDS (r = 0.77) at p < 0.05. Additionally, TDS and salinity were strongly correlated (r = 0.983; p < 0.01). Na+ showed positive correlations with TDS (r = 0.98), SO₄²⁻ (r = 0.93), salinity (r = 0.95), HCO₃⁻ (r = 0.85), CO₃²⁻ (r = 0.85), Cl⁻ (r = 0.88), and pH (r = 0.82) at p < 0.01. It also correlated positively with K⁺ (r = 0.767) at p < 0.05 and negatively with Ca²⁺ (r = -0.867) and Mg²⁺ (r = -0.433) at p < 0.01. K⁺ positively correlated with Cl⁻ (r = 0.833), TDS (r = 0.800), salinity (r = 0.867), and EC (r = 0.750) at p < 0.05, but negatively with Ca²⁺ (r = -0.567) and Mg²⁺ (r = -0.167). Ca²⁺ and Mg²⁺ showed negative correlations with other variables at both p < 0.05 and p < 0.01. HCO₃⁻ was positively

correlated with $CO_3^{2^-}$ (r = 0.91), $SO_4^{2^-}$ (r = 0.91), and pH (r = 0.81) at p < 0.01, and with Cl^- (r = 0.700), TDS (r = 0.783), and salinity (r = 0.73) at p < 0.05. $CO_3^{2^-}$ also positively correlated with $SO_4^{2^-}$ (r = 0.81), pH (r = 0.89), TDS (r = 0.75), and salinity (r = 0.68) at p < 0.01. $SO_4^{2^-}$ showed positive correlations with TDS (r = 0.90) and salinity (r = 0.85) at p < 0.01. Cl^- exhibited strong positive correlations with $SO_4^{2^-}$ (r = 0.85), TDS (r = 0.83), and salinity (r = 0.96) at p < 0.01.

Table 10: The Spearman correlations of the physiochemical variables of the investigated lakes (** represent significant correlation at p < 0.01, * represent significant correlation at p < 0.05)

	Na ⁺	K ⁺	Ca ²⁺	Mg^{2+}	HCO ₃ ⁻	CO ₃ ²⁻	Cl ⁻	SO ₄ ²⁻	pН	TDS	EC	salinity
Na ⁺	1.000					•	•	•	•			
K^+	.767*	1.000										
Ca^{2+}	867**	-0.567	1.000									
Mg^{2+}	-0.433	-0.167	0.633	1.000								
HCO_3^-	.850**	0.600	983**	-0.617	1.000							
$\mathrm{CO_3}^{2-}$.800**	0.617	933**	767*	.917**	1.000						
Cl^-	.883**	.833**	717*	-0.183	$.700^{*}$	0.617	1.000					
SO_4^{2-}	.933**	0.617	933**	-0.450	.917**	.817**	.850**	1.000				
pН	.820**	0.477	854**	820**	.812**	.895**	0.586	.795*	1.000			
TDS	.983**	.800**	817**	-0.367	.783*	$.750^{*}$.933**	.900**	.778*	1.000		
EC	0.600	$.750^{*}$	-0.400	0.067	0.383	0.467	0.617	0.500	0.393	0.633	1.000	
salinity	.950**	.867**	750*	-0.283	.733*	.683*	.967**	.850**	.695*	.983**	0.650	1.000

4.2.4 Saturation Indices (SI)

The saturation indices (SI) of the lake's mineral phases were computed using the PHREEQC Geochemical Model (Parkhurst. & Appelo, 1999). The results of this computation are reported in Table S3 and Figure 20 (a)—(d). The results revealed that the lakes are oversaturated with dolomite, calcite, goethite, hematite, manganite, aragonite (except lake Balangida), chrysolite (except lake Natron), pyrochroite (except lake Balangida Lelu and Natron), pyrolusite (except lake Natron), and sepiolite (except lake Balangida Lalu and Natron). Based on the results, it appears that the lakes contain high amounts of these minerals in their water. This discovery has important implications for the overall well-being of the lake's ecosystem and the potential opportunities for mining or extracting minerals in the area. Additionally, the lakes were found to be undersaturated with respect to anhydrite, chalcedony, celestite (except for Lake Balangida Lalu), gypsum, halite

(except for Lake Eyasi), Jarosite-K, melanterite, quartz, rhodochrosite (except for lake Natron), siderite, sylvite, and vivianite minerals. The undersaturation of these mineral phases in the lakes suggests that they can dissolve more of these minerals, which might alter the overall mineral composition of the water over time.

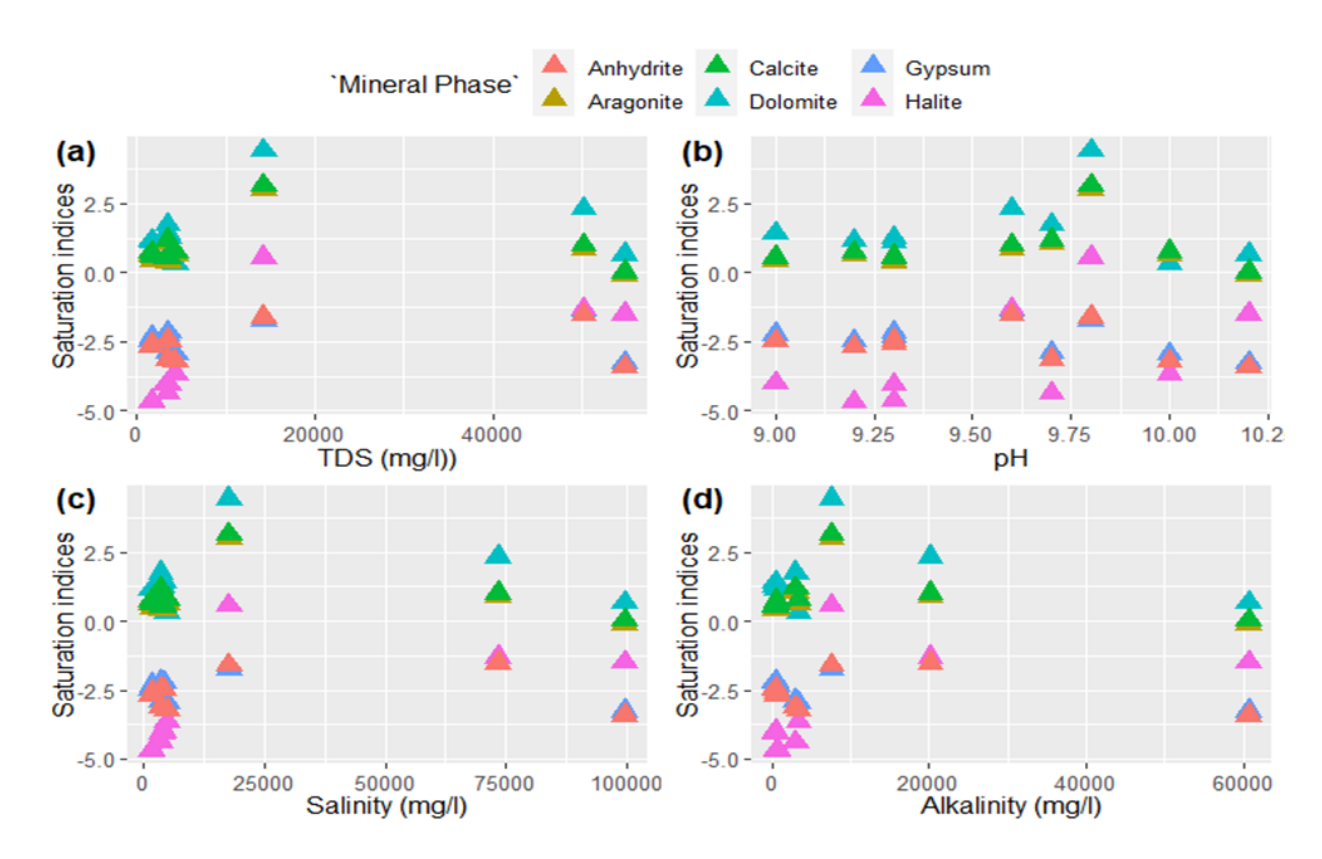


Figure 20: The plots of the mineral saturation indices (anhydrite, calcite, gypsum, aragonite, dolomite and halite) against (a) TDS, (b) pH, (c) salinity, and (d) alkalinity.

4.2.5 Hydrochemical Characteristics

The ETRV lakes demonstrate notable variations in the hydrochemical type, as seen in Figure 21. Lakes Natron and Manyara exhibit a Na-K-HCO₃ composition, while Lakes Balangida and Balangida Lalu are of the Na-SO₄ type. Lakes Sulunga, Kindai, Singidani, Mikuyu, and Eyasi are characterized by a Na-Cl type.

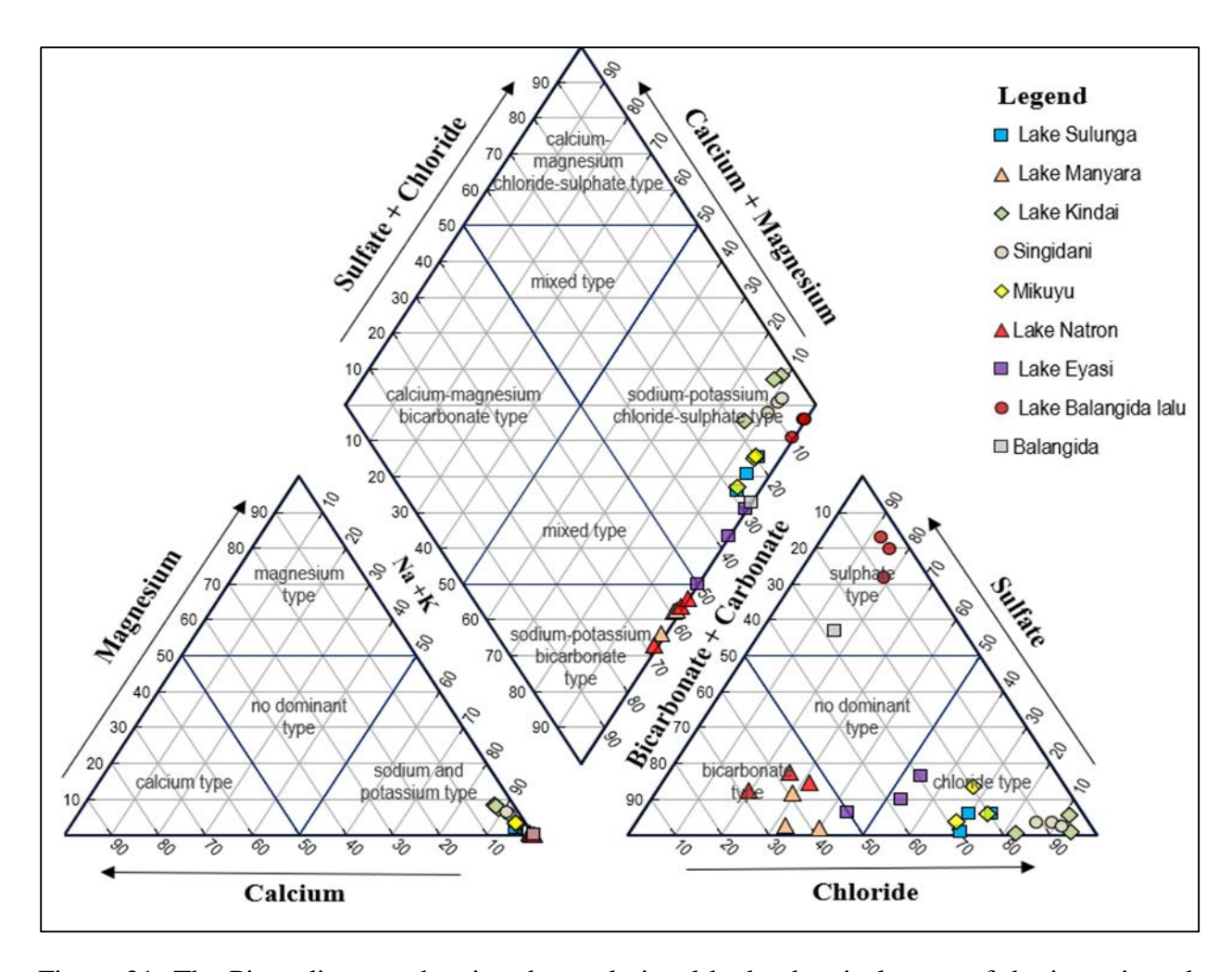


Figure 21: The Piper diagram showing the evolutional hydrochemical types of the investigated lake

4.2.6 Water chemical classification of the IASW of ETRV

Water chemical type of the of the IASW of the ETRV and percentage equivalents of the dominance of the major ions are detailed in Table 11 and Table 12 respectively. Na⁺ was the most abundant ion in all lakes, contributing more than 87% of the total cation composition. HCO₃⁻ + CO₃²⁻ dominated the anionic composition in Lake Natron and Manyara, accounting for over 50%. SO₄²⁻ was the dominant anion in Lake Balangida Lelu and Balangida, while Cl⁻ comprised about 50% of the anionic composition in Lake Kindai, Singida, Mikuyu, Eyasi, and Sulunga. Based on the classification system by Boros & Kolpakova, (2018), Lake Natron and Manyara are categorized as soda types, Lake Balangida and Eyasi as soda-saline types, and Lakes Singidani, Kindai, Mikuyu, Balangida Lalu, and Sulunga as saline types.

Table 11: The calculated equivalent percentages of the investigated lakes

	Percentage equivalent						
Lakes	Na ⁺	K ⁺	Ca ²⁺	Mg^{2+}	$HCO_3^- + CO_3^{2-}$	Cl-	SO ₄ ²⁻
Kindai	87.12	0.79	4.11	7.99	8.85	89.00	2.15
Singidani	91.19	0.58	2.41	5.81	8.01	89.08	2.92
Mikuyu	94.04	0.54	2.17	3.25	22.45	69.88	7.67
Balangida Lalu	97.64	2.16	0.01	0.20	5.49	15.19	79.32
Balangida	99.99	0.00	0.00	0.01	27.42	15.86	56.72
Eyasi	99.75	0.14	0.06	0.04	37.12	51.44	11.44
Natron	97.33	2.51	0.13	0.02	53.85	31.48	14.67
Manyara	98.57	0.32	0.76	0.35	60.48	33.98	5.54
Sulunga	94.43	0.84	2.88	1.85	23.59	72.09	4.33

Table 12: The dominance trend of the ionic concentrations and water chemical types of the ETRV lakes.

	Dominan		
lakes	Cations	Anions	Water chemical types
Kindai	$Na^{+}>Mg^{2+}>Ca^{2+}>K^{+}$	Cl ⁻ > HCO ₃ ⁻ + CO ₃ ²⁻ > SO ₄ ²⁻	Saline
Singidani	$Na^{+}>Mg^{2+}>Ca^{2+}>K^{+}$	$Cl^-> HCO_3^- + CO_3^2 -> SO_4^{2-}$	Saline
Mikuyu	$Na^{+}>Mg^{2+}\sim Ca^{2+}>K^{+}$	$Cl^-> HCO_3^- + CO_3^2 -> SO_4^{2-}$	Saline
Balangida Lalu	$Na^+>K^+>Mg^{2+}\sim Ca^{2+}$	SO ₄ ² ->Cl ⁻ > HCO ₃ ⁻ + CO ₃ ² -	Saline
Balangida	$Na^{+}>K^{+}\sim Mg^{2+}\sim Ca^{2+}$	$SO_4^2 > HCO_3^- + CO_3^2 > Cl^-$	Soda-saline
Eyasi	$Na^{+}>K^{+}\sim Mg^{2+}\sim Ca^{2+}$	$Cl^-> HCO_3^- + CO_3^2 -> SO_4^{2-}$	Soda-saline
Natron	$Na^+>K^+>Mg^{2+}\sim Ca^{2+}$	$HCO_3^- + CO_3^2 -> Cl^- > SO_4^{2-}$	Soda
Manyara	$Na^{+}>K^{+}\sim Mg^{2+}\sim Ca^{2+}$	$HCO_3^- + CO_3^{2-} > Cl^- > SO_4^{2-}$	Soda
Sulunga	$Na^{+}>Ca^{2+}>Mg^{2+}>K^{+}$	Cl ⁻ > HCO ₃ ⁻ + CO ₃ ² -> SO ₄ ² -	Saline

4.2.7 Geographical distributions of the IASW in ETRV

Figure 22 depicts the spatial geographical distribution of the soda-saline lakes in the eastern Tanzania rift valley. The study revealed a decreasing tendency in the soda-saline nature from the northern to the central part of the country. The soda-type and soda-saline lakes are most common in northern Tanzania, particularly in Arusha and Manyara. On the other hand, saline-type lakes are

common in the central part of the country, particularly in the Singida and Dodoma regions. Variations in geological settings, geographical features, and volcanic activity are believed to have an impact on the observed decrease in soda-saline properties from the northern to the central parts of the country. The geological features in the study area are depicted in Figure 23, and the figure demonstrates the dominance of the volcanic nature in northern Tanzania (Arusha and Manyara regions) as compared to the central part of Tanzania (Singida and Dodoma regions).

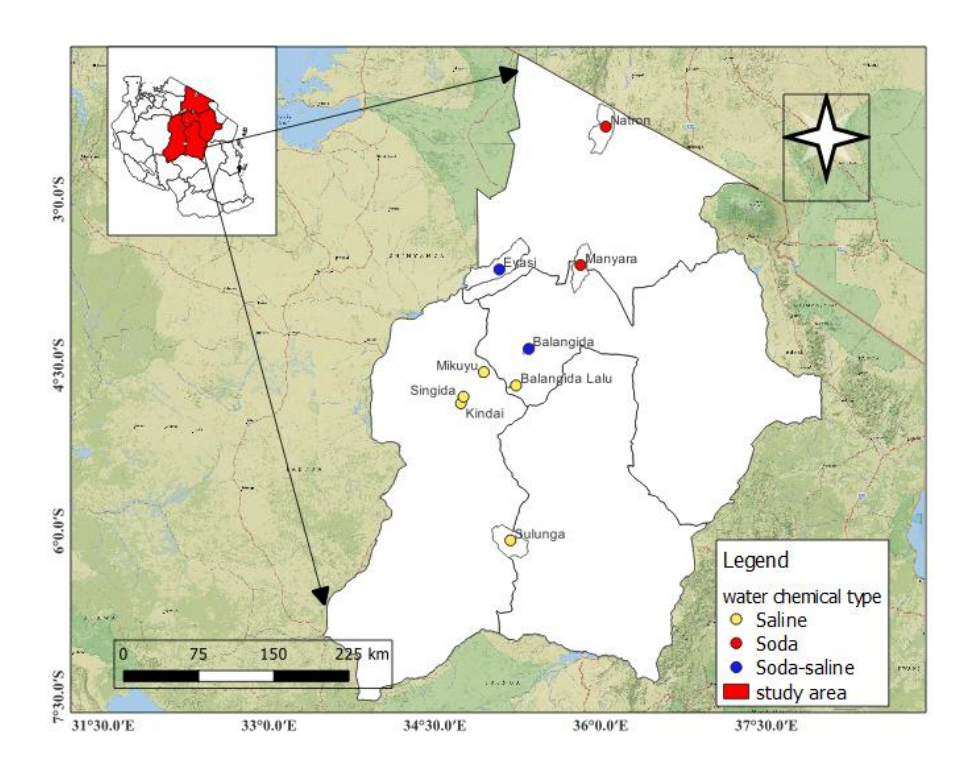


Figure 22: The geographical distributions of the Soda-saline lakes in ETRV

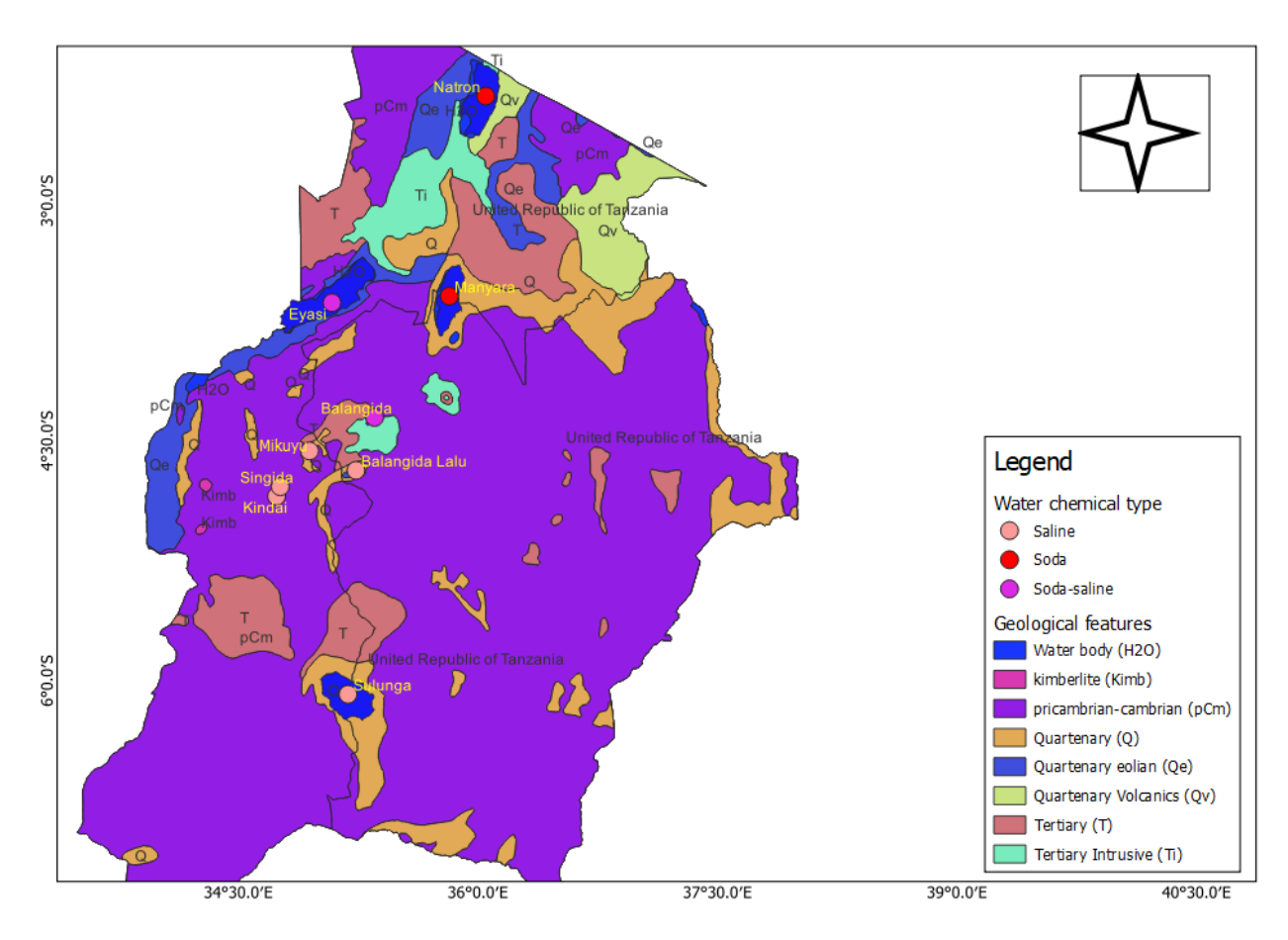


Figure 23: The geological features surrounding the IASW in the ETRV

4.3 Influence of environmental variables and anthropogenic activities on soda-saline lake chemistry in Northern Tanzania: A Remote Sensing and GIS-based approach.

4.3.1 Validation of CHIRPS and MERRA-2 data

Figure 24 presents the validation results for CHIRPS (precipitation) data and MERRA-2 (temperature) data against the station data. The results showed an RMSE of 0.94 ($R^2 = 0.54$) for the station-recorded temperature data and MERRA-2 temperature data, and an RMSE of 65.52 ($R^2 = 0.53$) for station-observed precipitation and CHIRPS data. The results suggest that the satellite-based MERRA-2 temperature data and CHIRPS precipitation data retrieved from the established stations are reliable and suitable for use in drought-related studies.

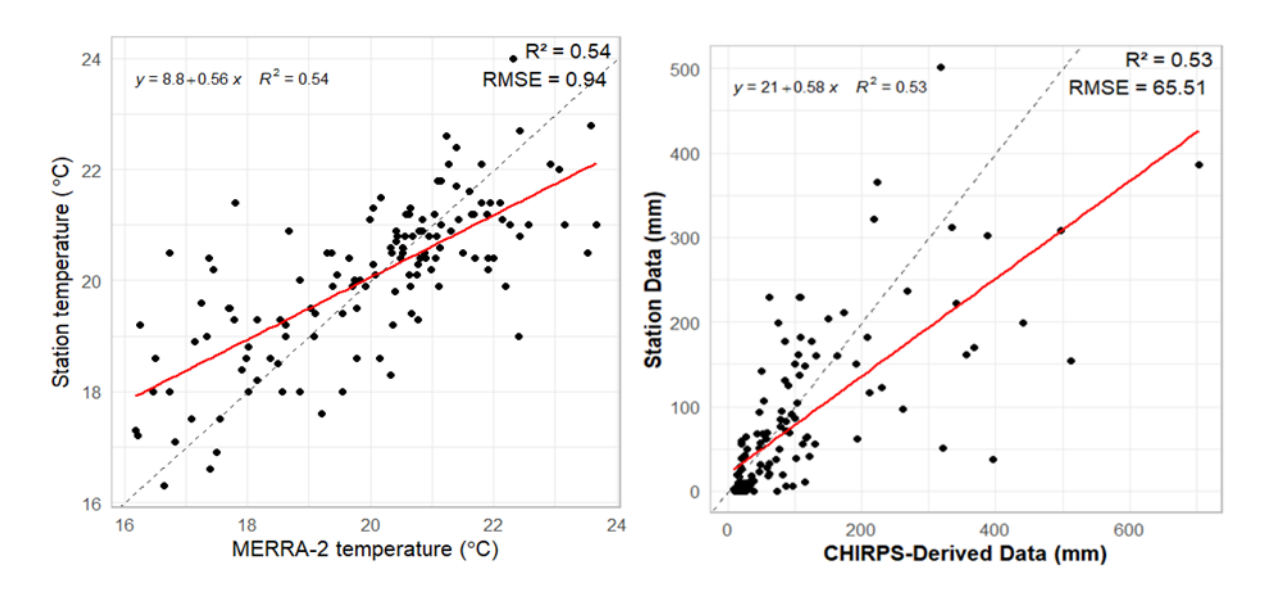


Figure 24: (a) Station temperature versus MERRA-2 temperature data (b) observed precipitation versus CHIRPS data

4.3.2 Climate Variability

Figure 25 (a–f) displays the satellite-derived data on rainfall and temperature in the catchments of the three soda-saline lakes (Manyara, Natron, and Eyasi) in Northern Tanzania, covering the period from 1981 to 2022. The results show similar trends in temperature and precipitation across the catchments of these lakes, with small variations among them. Rainfall occurs from late October to May, with the highest rainfall observed during the fall season (March-May) and the least rainfall in November through February. These months indicate a well-defined wet season in Northern Tanzania, consistent with previous studies (Borhara et al., 2020; Mwabumba et al., 2022)(Borhara et al., 2020; Mwabumba et al., 2022). Temperature data reveals maximum temperatures ranging from 25-35°C, peaking in January, February, March, September, and October. Minimum temperatures range from 6-17°C during June and July. The temperature distribution aligns with previous findings by Mwabumba et al., (2022).

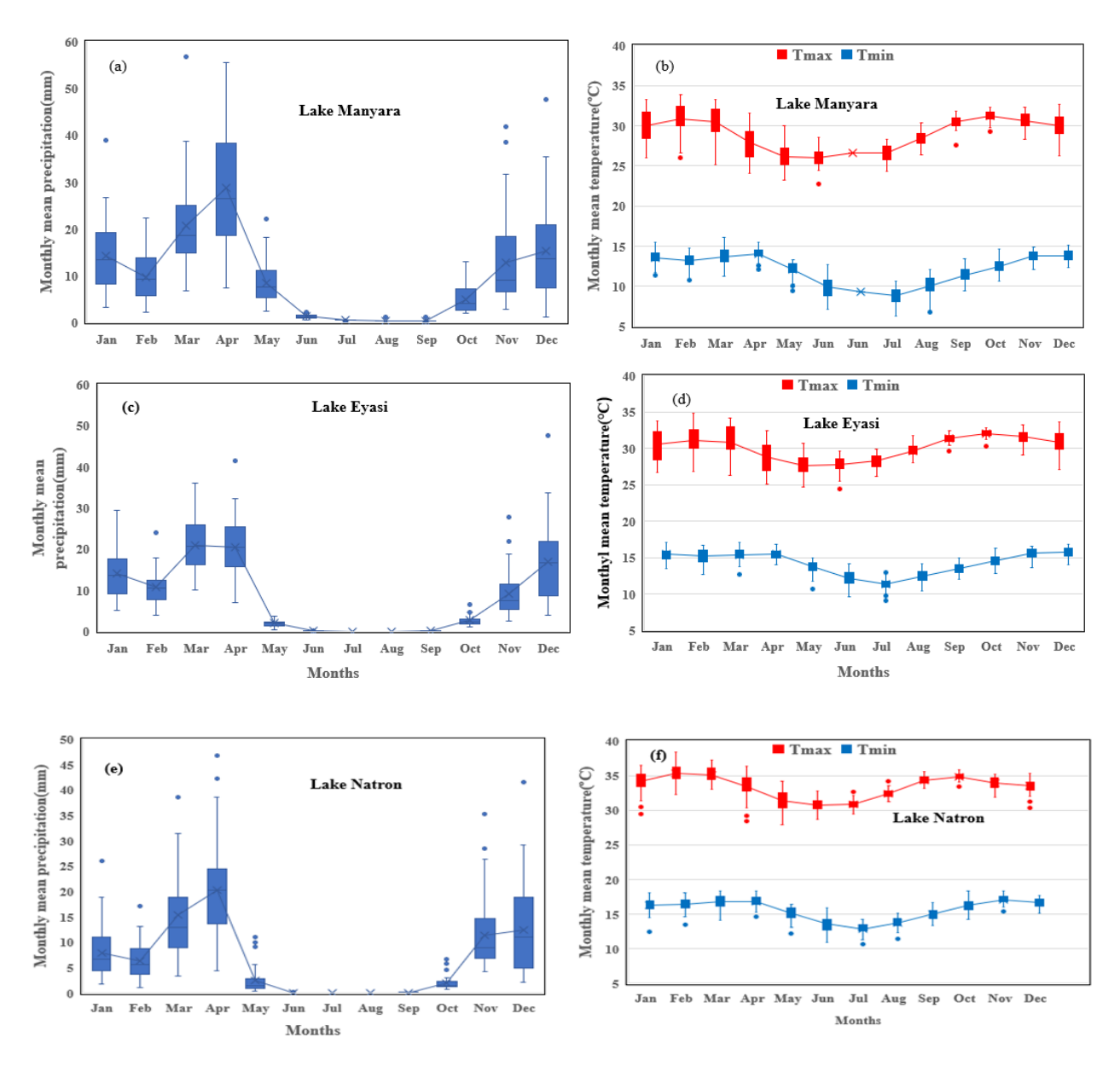
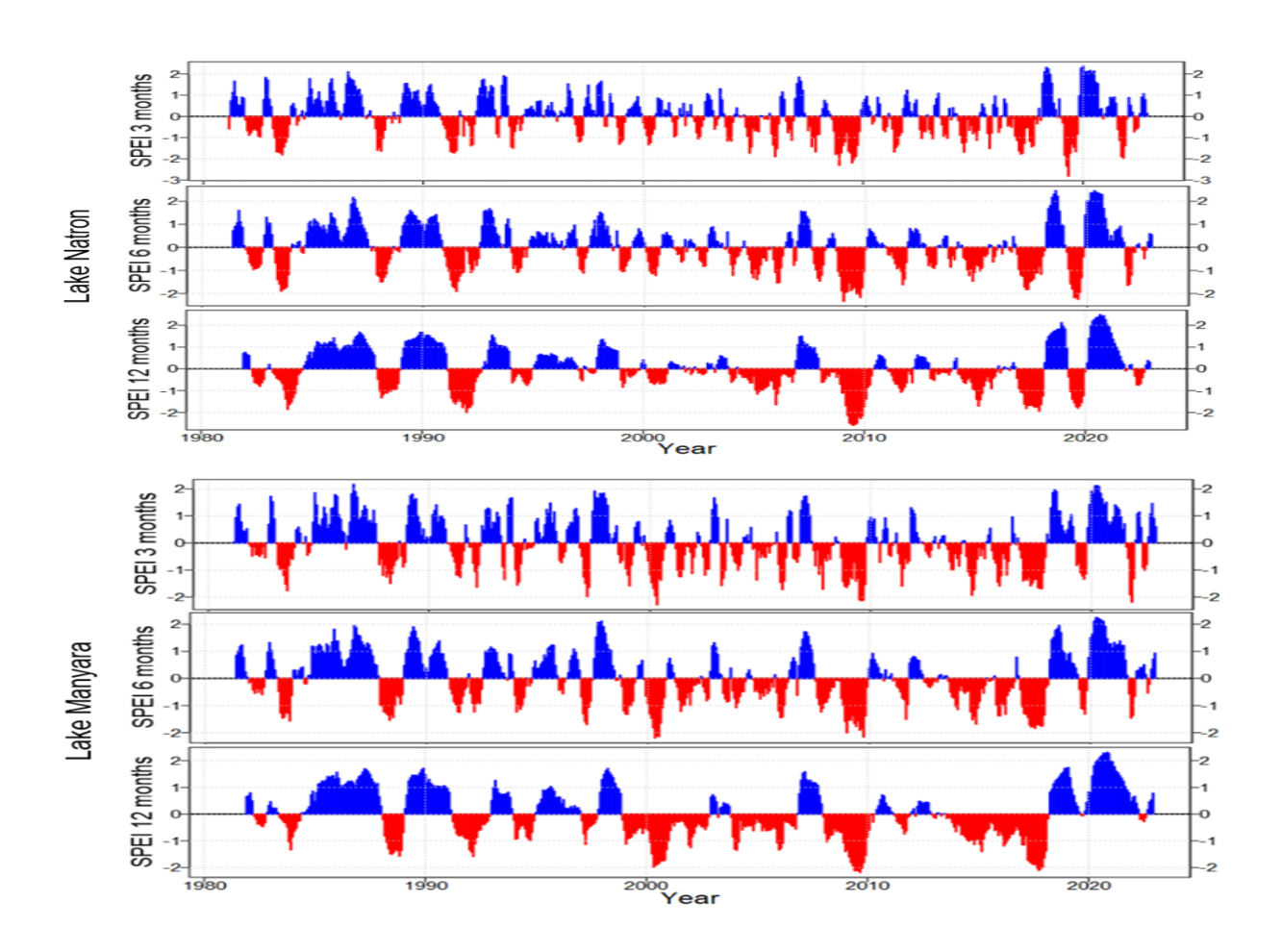


Figure 25: The average monthly precipitation (mm) and temperatures (°C) for Lake Manyara (a and b), Lake Eyasi (c and d), and Lake Natron (e and f), respectively.

4.3.3 Drought Analysis

displays the temporal sequence of the SPEI at 3-month, 6-month, and 12-month intervals. The SPEI values were computed using a dataset spanning 40 years of rainfall and temperature data in three lake basins (Natron, Manyara and Eyasi). The SPEI values were used to analyze the spatial and temporal patterns of drought in the study area. The SPEI curves indicate both dry and wet

events, with negative values (red) signifying drought years and positive values (blue) indicating years with sufficient water conditions. The 3-month SPEI showed a higher frequency of short-term dry and wet events but did not reveal major drought occurrences or long-term trends. In contrast, the 6-month and 12-month periods provided a more appropriate scale (Polong et al., 2019) for analyzing significant drought events, as they helped identify long-term drought patterns. The results show that drought intensities in all lake basins increased over time, with notable drought events observed from 1987-1992, 2000-2010, and 2012-2017. Additionally, the drought analysis demonstrated that the lake basins under investigation experienced an extended drought from 2012 to 2017.



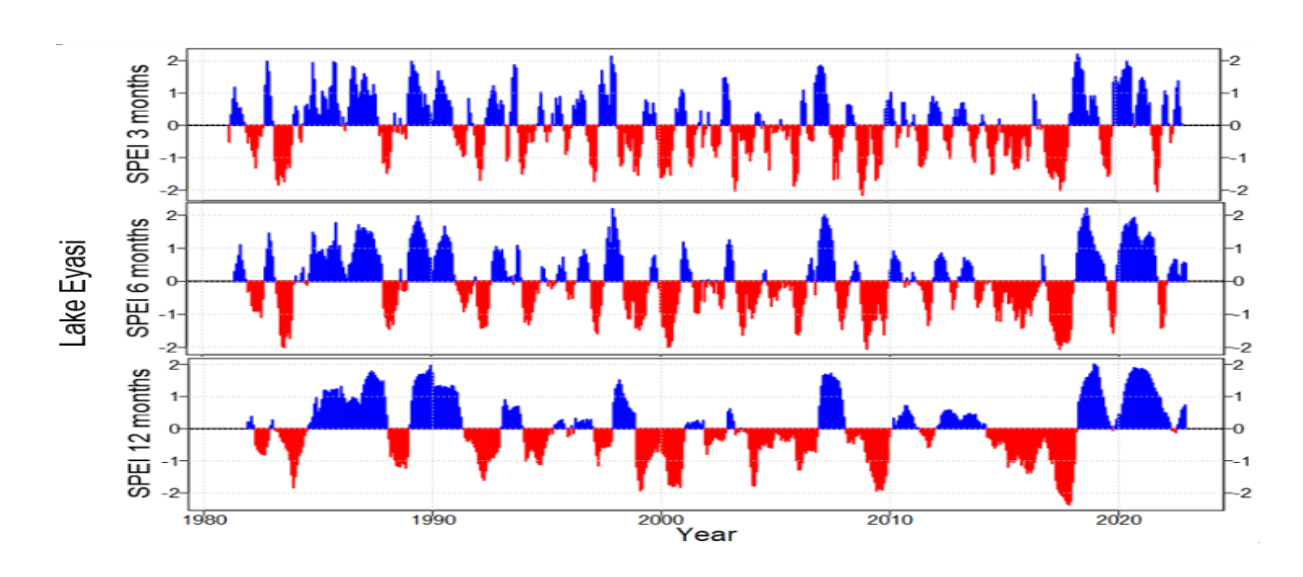


Figure 26: The evolution of the SPEI for 3, 6, and 12-month timescale in Lake Manyara, Lake Natron, and Lake Eyasi basin showing the variation in the duration, severity, and intensity of dry and wet events

4.3.4 Soil Types Classification

Figure 27 illustrates the reference soil types observed around the soda-saline lakes in Northern Tanzania with their key chemical characteristics detailed in Table 13. The soil types identified include ferric acrisols (Af), chromic cambisols (Bc), calcic cambisols (Bk), entisols (E), inceptisols (I), eutric fluvisols (Je), distric nitisols (Nd), humic nitisols (Nh), mollic andosols (Tm), ochric andosols (To), and pellic vertisols (Vp). Each soil type is derived from a distinct parent rock material and has unique chemical properties. These different soil types can significantly impact the chemistry of the adjacent soda-saline lakes.

Ferric acrisols were found near Lake Eyasi, suggesting clayey soils with high iron content (Lyu et al., 2018) and formed due to extensive chemical weathering and are commonly found in tropical regions (Domínguez-rodrigo et al., 2007). Pellic vertisols were predominantly observed in the western region of Lake Natron, with a neutral to slightly alkaline pH and lime accumulation(Pierre *et al.*, 2015; Orzechowski *et al.*, 2020) high base saturation, and moderate to low organic content, and, generating deep cracks during the dry season (Pierre *et al.*, 2015; Orzechowski *et al.*, 2020). Entisols, which were widely spread near Mount Hanang, are young soils with minimal horizon development (Singh and Chandran, 2017), while inceptisols, which were dominant around Lake

Natron and between Lakes Manyara and Eyasi, exhibit slight horizon development (Singh and Chandran, 2017). Eutric fluvisols, identified in lowland areas around Lakes Manyara and Eyasi, are formed by the deposition of alluvial sediments (Asongwe et al., 2020; Šimanský, 2018). Fluvisols (depending on the sediment source), have a neutral to alkaline pH, high organic matter and nutritional content, and significant levels of pyrite in the subsoil (Šimanský, 2018). Cambisols, including chromic and calcic variants, were observed in the western regions of Lake Natron and Eyasi and parts of Lake Manyara. Chromic cambisols have a neutral to mildly acidic response, whereas calcic cambisols are alkaline (ISRIC, 2014). Mollic andosols and ochric andosols, associated with volcanic activity, were observed near Lake Natron, Manyara, and Ngorongoro. This is evidenced by the occurrence of lavas, ash, tuffs, pumice, and other volcanic ejecta in the region (Deocampo, 2004; Scoon, 2020). Nitisols, including humic and distric types, were found across the Ngorongoro crater and in the area between Lake Manyara and Eyasi. The presence of andosols in the study area is consistent with their widespread distribution throughout Africa's rift systems (ISRIC, 2016; Ring et al., 2014; Sisay et al., 2024). These soils originate from volcanic ash and other materials expelled by volcanoes. They are distinguished by the presence of allophanes, imogolite, and ferrihydrite (ISRIC, 2016). Andosols are abundant along the East African Rift Valley due to volcanic activity in the area (Ring et al., 2014; Sisay et al., 2024). The occurrence of andosols also indicates a history of violent volcanic eruptions in the area, resulting in the deposition of volcanic elements throughout time. Furthermore, we identified the existence of severely weathered basaltic volcanic deposits (Nitisols) in the area. Humic nitisols are frequently observed across the Ngorongoro crater and have a significant impact on the alkalinity of Lake Magadi (Deocampo, 2004). Distric nitisols are extensively distributed in the area between Lake Manyara and Eyasi, as well as in the Katesh area of Mount Hanang.

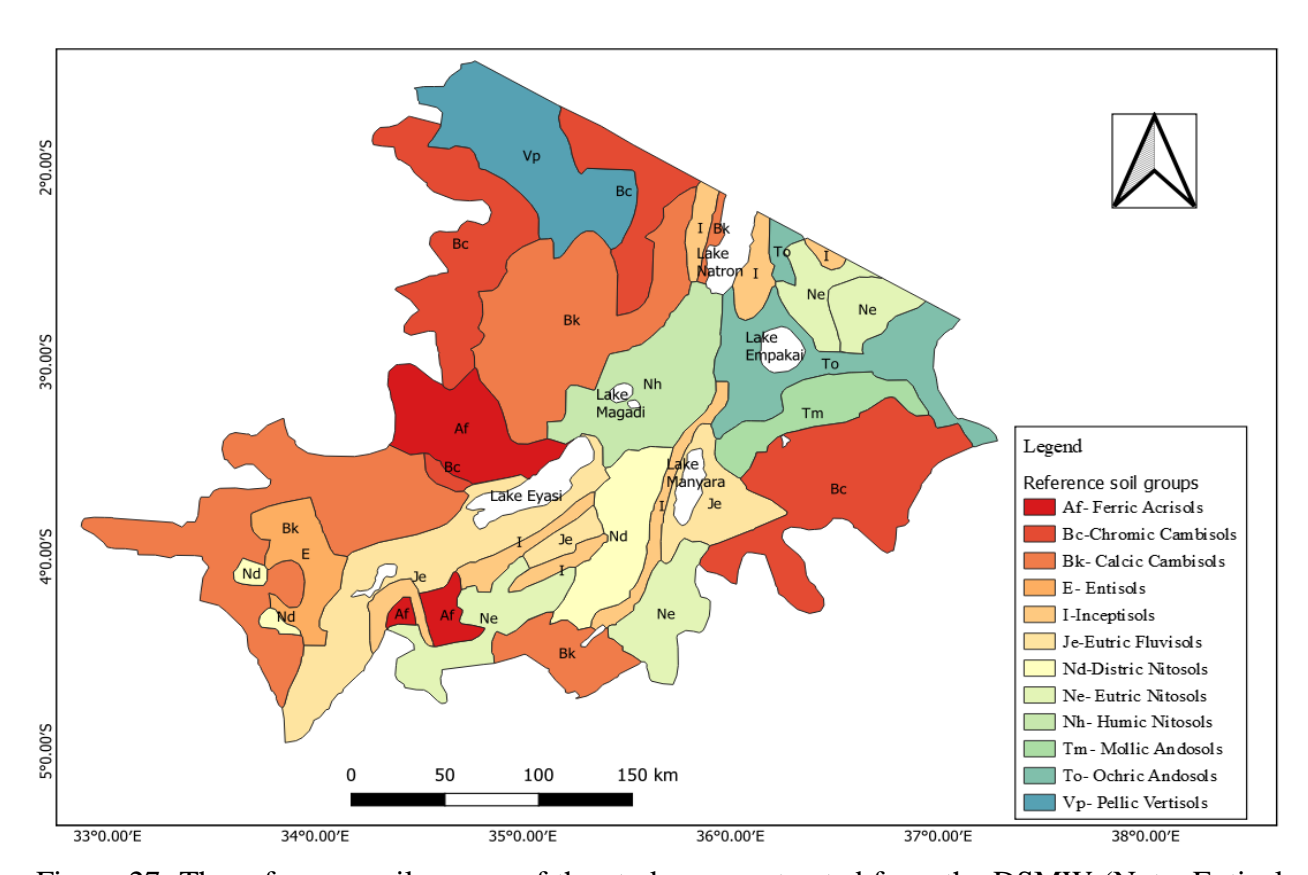


Figure 27: The reference soil groups of the study area extracted from the DSMW (Note, Entisol (USDA Taxonomy)/Regosol (FAO), Inceptisols (USDA Taxonomy)/Cambisol (FAO))

Table 13: The key characteristics of the soil groups in the study area (Northern Tanzania)

soil groups	Key Characteristics	Reference
ferric acrisols	highly weathered soil rich in Fe oxides (especially rich in hematite), low-activity clays, and low base saturation, acidic soils	(Schad, 2016, 2023)
chromic cambisols and calcic cambisols	The soil profile is characterized by the presence of accumulated carbonate in the soil profile, weakly alkaline or alkaline reaction low content of humus, equal distribution of main oxides, high base saturation, Al or Fe compounds, predominant silicate iron over non-silicate iron, powerful, well-expressed carbonate - illuvial horizon	(Schad, 2016, 2023)
entisols	The soil is characterized by neutral-to-alkaline reactions, low to high base saturation, low to moderate levels of iron (Fe ³⁺) and aluminium oxides (Al ³⁺) and can accumulate calcium carbonate (CaCO ₃)	(Roozitalab, <i>et al.</i> ,2018)
inceptisols	The soil is characterized by neutral to slightly alkaline reactions, the clay minerals are often illite, kaolinite, or smectite, with low to moderate base saturation, moderate levels of Iron and Aluminum Oxides and contain calcium carbonate (CaCO ₃)	(Roozitalab, et al.,2018)
eutric fluvisols	The soil forms as alluvial deposits in the river basins or lowlands, with acid, neutral or alkaline reactions, high base saturation of 50% or more, content of silicate iron sharply predominates non-silicate iron.	(Schad, 2016, 2023)
	The soil is associated with volcanic regions and weathered basaltic rocks, High concentrations of iron (Fe ³⁺) and aluminium (Al ³⁺) oxides, low-	(Schad, 2016, 2023)

distric nitisols and humic	activity clays, rich in secondary clay minerals (especially kaolinite, and sometimes illite), high organic Matter Content, and the reaction slight acidic	
nitisols	to neutral	
mollic andosols and ochric andosols	The soil formed from volcanoclastic materials (volcanic ashes and ejecta), moderate to high organic matter contents, non-crystalline aluminium (Al ³⁺) and iron oxides (Fe ³⁺), and moderate to high base saturation	(Schad, 2016, 2023)
pellic vertisols	The soil profile is characterized by the humus horizon, presence of carbonate–illuvial horizon, uniform distribution of main oxides, weakly alkaline reaction, and in some cases labile soluble salts and gypsum accumulate in the soil profile.	(Schad, 2016, 2023)

4.3.5 Geological and Hydrogeological Features

Figure 28 presents detailed geological features surrounding the soda-saline lakes in northern Tanzania, and the key chemical constituents are detailed in Table 14. The geological map of the study area reveals a variety of geological characteristics, including Kimberlite (Kimb), Precambrian-Cambrian (pCm), Quaternary (Q), Quaternary Eolian (Qe), Quaternary Volcanics (Qv), Tertiary (T), and Tertiary Intrusive (Ti).

The distribution of Kimberlite mineral deposits is concentrated in clusters in the western areas adjacent to Lake Eyasi, specifically in the Meatu and Bariadi districts. Kimberlite, an igneous rock, comprises a diverse range of minerals such as olivine, mica, serpentine, calcite, monticellite, apatite, and lesser quantities of dolomite, phlogopite, spinel, perovskite, and ilmenite (Giuliani et al., 2017; Kamenetsky, Belousova, et al., 2014; Kamenetsky, Golovin, et al., 2014; Ringwood et al., 1992; Sparks et al., 2009). Olivines (in mafic igneous/magmatic rocks in basaltic volcanoes or intrusive volcanoes) and spinel (found in ultramafic rocks like peridotite) are minerals composed of dolomite, calcite, and alkali carbonates, with a lesser proportion of silicate and oxide minerals (Giuliani et al., 2017; Kamenetsky, Belousova, et al., 2014). The olivine contains a combination of Na-K carbonates and chloride (Giuliani et al., 2017). Weathering of kimberlite mineral deposits can contribute to alkali carbonates and silicates, which raise sodium and potassium levels in the lakes, enhancing the alkaline nature of the soda and soda-saline lakes.

The Precambrian-Cambrian (pCm) rocks were extensively distributed in the western, southern, and eastern parts of the study area. This suggests stable geological (constant sediment deposition) conditions throughout the transition from the Precambrian to the Cambrian epoch. Precambrian rocks, including intrusive granitic and volcanic rocks, exhibit minerals such as feldspar, pyroxene, microcrystalline quartz, olivine, calcium carbonates, iron carbonates, dolomites, and magnetite (Kuznetsov, 2020; Saber, 2020; Tetiker et al., 2015). Precambrian rocks, rich in calcium

carbonates and silicates, provide carbonate ions that help maintain high pH and support the formation of soda minerals like trona which correlates to the trona formation in the soda lakes. Cambrian sediments, which include basal conglomerates, sandstone, and siltstone, include quartz, moganite, calcite, dolomite, feldspar, phyllosilicates, zircon, monazite, uranophane, thoriante, xenotime, pyrite, and gold (Saber, 2020; Tetiker et al., 2015). Cambrian sediments, containing quartz, dolomite, and feldspar, supply additional carbonate and silicate minerals and can contribute to the alkaline environment of the soda and soda-saline lake.

Quaternary (Q) formations are distributed and found in scattered patches surrounding Lake Manyara, Eyasi, and the southern region. On the other hand, Quaternary Volcanic (Qv) formations are mostly located in the eastern part of Lake Natron, southeastern Longido, and eastern Monduli districts. The spread of this geological formation suggests substantial volcanic activity and the presence of sedimentary deposits from the Quaternary era. The patches of Quaternary Eolian (Qe) formations were observed, in the western portion of Lake Natron, the western part of Longido and Monduli districts, and the southern portion of the Eyasi rift. This suggests that wind deposition plays a significant role in changing the terrain in the region. Tertiary (T) formations occur in the Monduli districts northeast of Lake Manyara, southwest of Lake Eyasi, and around Mount Hanang in the Katesh districts. The Ngorongoro Crater in the Southern region of Lake Natron is the primary location of Tertiary intrusive (Ti) formations, which extend to Lake Eyasi in the North. Substantial portions of these formations are also present in the Northern part of Lake Natron and on Mount Hanang in the Katesh districts.

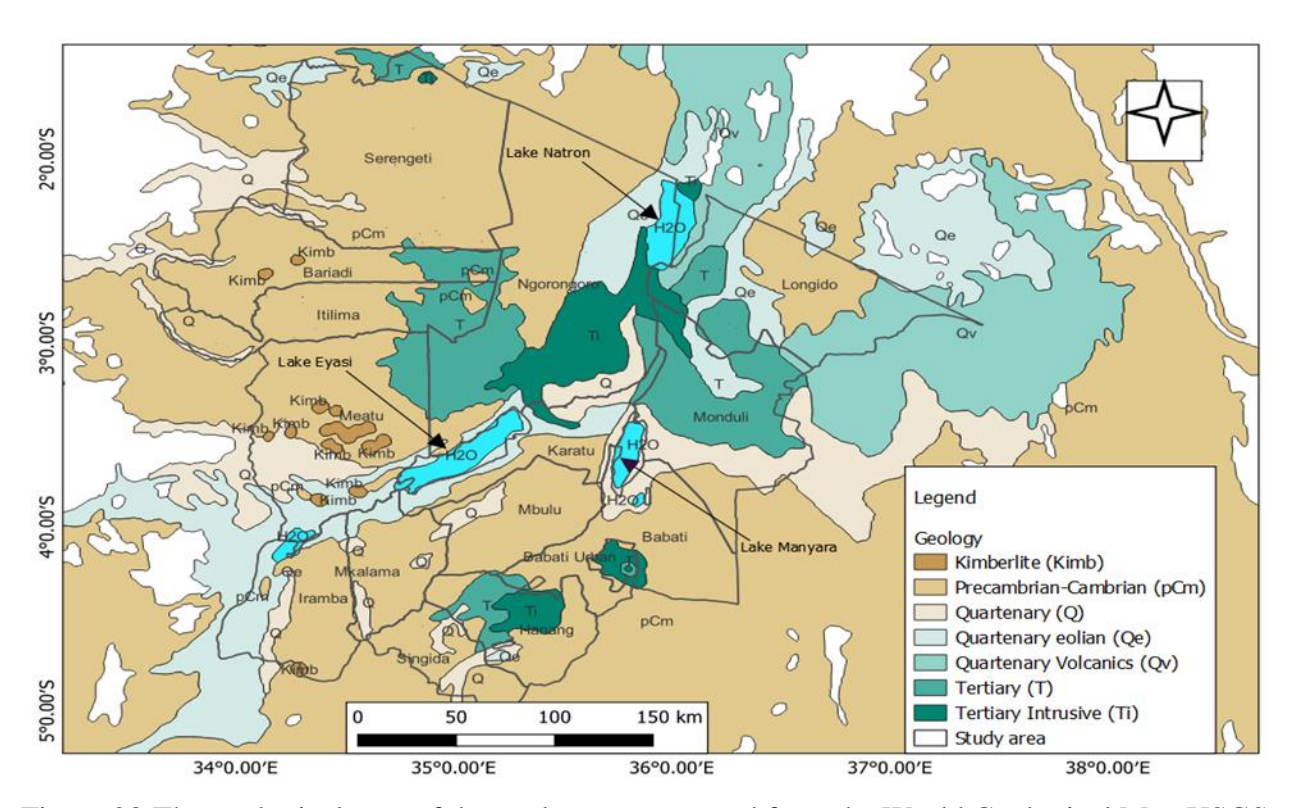


Figure 28:The geological map of the study area generated from the World Geological Map USGS database

Table 14: The geological features and key chemical constituents in the study area (Northern Tanzania)

Geological features	rock minerals	Key Chemical Constituents	Reference
Kimberlite mineral deposits	olivine, mica, serpentine, calcite, monticellite, apatite, and smaller amounts of dolomite, phlogopite, spinel, perovskite, and ilmenite	alkali carbonates (Na-K carbonates), chloride, silicate and oxide minerals	(Ringwood <i>et al.</i> , 1992; Sparks <i>et al.</i> , 2009; Kamenetsky <i>et al.</i> , 2014; Giuliani <i>et al.</i> , 2017)
Precambrian rocks	intrusive granitic and volcanic rocks	feldspar, pyroxene, microcrystalline quartz, olivine, calcium carbonates, iron carbonates, dolomites, and magnesite	(Tetiker <i>et al.</i> , 2015; Kuznetsov, 2020; Saber, 2020).
Cambrian sediments		basal conglomerates, sandstone, and siltstone, contain quartz, moganite, calcite, dolomite, feldspar, phyllosilicates, zircon, monazite, uranophane, thoriante, xenotime, pyrite, gold	(Tetiker <i>et al.</i> , 2015; Saber, 2020)
quaternary to tertiary	natrocarbonatite volcanoes (cinder cones, lava flows,	alkali carbonate minerals, such as nahcolite (NaHCO ₃), trona (Na ₃ H(CO ₃) ₂ ·2H ₂ O), thermonatrite	(Zaitsev <i>et al.</i> , 2006; Dawson, 2008b, 2010; Sherrod <i>et al.</i> , 2013)

intrusive volcanoes	mudflows, pyroclastic flows, pumice, and volcanic ash)	(Na ₂ CO ₃ ·H ₂ O), pirssonite (CaCO ₃ ·Na ₂ CO ₃ ·2H ₂ O), gaylussite (CaCO ₃ ·Na ₂ CO ₃ ·5H ₂ O), and calcite
		(CaCO ₃), and carefte (CaCO ₃)

4.3.6 Land Use and Land Cover (LULC) Changes

4.3.6.1 Accuracy statement

As shown in Table 15, the overall accuracies were higher than 80%, and the Kappa values were higher than 0.70. We continued using the classification outputs because the accuracy was within acceptable limits (Landis & Koch, 1977).

Table 15: Accuracy Assessment

	2000	2014	2023	
Overall accuracy	92.55	84.59	81.57	
Kappa hat	0.87	0.75	0.72	

4.3.6.2 LULC and Lake areas statistics and maps

The LULC classes demonstrated spatial and temporal changes, as shown in Table 16 and Figure 29. In 2000 and 2014, bareland covered most of our study area (58.73% and 50.77%), while shrubs and grasses comprised the second largest LULC type (21.80% and 33.47%) respectively. As of 2023 shrubs and grasses dominated the study area (37.66%) which is closely followed by bareland (37.48%). Built-up areas formed the least cover of the study area for all three years. Water bodies covered the second smallest area (5.07%, 2.87% and 3.05%) throughout the study years (Table 16). The analysis of the individual lakes revealed that Lake Eyasi had the largest area coverage across all three study years, as shown in Table 17. In contrast, Lake Manyara had the smallest area in both 2000 (54,873.81 ha) and 2014 (21,760.61 ha). By 2023, however, Lake Natron had the smallest area (20,368.59 ha) indicating distinct patterns of area change among the lakes over time. In 2014, both Lakes declined in their catchment areas, as shown in Figure 30. This reduction may be attributed to the prolonged droughts between 2000 and 2017, as depicted in Figure 5. The extended periods of drought likely played a significant role in reducing precipitation, and water inflow, leading to the observed shrinkage in lake size during this period.

Table 16: LULC areas and percentages for 2000, 2014 and 2023

LULC Class	20	00	201	14	2023		
	Area (ha)	Area (%)	Area (ha)	Area (%)	Area (ha)	Area (%)	
Water bodies	262304.42	5.07	148491.07	2.87	157900.61	3.05	
Forest	334007.72	6.46	183211.33	3.54	258615.37	5	
Shrubs & grasses	1127623.3	21.8	1731349.05	33.47	1948192.3	37.66	
Bareland	3037905.51	58.73	2626045.29	50.77	1938675.6	37.48	
Agricultural land	410050.59	7.93	479914.71	9.28	865253.47	16.73	
Built up	748.8	0.01	3628.89	0.07	4003.99	0.08	
Total	5172640.34	100	5172640.34	100	5172641.34	100	

Table 17: Individual Lakes statistics for 2000, 2014 and 2023 in the study area

Lake name	2000	2014	2023
	Area (ha)	Area (ha)	Area (ha)
Lake Natron	73332.90	34970.02	20368.59
Lake Eyasi	115284.80	35788.93	68479.04
Lake Manyara	54873.81	21760.61	55036.17

In terms of spatial distribution of LULC classes, water bodies were situated in the southern and northern regions of the study area, while the middle area was covered by forests. Shrubs and grasses were found in the south and southwest, agricultural areas were located in the southeast, and barren lands were present across the whole study area (Figure 29). The classes exhibited variations in coverage throughout time. The LULC exposed the soils and rocks to the weathering and erosion agents and influenced the alterations in the lakes' chemistry.

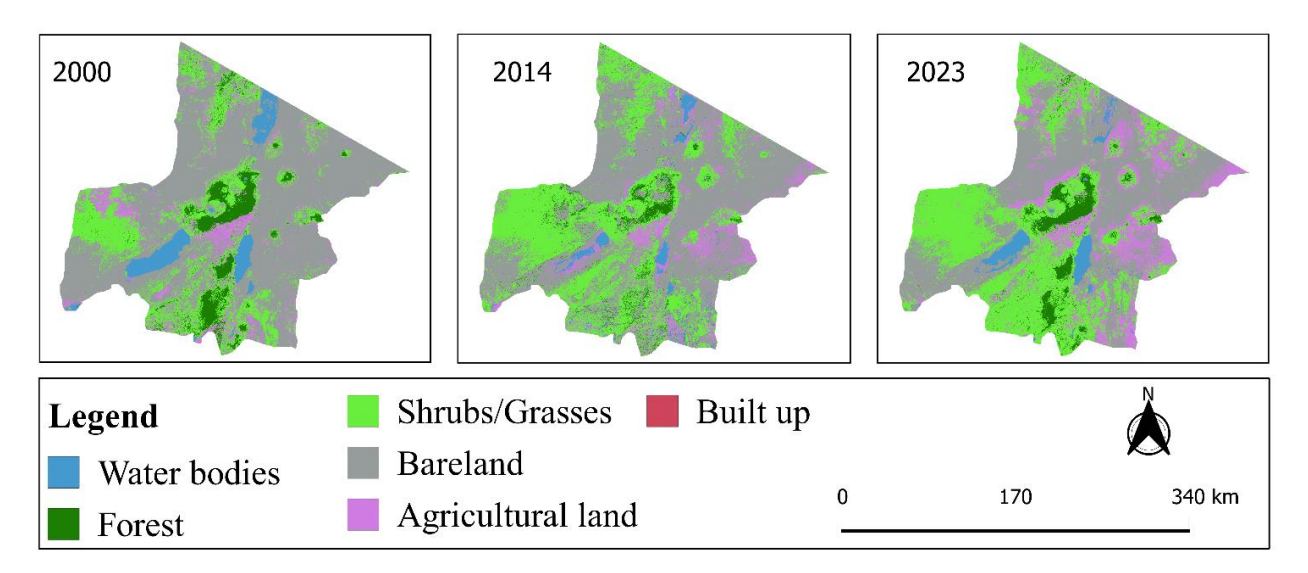


Figure 29: Map showing the spatial distribution of the various LULC classes over the study period

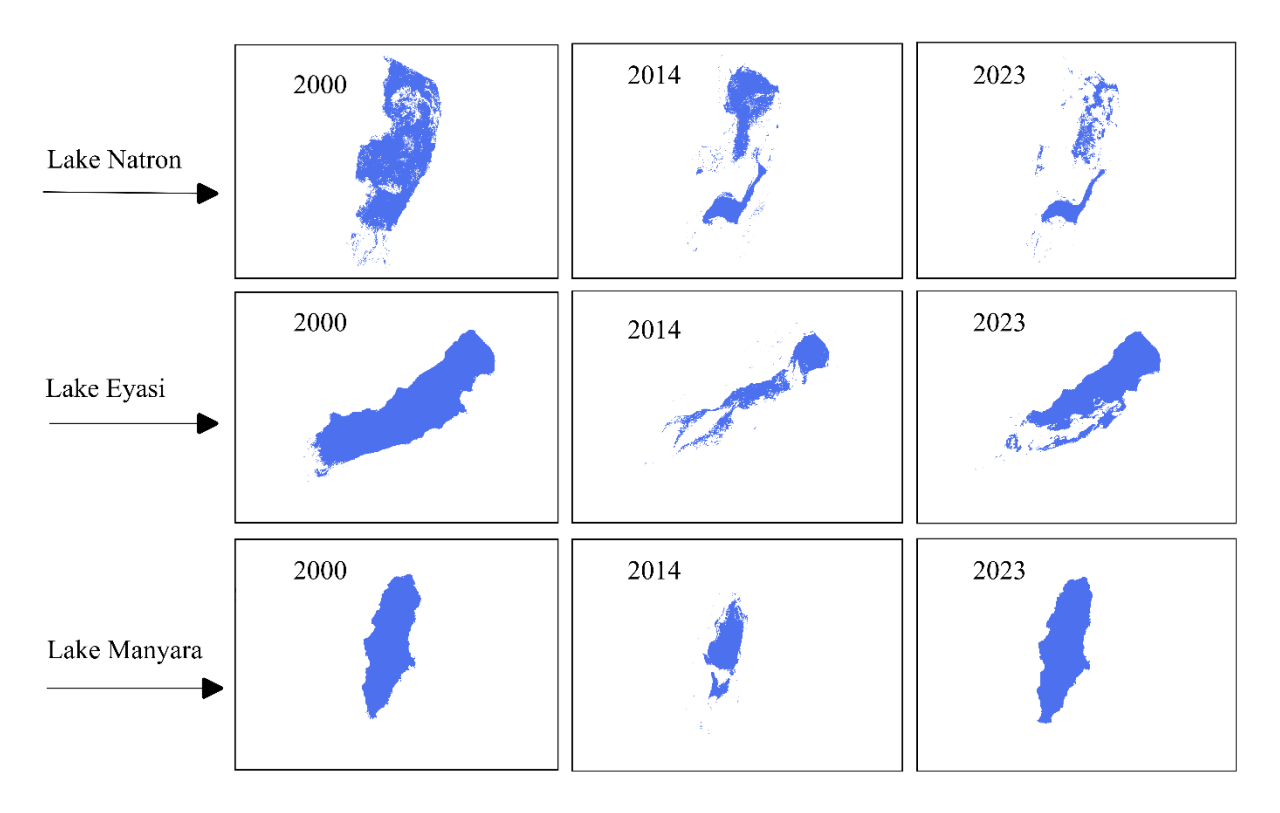


Figure 30: Maps showing the spatio-temporal dynamics of the three lakes in the study area

4.3.6.3 LULC and Lake Changes

Table 18 illustrates the dynamics of various LULC classes that occurred over time in the study area. There was a significant decline in bareland (-13.56%), water bodies (-43.39%), and forest areas (-45.15%) during the first study period (2000–2014). Conversely, there was a rise in built-up areas (384.63%), agricultural land (17.04%), and grasses and bushes (53.54%) areas. Except for bareland, all LULC classes increased in size throughout the second phase (2014-2023). Overall, from 2000 to 2023, there was a decline in areas under water bodies (-39.80%), forests (-22.57%), and bare land (-36.18%), whereas a significant increase was observed in agricultural land (111.01%), built-up areas (434.72%), and shrubs and grasses (72.77%). Overall, negative area changes were recorded for Lake Natron (-52,964.31 ha) and Lake Eyasi (-46,805.76 ha) while a positive area change was noted for Lake Manyara (162.36 ha) (Table 8).

Table 18: LULC changes between the study years

LULC class	2000-2014		2014-2023		2000-2023	
LULC Class	ha	%	ha	%	ha	%
Water bodies	-113813.35	-43.39	9409.54	6.34	-104403.81	-39.8
Forest	-150796.39	-45.15	75404.04	41.16	-75392.35	-22.57
Shrubs & grasses	603725.75	53.54	216843.25	12.52	820569	72.77
Bareland	-411860.22	-13.56	-687369.69	-26.18	-1099229.91	-36.18
Agricultural land	69864.12	17.04	385338.76	80.29	455202.88	111.01
Built up	2880.09	384.63	375.1	10.34	3255.19	434.72

Table 19: Changes in individual Lake area coverage between the study years

Lake name	2000-2014	2014-2023	2000-2023
	Area (ha)	Area (ha)	Area (ha)
Lake Natron	-38,362.88	-14,601.43	-52,964.31
Lake Eyasi	-79,495.87	32,690.11	-46,805.76
Lake Manyara	-33,113.20	33,275.56	162.36

5. DISCUSSION

5.1 Review of chemical properties of the IASW of EARV

The high pH levels (Table 1) observed in IASW of the EARV can be explained by the natural weathering of alkaline volcanic rocks in the surrounding escarpments, which elevates pH levels in lake waters (Deocampo & Jones, 2013; Kebede et al., 1994; Masresha et al., 2011; Nanyaro et al., 1984; Yuretich & Cerling, 1983). This weathering releases alkaline components into the lakes, leading to increased pH levels in the water.

The dominance of Na⁺ (Table 1, Table 4 and Figure 11b) over other cations in IASW of the EARV can be explained by the dissolution of nephelinite minerals containing nepheline, augite, anorthoclase, and albite, which release Na⁺ and K⁺ during weathering (Gaciri & Davies, 1993; Ghiglieri et al., 2012). The dissolution of alkaline rocks results in a greater discharge of Na⁺ into the lake water, which explains the prevalence of Na⁺ in IASW. Nephelinite minerals with nepheline (Na₃KAl₄Si₄O₁₆), augite, anorthoclase, and albite are dominant in the EARV, releasing Na⁺ and K⁺ during weathering (Ghiglieri et al., 2012; Makoba & Muzuka, 2019). Although monovalent elements predominate, Na⁺ is more abundant than K⁺. The enrichment of Na⁺ over K⁺ is due to the conservative nature of Na⁺ which remains constant during evaporation, while K⁺ can be removed by adsorption on the lake's active surface (Deocampo, 2004; Eugster & Jones, 1979; Kilham & Cloke, 1990). The loss of K⁺ due to clay mineral absorption during reverse weathering favours Na⁺ dominance (Garrels & Mackenzie, 1967; Mackenzie et al., 1995). Also, the parent materials' dominance of Na⁺ over K-bearing minerals and K-feldspar's weathering resilience could account for the low K⁺ compared to Na⁺ (Makoba & Muzuka, 2019). The low concentrations of Ca²⁺ and Mg²⁺ (Table 1, Table 4 and Figure 11a) are attributed to the early precipitation of calcite and dolomite minerals, which reduces the availability of these ions in lake water (Deocampo, 2004; Eugster & Jones, 1979; Getenet et al., 2023; Getenet, García-Ruiz, et al., 2022; Kilham, 1990; Kilham & Cloke, 1990). Carbonate precipitation (calcite, magnesite) lowers the amounts of calcium and magnesium in water (Jobbágy et al., 2017). The lower solubility of calcium and magnesium salts in water and the accumulation of soluble salts promote Na⁺ concentration while suppressing Ca²⁺ and Mg²⁺ (Chebotarev, 1955).

The high concentrations of HCO₃⁻ and CO₃²⁻ in IASW of the EARV are associated with the hydrolysis of silicate minerals, volcanic glass, and lava from surrounding rocks, which contain

high levels of Na⁺ and HCO₃⁻ + CO₃²⁻ (Deocampo & Jones, 2014; Jones et al., 1977). The dissolution of soluble naturally occurring minerals, chemical weathering of parent rock materials, and mineral-bearing rock's interaction with runoff water, and river input water also accounts for higher alkalinity in IASW of EARV (Chernet et al., 2001; Yechieli & Wood, 2002). The dominance of the Cl⁻ ions in IASW of the EARV (Table 1) can be due to the high precipitation rate and trona depositions (HCO₃⁻ depletion and Cl⁻ enrichment in brines), which co-occur with a rise in chlorinity (Eugster & Jones, 1979; Eugster, 1970; Kaufman et al., 1990). Due to its conservative nature, Cl⁻ can remain in solutions despite rapid evaporation rates, as the halite product remains below saturation levels even at high chloride concentrations. Evaporation-concentrated spring water discharges into lakes, alkaline hot spring recharge, seasonal runoff, and host volcanic bedrock dissolution also account for Cl⁻ dominance in IASW (Kaufman et al., 1990; Pecoraino et al., 2015; Renaut et al., 2021). Microbial conversion of sulphate ions to sulphide during organic matter degradation and loss of sulphate via sorption on the surface accounts for the sulphate ion content in Rift Valley IASW (Dunnette et al., 1985; Kilham, 1984). Anthropogenic activities including sewage effluent discharge and fertilizer residue also contribute to the $\mathrm{SO_4^{2^-}}$ concentration (Jiang et al., 2009). In addition, the amount of sulphate ions is linked to the dissolution of the gypsum minerals (Awaleh et al., 2022). The Spearman results (Table 3) suggest that monovalent ions, particularly Na⁺ and K⁺, are primary contributors to the cationic composition of IASW and are key influencers of TDS concentrations in lake water. The significant positive correlations between TDS and these monovalent ions reflect their high concentrations relative to other cations. Conversely, the negative correlation between TDS and Ca²⁺ and Mg²⁺ implies that divalent ions (alkaline earth metals) contribute minimally to the overall cationic composition of IASW. Meanwhile, the positive correlations between TDS and anions HCO₃⁻, CO₃²⁻, Cl⁻, and SO₄²⁻ emphasize the dominance of these anions within the IASW. Most correlations are significant, likely due to interactions among ions in the solution, reflecting the complex geochemical processes within the lake systems.

5.1.1 Spatial distributions of the IASW in EARV

The chemical diversity of IASW in the EARV reflects the region's complex hydrogeochemical and geological conditions, which give rise to distinct water types: soda, soda-saline, and saline

(Table 4, Table 5 and Figure 12). The predominance of soda-type lakes, particularly in Tanzania, is closely related to the extensive weathering of alkaline volcanic rocks, especially in northern Tanzania (Deocampo & Renaut, 2016; Deocampo, 2014; Makoba & Muzuka, 2019; Nanyaro et al., 1984) that release these ions into the lake water, combined with arid and semi-arid climate conditions that reduce water dilution and increase ion concentrations. In contrast, the presence of soda-saline lakes (transitional chemical type), which are less common but significant in number, especially in Tanzania, suggests the influence of additional processes like increased evaporation. Under high evaporation rates, typically seen in semi-arid regions, the lake water concentrates further, raising the levels of Cl⁻ and SO₄²⁻ while retaining high levels of sodium and carbonate. This indicates an intricate balance between mineral input from rock weathering and intensified evaporative concentration. The saline water type, observed less frequently but identified in Uganda, Tanzania, and Ethiopia, emphasizes the role of localized geological and hydrological conditions that contribute high levels of Cl⁻ and SO₄²⁻ to the lakes. The saline profile in these lakes can be attributed to high evaporation rates, groundwater flow paths enriched with chloride and sulfate ions, and contributions from hydrothermal sources. Thus, the diversity of lake water chemistries across the EARV from soda to soda-saline and saline demonstrates the complex interplay between geological substrate, climatic conditions, hydrology, and mineral input.

The observed clustering of ions such as Na⁺, Cl⁻, and SO₄²⁻ (Table *6*) across the EARV likely reflects regional geological and environmental influences. High concentrations of these ions may be associated with mineral dissolution, resulting from the weathering of volcanic and alkaline rocks common in the region. Additionally, processes like hydrological connectivity and evaporation rates can contribute to localized ion concentrations, enhancing the clustering of specific ions in certain areas. The weaker clustering of HCO₃⁻ + CO₃²⁻ may reflect more dispersed geological or biological processes, such as carbonate dissolution or aquatic biological activity, which tend to vary more subtly across different parts of the rift valley. These patterns underscore the role of geological sources, regional hydrology, and climate in shaping the spatial distribution of water chemistry in the EARV. The LMM (Table 7) suggest that carbonate concentrations (HCO₃⁻ + CO₃²⁻) are influenced by proximity to Pleistocene volcanoes, the elevation of Holocene volcanoes, and the soil types (Chromic Cambisols, Humic Gleysols, Inceptisols, Ochric Andosols, Haplic Xerosols, and Calcic Xerosols) indicating a spatial dependency on surface geological features and soil types. The observed inverse relationship between HCO₃⁻ + CO₃²⁻ and Pleistocene

volcano distance and positive correlation with Holocene volcano elevation (Table 7) underscore the role of local volcanic spatial pattern and soil type in shaping carbonate in the lake watershed. This phenomenon may also be explained by the importance of local gravity-driven groundwater inflow in the IASW water cycle (Tóth, 1999). In contrast, other saline water types dominated by SO₄²⁻ or Cl⁻ (Table 9 and Table 8) are primarily sourced from a longer groundwater gravity flow, making their genesis less connected to volcanic spatial patterns.

The observed north-to-south gradient in ion concentrations (Na⁺, Cl⁻, HCO₃⁻ + CO₃²⁻, and TDS) (Figure 13, Figure 14, Figure 15, Figure 16) in the Eastern Rift Valley is likely driven by several interlinked geological, climatic, and hydrological factors. Active volcanic and tectonic activities in northern Tanzania and southern Kenya create favourable conditions for mineral-rich waters through weathering of volcanic rocks and recharge from alkaline hot springs (Eugster, 1970; Fazi et al., 2018; Schagerl & Renaut, 2016). The dominance of volcanic rock formations in these areas provides abundant sources of ions through weathering processes, while recharge from alkaline hot springs further enhances the mineral content (Eugster, 1970; Fazi et al., 2018; Schagerl & Renaut, 2016). Furthermore, deep underground water connectivity beneath the Rift Valley aids the transport and concentration of ions, reinforcing the observed chemical gradient (Fazi et al., 2018). The semi-arid to arid climate in northern Tanzania and southern Kenya, with limited and fluctuating precipitation (Borhara et al., 2020), leads to reduced dilution of dissolved ions, contributing to higher mineral concentrations in local lakes and groundwater. The major consequence of the large spatial concentrations of major ions in the lakes of the EARV might potentially lead to the salinization of both the freshwater and the soil (Kaushal et al., 2021). The primary environmental variables responsible for the salinization of freshwater and soil in the Rift Valley regions are the intrusions of dissolved salts into the land and climate change (Godebo et al., 2021; Musie & Gonfa, 2023; Zebire et al., 2019). Moreover, the increasing temperatures in the area might result in elevated rates of evaporation, resulting in the accumulation of concentrated salt deposits in the soil.

5.2 The chemical composition, classification, and geographical distributions of sodasaline lakes in ETRV.

5.2.1 Physiochemical properties of the ETRV

The higher pH values observed in most lakes (Table S1 and Figure 17), particularly in Lake Eyasi, Natron, and Balangida, are likely due to the hydrolysis of aluminosilicate minerals, as previously reported in studies of Tanzanian Rift Valley lakes (Ghiglieri et al., 2012; Makoba & Muzuka, 2019). The pH observed aligns with what was reported in previous studies done in the Tanzania Rift Valley lakes (Deocampo, 2005; Hecky & Kilham, 1973; Mgimwa et al., 2021; Yona et al., 2022). However, the pH levels (>9) observed, especially in Lake Kindai and Singida, differ from previous findings by Hecky & Kilham, (1973) and may be linked to human activities and climate change, which could contribute to water pollution and changes in water chemistry. The variations in EC and salinity are largely attributed to evaporation rates. Lakes like Balangida Lelu and Balangida Lelu, which showed high EC and salinity, were almost completely dry during the fieldwork (Lameck et al., 2024) confirming that evaporation played a significant role in salinization. Lakes with lower EC and salinity, such as Eyasi, Mikuyu, and Sulunga, likely experience less evaporation and have more dilute waters. Turbidity values suggest a high concentration of suspended particles in the water, likely due to runoff from surrounding land, transporting silt and pollutants. The high turbidity in lakes like Manyara and Sulunga may affect water quality and biodiversity. The observed water temperatures, ranging from 26.5 to 33.7°C, likely contribute to the increased evaporation rates in the region, promoting salinization. The higher temperatures are conducive to evapotranspiration, further concentrating salts and other dissolved substances in the lakes.

5.2.2 The major ions chemistry of the ETRV

The observed variation in ion concentrations (Figure 18 and Figure 19) is attributed to a combination of geological, hydrological, and climatic factors. The higher Na⁺ concentrations in lakes Balangida, Balangida Lelu, and Eyasi might be related to geology, alkaline rock weathering, and evaporation. The higher Na⁺ concentrations in Lake Balangida, Balangida Lelu and Eyasi compared to other lakes, can be due to higher evapotranspiration and lake volume declines as

reported by Lameck et al.,(2024) in Figures 1 (a) and (b). The findings demonstrated that Na⁺ is the dominant cation, accounting for more than 87.12% (Table 11) of the total cation content in each lake. Dissolution of alkaline rocks (feldspars), weathering of alkaline minerals from surrounding escarpments, and volcanic ash deposition in depressions accounts for Na⁺ dominance in the ETRV (Gaciri & Davies, 1993; Ghiglieri et al., 2012; Makoba & Muzuka, 2019; Zango et al., 2019). The strong positive correlations seen between Na⁺ (Table 10) and TDS, salinity, HCO₃⁻, CO₃²⁻, SO₄²⁻, Cl⁻, and pH, together with the negative correlation with Ca²⁺ and Mg²⁺, indicate that Na⁺ is the dominant cation in the eastern rift valley lakes. The prevalence of Na⁺ in the soda-saline lakes in the ETRV aligns with the prevalence of sodium in soda lakes globally (Boros et al., 2017; Boros & Kolpakova, 2018; Borzenko, 2019; Deocampo & Renaut, 2016; Eugster & Hardie, 1978). The higher concentrations of K⁺ (Figure 18) in Lake Balangida, Balangida Lelu, and Natron may be due to increased evapotranspiration and reduced volume, leading to an increase in dissolved ions in the water. The K⁺ cations were the second most prevalent cations, and they contributed less than 5% to the overall cation composition of the examined lakes as seen in Table 11. An adsorptive process of K⁺ by the active clay minerals (Garrels & Mackenzie, 1967; Mackenzie et al., 1995), particularly in the bottom layers, might explain the lower potassium content in lake water. This adsorption process hinders the dissolution of K⁺ in water. The high concentrations of Ca²⁺ and Mg²⁺ observed in Lake Kindai and Singida (Table S1 and Figure 18) agree with the results reported by Hecky & Kilham, (1973). The higher Ca²⁺ and Mg²⁺ levels seen in Lake Kindai and Singida might be due to the geological characteristics of their surrounding drainage basins. The results demonstrated that the soda-saline lakes in the Eastern Tanzania rift valley had a low concentration of Ca²⁺ and Mg²⁺ ions, accounting for less than 10% of the total cationic composition (Table 11). The lower prevalence of Ca²⁺ and Mg²⁺ ions in the ETRV soda-saline lakes aligns with global soda lake hydrochemistry patterns (Boros et al., 2017; Boros & Kolpakova, 2018; Borzenko & Shvartsev, 2019; Deocampo & Renaut, 2016). The precipitation of secondary carbonate minerals (calcite, sepiolite, and aragonite) explains lower Ca²⁺ and Mg²⁺ concentrations (Deocampo & Jones, 2014; Eugster & Jones, 1979; Getenet et al., 2022; Kilham & Cloke, 1990). The supersaturation of calcite, dolomite, sepiolite, and aragonite in the studied lakes (Figure 20 (a)-(d), Table S3), indicates that precipitation had a direct impact on the lake's lower Ca²⁺ and Mg²⁺ concentrations.

The lakes Balangida, Balangida Lelu, and Natron exhibited the highest levels of HCO₃⁻ and CO₃²⁻, while lakes Singida, Kindai, and Sulunga displayed the lowest concentrations. Lakes Natron and Manyara displayed an anion composition with over 50% equivalent of HCO₃⁻, as shown in Figure 21 and Table 11. The proportions of HCO₃ were above 25% in lakes Balangida, Balangida Lelu, and Eyasi, whereas they were below 25% in Kindai, Singidani, Sulunga, Mikuyu, and Balangida. The variability observed is likely due to variations in geological factors, such as the unique rock formations and hydrological inputs present in each lake. The weathering of volcanic soils, silicate minerals, sedimentary rocks from nearby hills and escarpments, as well as the leaching and weathering processes of water-bearing rocks, enriches the soda-saline lakes with HCO₃⁻ and CO₃²⁻ levels (Gaciri & Davies, 1993; Ghiglieri et al., 2012; Gizaw, 1996; Jones et al., 1977; Makoba & Muzuka, 2019). The results revealed that Cl⁻ is the dominant anion in lakes Singidani, Kindai, Mikuyu, Sulunga, and Eyasi, accounting for more than 50% of the anionic composition as shown in Table 11 and Figure 21. In contrast, other lakes showed an anion composition with less than 50% Cl⁻. The prevalence of Cl⁻ in lakes Singidani, Kindai, Mikuyu, Sulunga, and Eyasi may be attributed to the evaporation and dissolution of halite and other minerals rich in chloride (Deocampo, 2005; Jones & Deocampo, 2003). Lakes Balangida and Balangida Lalu showed higher concentrations of SO_4^{2-} compared to the other lakes, with equivalent percentages of 56.72 and 79.32, respectively (Table 3). On the other hand, the concentration of SO_4^{2-} in the other lakes was much lower, accounting for less than 25% of the overall anionic compositions. The study reported considerably higher SO_4^{2-} concentrations in Lakes Balangida and Balangida Lalu compared to previously reported by Hecky & Kilham, (1973). This implies that Lakes Balangida and Balangida Lalu, unlike the other lakes, may have different SO₄²⁻ sources. Sulphur-containing rocks, natural geological processes (Awaleh et al., 2022; Borzenko, 2021; Borzenko & Shvartsev, 2019; Dunnette et al., 1985; Kilham, 1984), and artificial fertilizer applications in agricultural fields surrounding these lakes might be the possible sources of the higher SO_4^{2-} concentrations observed. Overall, the anionic composition of the eastern Tanzania rift valley lakes examined exhibited a mixed dominance of Cl⁻, HCO₃⁻ + CO₃²-, and SO₄²-. The mixed dominance of Cl⁻, HCO₃⁻ + ${\rm CO_3}^{2^-}$, and ${\rm SO_4}^{2^-}$ in the eastern Tanzanian rift valley is further supported by the significant positive correlations (Table 10) between Cl⁻, HCO₃⁻, and SO₄²⁻ with Na⁺, K⁺, TDS, EC, and salinity. The existence of soda, soda-saline, and saline water types (Table 4) supports the mixed dominance of Cl^- , $\text{HCO}_3^- + \text{CO}_3^{2-}$, and SO_4^{2-} in the Tanzanian rift valley. The hydrochemical variation in the

ETRV lakes is linked to geological processes and interactions with surrounding rocks and sediments. The Na-K-HCO₃ type in Lake Natron and Manyara can be linked to volcanic activity in northern Tanzania (Abdallah et al., 2023; Deocampo & Renaut, 2016; Deocampo, 2004; Foster et al., 1997; Pecoraino et al., 2015). In contrast, the Na-SO4 composition in Lakes Balangida and Balangida Lalu may be due to the weathering of sulphide minerals or human activities, such as fertilizer use in nearby agricultural areas. The Na-Cl type in Lakes Sulunga, Kindai, Singidani, Mikuyu, and Eyasi is likely associated with halite weathering, evaporation, and increased salt concentration in these lakes.

5.2.3 Chemical Classification of IASW of the ETRV

The Na⁺ dominance is consistent across all lakes in ETRV, with the mixed dominance of the anions (such as $HCO_3^- + CO_3^{2-}$, SO_4^{2-} , and Cl^-) (Table 11 and Table 12). The classification of Lake Natron and Manyara as soda types and Eyasi as soda-saline types aligns with previous studies (Lameck et al., 2023). In this study lake, Balangida is classified as soda-saline which deviates from the previous study by Lameck et al., (2023). This discrepancy in the classifications of Lake Balangida and Eyasi in this study compared to our previous work suggest that human activities may have affected the water composition in these areas. The applications of synthetic fertilizers in nearby agricultural fields could have led to the addition of the sulphate and chloride components, altering the chemical composition of these lakes. The classification of Lake Kindai and Singidani as saline-type aligns with our previous study (Lameck et al., 2023). On the other hand, the consistent classification of Lakes Kindai and Singidani as saline types implies a more stable ecosystem despite external influences. The observed decrease in soda-saline lake properties (Figure 22) from the northern to the central parts of Tanzania is likely influenced by variations in geological settings and volcanic activity (Dawson, 2008; Ghiglieri et al., 2012; Kisaka et al., 2021; Lyu et al., 2018; Mizota et al., 1988; Nanyaro et al., 1984; Scoon, 2018). This is evidenced by the dominant volcanic features highlighted in Figure 23. The extensive volcanic landscape provides a strong geological imprint on local hydrology and water chemistry, reinforcing the soda-saline characteristics observed in the northern parts of Tanzania's rift zone. In the central part of the country, particularly in Dodoma and Singida regions, the landscapes are characterized by basement rocks and consolidated sedimentary rocks (Eriksson & Sandgren, 1999; Macdonald et al., 2000),

that might have contributed to the formation of non-soda lakes. Additionally, the groundwater movements within basinal-flow systems likely drive the sequential chemical transformation from HCO_3^- to sulfate SO_4^{2-} and finally to chloride Cl^- (Tóth, 1999). Various factors can influence the evolution of these anions, including lithology, water-rock interactions, and hydrological conditions. Understanding the processes involved in the transformation of anions can provide valuable insights into the formation and behaviour of soda-saline lakes.

5.3 Influence of environmental variables and anthropogenic activities on soda-saline lake chemistry in Northern Tanzania: A Remote Sensing and GIS-based approach.

5.3.1 Climate Variability and Drought Analysis

The observed rainfall pattern (Figure 25), with its peak during the fall season, is consistent with the semi-arid climate of Northern Tanzania (Mwabumba et al., 2022). This seasonal precipitation can intensify the weathering of nearby rocks and minerals, leading to the influx of chemical components into the lakes, which may alter their chemical compositions. The consistent temperature pattern, with maximum temperatures reaching 25-35°C, is favourable to induce a high evaporation rate in lake water. This evaporation can contribute to the accumulation of salts and minerals in the soda-saline lakes, further influencing their high salinity levels.

The severe drought events observed from 1987 to 1992, 2000 to 2010, and 2012 to 2017 (Figure 26) align with previous research confirming an increase in drought frequency in the region since 2000 (Slegers, 2008; Kijazi and Reason, 2009; Leweri *et al.*, 2021; Mdemu, 2021; Verhoeve *et al.*, 2021). On a broader scope, the increased incidence of drought patterns and their corresponding intensities align with previous comprehensive studies conducted in East Africa and Africa (Gebremeskel et al., 2019; Polong et al., 2019). The extended drought occurrences reported in the region in recent years may be attributed to variations in precipitation and temperature patterns caused by climate change implications. Increased frequency of droughts may impact and pose potential risks to the health of soda-saline lakes. The findings underscore the importance of implementing effective management strategies and policies to protect water and natural resources, ensuring the long-term sustainability of these lake systems.

5.3.2 Influence of Soil Type

The different soil types (Figure 27) surrounding the soda-saline lakes can significantly impact the chemistry of these lakes. The ferric acrisols, found near Lake Eyasi, are highly weathered soils rich in iron (Domínguez-rodrigo et al., 2007; Lyu et al., 2018), which may influence the lake's chemical composition. Pellic vertisols in the Lake Natron area are characterized by lime accumulation and deep cracks during dry seasons (Pierre et al., 2015; Orzechowski et al., 2020), which can contribute to the lake's alkaline conditions. Entisols and inceptisols in the region suggest active geological processes, including erosion and weathering (Singh and Chandran, 2017), that could introduce minerals into the lakes through runoff. Eutric fluvisols, found in the lowlands around Lakes Manyara and Eyasi, supply essential salts and ions due to their high organic matter and nutrient content (Asongwe et al., 2020; Šimanský, 2018). Cambisols, both chromic and calcic, can influence the lakes' chemistry by providing different pH conditions (neutral to alkaline) and minerals from slight to moderate weathering (ISRIC, 2014). Andosols, particularly mollic and ochric types, are linked to volcanic activity and contribute volcanic minerals to the lakes (ISRIC, 2016; Ring et al., 2014; Sisay et al., 2024), which may increase alkalinity. The presence of nitisols, particularly humic nitisols in the Ngorongoro area, indicates highly weathered basaltic volcanic deposits (Ring et al., 2014; Sisay et al., 2024) that can affect the alkalinity of nearby lakes. The diverse soil types, each with distinct chemical characteristics, interact with the lake water through weathering, leaching, runoff, and sediment deposition processes. These interactions introduce various chemical constituents into the lakes, influencing their alkalinity, salinity, and overall water chemistry. The high alkalinity of soda and soda-saline lakes can be attributed to the presence of carbonate-rich soils like Cambisols and Inceptisols, while volcanic soils like Andosols and Nitisols contribute additional minerals and influence the lakes' chemical balance, affecting primary productivity, algal growth, and ecosystem health.

5.3.3 Influence of Geological Features

The results as detailed in Figure 28 revealed the northern region of Tanzania is predominant with volcanic activities Ranging from Precambrian-Cambrian (pCm) to Tertiary Intrusive (Ti). Our observations agree with the previous studies that noted the dominance of volcanic and tectonic

activity in the region (Dawson, 2008a, 2010; Biggs et al., 2013; Sherrod et al., 2013; Scoon, 2018, 2020). The presence and distribution of quaternary to tertiary intrusive volcanoes suggest tectonic and volcanic activity in the area. Natrocarbonatite volcanoes like Oldonyo Lengai, as well as different geological features including cinder cones, lava flows, mudflows, pyroclastic flows, pumice, and volcanic ash (Zaitsev et al., 2006; Dawson, 2008b, 2010; Sherrod et al., 2013), are evidence of this continuous volcanic activity. The region's major volcanic deposits contain alkali carbonate minerals such as Na₂Ca(CO₃)₂ and Na₂CO₃ (Zaitsev et al., 2006), which have a significant impact on the chemistry of the soda-saline lakes. The interaction of volcanic rocks and lake waters adds to the lake's unique chemical composition and influences the higher alkalinity of soda-saline lakes (Pecoraino et al., 2015; Deocampo and Renaut, 2016). The ongoing influx of volcanic gases and minerals into these lakes is crucial for creating the physical terrain and preserving the biological variety and distinctive features of the soda-saline lakes.

5.3.4 Land use and Land Cover changes

The observed dynamics in LULC classes (Table 16 and Table 18) revealed a decrease in water bodies, forests, and bare land and a significant increase was observed in agricultural land, built-up areas, and shrubs and grasses. The findings align with other studies conducted in the Urmia Lake basin in Northwestern Iran and Lake Naivasha in Kenya (Chaudhari et al., 2018; Onywere, 2012) have demonstrated a consistent rise in agricultural lands and urban/built-up regions, accompanied by a decline in the extent of the lake/water bodies. The decline in the extent of the lake/water bodies may be primarily attributed to human activities and climate changes as evidenced by an extended drought from 2012 to 2017 (Figure 26). The prolonged drought caused by climate change leads to increased evaporation, resulting in a decrease in the extent of the lake/water bodies (Figure 30). The expansion of built-up areas in our study area can be linked to population increase over the years (Ministry of Finance and Planning, 2022). The population increase subsequently results in agricultural expansion and intensification to meet the food and commercial demands of the population (Onyango et al., 2015). An increase in agricultural activities is often associated with increased water abstraction through irrigation, and the use of inorganic fertilizers, pesticides and herbicides which eventually alter the chemical composition of the water bodies in addition to promoting algal bloom (Evans et al., 2019; Zahoor & Mushtaq, 2023). Population increase also

translates to an increase in domestic and commercial effluent discharge which results in water resources contamination. Earlier research has also shown anthropogenic alterations as the leading cause of significant changes in land use and water storage for most lakes (Chaudhari et al., 2018). There was a notable decrease in the forest cover in the study area over the two decades most likely due to anthropogenic activities. Deforestation and forest degradation expose soils and rocks to weathering and erosion, resulting in increased sediment loads and nutrient inputs into lake waters thereby altering their chemical compositions (Hay, 1998). Analysis of the individual lakes also showed changes in their area coverage between the study years (Table 17 and Table 19). Lake Natron steadily decreased between 2000–2014 and 2014–2023 while Lakes Eyasi and Manyara likewise decreased between 2000–2014 but later increased between 2014–2023 (Table 19) (Figure 30). The reductions in lake surface areas can be linked to water abstraction (Goshime et al., 2019) and climate variability (Yao et al., 2023), which have had a considerable effect on water volumes. These decreases in volume, in turn, influence the dynamic water chemistry of the lakes by altering the concentration of dissolved minerals and other key chemical elements, thereby affecting the overall ecological balance and health of the lake ecosystems. Our results align with a time series study of Lake Natron's surface area between 1984–2011 which similarly showed a high degree of variability in the lake levels due to climate variability and catchment degradation (Tebbs et al., 2013). A mixed-method approach, involving a multidisciplinary stakeholders' engagement identified decreasing water levels, human activities near the lake, siltation and evaporation as the key challenges facing Lake Manyara (Janssens de Bisthoven et al., 2020). The study of Northern Tanzania comprising the three lakes (Natron, Eyasi, Manyara) among others also linked the fluctuations in lake water levels to geologic, climatic, and biological events occurring within and outside the lake (Yanda & Madulu, 2005).

6. CONCLUSIONS AND RECOMMENDATIONS

6.1 CONCLUSIONS

This dissertation presents a detailed analysis of the chemistry of the IASW in the EARV system, focusing on the ETRV. We compiled and reported chemical data from 56 inland saline waters in the EARV into a comprehensive database. The results of our study revealed that the dominance sequence of major cations and anions in the EARV is as follows: $Na^+ > K^+ > Ca^{2+} > Mg^{2+}$ and $HCO_3^- + CO_3^{2-} > Cl^- > SO_4^{2-}$. Among the examined lakes, 73.2% were soda water chemical types, 12.5% were soda-saline water, and 14.3% were saline water chemical types. The carbonates as the dominant anions in IASW, displayed an inverse spatial relationship with the distance from Pleistocene volcanoes while showing a positive correlation with the elevation of Holocene volcanoes. Furthermore, different soil types, including Chromic Cambisols, Humic Gleysols, Inceptsol, Ochric Andosol, Haplic Xerosols, and Calcic Xerosols, were also significant in the mixed models. This pattern can be explained by the spatial distribution of volcanoes and the associated local gravity flows. However, other saline water types dominated by sulfate or chloride are more likely associated with longer gravity-driven groundwater flows (Tóth, 1999), making their genesis less connected directly to the volcanoes. The spatial distributions of Na⁺, Cl⁻, HCO₃⁻+CO₃²⁻, and TDS in the EARV revealed a gradual increase in the concentration gradient of Na⁺, Cl⁻, HCO₃⁻+CO₃²⁻, and TDS (salinity) from the northern to the southern regions of the eastern branch of the EARV. However, Lake Afrera, situated in the Danakil depression in the north of Ethiopia and Ugandan lakes (Western Rift), stands out as a significant exception from this pattern.

In the ETRV lakes, Na^+ dominates, with lower amounts of K^+ , Ca^{2+} , and Mg^{2+} , and mixed dominance of $HCO_3^- + CO_3^{2-}$, Cl^- , and SO_4^{2-} . From North to Central Tanzania, we observed decreasing soda lake characteristics. Soda-type and soda-saline lakes were more widespread in northern Tanzania (Arusha and Manyara), whereas saline lakes were common in the middle region between Dodoma and Singida. The predominance of volcanic in northern Tanzania likely influenced the dominance of soda and soda-saline lakes in northern Tanzania (Arusha and Manyara). These patterns can also be associated with regional groundwater gravity flow which influences their genesis. We observed temperature and precipitation variability in northern Tanzania. The SPEI results showed drought episodes from 1987, with prolonged droughts

between 2000 and 2017 perhaps caused by regional and global climate change. The intricate relationship between the climate, soils, and geological features in northern Tanzania plays a crucial role in triggering the creation of soda-saline lakes. For the 23-year study period (2000–2023), we noted LULC changes. Water bodies decreased by 39.80%, forests by 22.57%, and bare land by 36.18%. Water bodies fell 39.80%, woods 22.57%, and barren ground 36.18%. Conversely, agricultural land rose 111.01%, built-up areas 434.72%, and bushes and grasses 72.77%. The analysis of the individual lakes revealed decreased area coverage in 2014 for all lakes while in 2023 lake area coverage of Natron decreased while for Lake Eyasi and Manyara, the coverage area increased. Human actions such as an increase in agricultural and built-up areas reflect population increases and suggest the LULC alterations. The decrease in waterbodies and forests negatively harms lake ecosystems and biodiversity. Policymakers and stakeholders must consider LULC trends for sustainable development and conservation. Understanding the complex interactions between climate change, drought, and the ecosystem in this region requires more investigation.

6.2 RECOMMENDATIONS

According to the findings of this study, the following recommendations can be made:

- ✓ Establish a Regular Monitoring System: It is important to establish and implement a continuous monitoring system to track changes in the chemistry of soda-saline lakes over time. Ongoing monitoring will provide valuable insights into any shifts in lake chemistry and offer early warnings of potential changes due to climatic or anthropogenic influences.
- ✓ Implement Climate Change Mitigation Strategies: Climate change initiatives aiming at reducing the frequency and severity of droughts should be prioritized. This includes optimizing water management practices, reforestation and anti-deforestation programmes, controlling the emission of pollutants from industry and promoting sustainable land use practices.
- ✓ Incorporate Land Use and Land Cover (LULC) Change into Regional Planning: It is important to integrate patterns of land use and land cover change into regional planning frameworks. This should include policies that address deforestation and promote sustainable land use practices, as the reduction in water bodies and forests, coupled with the expansion of

- agricultural and urban areas, highlights the urgent need for sustainable land management to preserve biodiversity and ecosystem services.
- ✓ Raise Public Awareness on the Ecological Importance of Soda Lakes: Raising public awareness about the ecological value of soda lakes is vital for fostering community support for conservation efforts. Initiatives of educating the public on the importance of these ecosystems will encourage sustainable practices that help reduce environmental degradation.

7. KEY SCIENTIFIC FINDINGS AND IMPORTANT OUTPUT

- 1. I have compiled and reported chemical data and classified EARV inland soda salt waters into a comprehensive database based on their distinctive water chemical type. I have determined that 73.2% of the lakes were soda type, 12.5% soda-saline type and 14.3% saline type.
- 2. This study revealed a north-to-south gradual increase in the concentration gradient of Na⁺, Cl⁻, HCO₃⁻ + CO₃²⁻ in relation with vulcanic spatial pattern, and TDS (salinity) across the eastern branch of the EARV.
- 3. Soda and soda-saline lakes were predominant in northern Tanzania (Arusha and Manyara), while saline lakes were more common in the central region (Singida and Dodoma).
- 4. In northern Tanzania, prolonged drought episodes were observed between 2000 and 2017.
- 5. LULC analysis showed declines in water bodies, forests, and bare land, with increases in agricultural land, built-up areas, and bush/grassland
- 6. Between 2000 to 2014, all lake catchment areas decreased, but between 2014 and 2023, only Lake Natron continued to shrink, while Lakes Eyasi and Manyara expanded.

8. SUMMARY

This dissertation explores the chemistry of the inland soda-saline lake waters of the EARV system, specifically emphasizing the ETRV. We conducted a comprehensive review of the chemical properties of inland soda-saline lakes with a salinity (TDS) exceeding 1 g/l, classified these lakes into their distinctive water chemical types and assessed the spatial geographical distributions of Na^+ , Cl^- , $HCO_3^- + CO_3^{2-}$, and TDS across the EARV region. We collected chemistry data on the EASL from published articles from 1968 to 2022. Additionally, we used the modified formula to

estimate the concrete proportions of CO_3^{2-} and HCO_3^{-} based on the pH and total alkalinity. Furthermore, we examined the current chemical composition, classified them into their respective chemical types, and investigated the geographical distribution of soda-saline lakes in the eastern Tanzania rift valley. In addition, we used remote sensing and GIS to assess the influence of environmental variables and human activities on soda-saline lake chemistry in northern Tanzania. The results showed that the cations and anions in the EARV soda saline lakes followed the order: $Na^+ > K^+ > Ca^{2+} > Mg^{2+}$ and $HCO_3^- + CO_3^{2-} > CI^- > SO_4^{2-}$. The results demonstrated considerable variability in soda-saline lakes across the EARV area. Tanzania has the most soda-chemical types of inland waters (20), followed by Ethiopia (9), Kenya (8), and Uganda (4). Soda-saline lakes were the most prevalent in Tanzania (7). Saline lakes were most commonly observed in Uganda (4), Tanzania (3), and Ethiopia (1). From the northern to the southern regions in the eastern branch of the EARV, we noticed a gradual increase in the concentration gradient of Na^+ , Cl^- , $HCO_3^- + CO_3^{2-}$, and TDS. Nevertheless, Lake Afrera in north Ethiopia and Uganda (Western Rift) is a notable exception to this pattern. This increase in concentration could be attributed to the volcanic spatial pattern occurring in southern Kenya and northern Tanzania.

Results show that the ETRV lake water pH ranged from 9.0 to 10.2, EC from 2843 to 109,800 μS/cm, and Na⁺ prevailed over other cations, with mixed dominance of HCO₃⁻ + CO₃²⁻, CI⁻, and SO₄²⁻. The study also found that lakes Balangida and Balangida Lelu had elevated SO₄²⁻ concentrations compared to the other lakes. The variation in gravity flows, including local (Soda), transitional (sulfate), and regional (chloride) groundwater flows, along with the presence of sulphate-rich bedrock and nearby agricultural input, are the probable causes for this phenomenon. The regional distribution patterns revealed that soda-type and soda-saline lakes were more prevalent in northern Tanzania (Arusha and Manyara). In contrast, saline lakes were prevalent in the central areas between Dodoma and Singida. The variation in volcanic spatial dsitribution and diversity of gravity flows, which encompass local (soda), transitional (Sulphate), and regional (chloride) groundwater flows in the ETRV, possibly influences the observed decline in soda and soda-saline characteristics from northern to central Tanzania.

Results also highlighted that temperature and precipitation variability in northern Tanzania are favourable for inducing evapotranspiration, affecting mineral precipitation and soda-saline lake chemistry. The SPEI results revealed increased drought events since 1987, with extended droughts between 2000 and 2017. Soil types in northern Tanzania include ferric acrisols, chromic

cambisols, calcic cambisols, entisols, inceptisols, eutric fluvisols, distric nitisols, humic nitisols, mollic andosols, ochric andosols, and pellic vertisols. The region's geological processes range from Precambrian-Cambrian to tertiary intrusions triggered by volcanic and tectonic activity. Throughout the study period (2000-2023), the results revealed dynamics in the various classes of land use and land cover (LULC). Areas under water bodies decreased by -39.80%, forests by -22.57%, and bareland by -36.18%. In contrast, agricultural land increased by 111.01%, built-up areas by 434.72%, and shrubs and grasses by 72.77%. This study highlights the intricate relationship between environmental factors and human actions in influencing the chemical composition of soda-saline lakes. Comprehending these interactions is essential for formulating efficient conservation and management measures to safeguard the ecological well-being of soda-saline lakes.

9. ACKNOWLEDGEMENTS

I am profoundly grateful to everyone who contributed to the successful completion of my dissertation, a journey marked by extensive learning and personal growth. My deepest appreciation goes to **Dr. Emil Boros**, my supervisor, whose invaluable guidance, patience, and support were pivotal throughout my Ph.D. journey. His expertise and insight have profoundly shaped this work, providing continuous motivation and inspiration. I extend my heartfelt thanks to my co-supervisor, Dr. Akos Pető, whose knowledge and insights played a significant role in my study. His recommendations and administrative assistance were crucial in navigating the complexities of my work. I also extend my heartfelt thanks to the support and cooperation I received from the Doctoral School of Environmental Science at the Hungarian University of Agriculture and Life Sciences (MATE) Gödöllő Campus have been instrumental in this journey, and I am deeply appreciative of their help in advancing my academic aspirations. My sincere gratitude is also directed towards the Stipendium Hungaricum Scholarship for funding for my PhD studies. This funding enables me to dedicate myself entirely to my studies and make meaningful contributions to my field. I am grateful to my wife, Eva James Machesse, and my children, Eliazary, Adriely, and Ariana, for their endless love, understanding, and patience throughout my absence. Your emotional support and regular encouragement have carried me through the highs and lows of this journey. I also wish to acknowledge my fellow PhD candidates for their companionship, motivating discussions, and the intellectually enriching environment we shared. Additionally, my gratitude extends to Mr

Mesia Lufingo, Mr Godwin Masumbuko, Mr Francis Asajile Mwasyeba, Mr Daniel Mwakagile, Mr Melckzedeck Tsere, and Mr Rajabu Shaban for their indispensable assistance during my fieldwork, which was crucial to the success of this dissertation.

This dissertation marks a significant milestone in my academic journey, and I am thankful for the opportunity to learn, grow, and contribute to my field. Thank you all for being an integral part of this fulfilling experience.

10. RELATED PUBLICATIONS

- 1. **Lameck, S. A.**, Skutai, J., & Boros, E. (2023). Review of chemical properties of inland soda and saline waters in East Africa (Rift Valley region). Journal of Hydrology: Regional Studies, 46(January), 101323. DOI: 10.1016/j.ejrh.2023.101323 (Q1).
- Lameck, A. S., Saeed, O., & Boros, E. (2024). The chemical composition, classification, and geographical distributions of soda-saline lakes in Eastern Tanzania's rift valley. Journal of Hydrology: Regional Studies, 51, 101668.
 DOI: 10.1016/j.ejrh.2024.101668
 (Q1).
- 3. Lameck, Azaria, S., Saeed, O., Nsima, P., Mwakagile, D., Peto, A., & Emil, B. (2024). Hydrochemical properties and heavy metal concentrations (ecological and human risk) of Lake Rukwa. Environmental Challenges, 15(April), 100940.

DOI: 10.1016/j.envc.2024.100940 (Q1).

11. APPENDICES

Table S1: Lakes under investigation, location, and field measurements (pH, temperature, DO, average specific conductivity, salinity, turbidity, and TDS).

	Sampling		Temp	DO	EC	Salinity	Turbidity	TDS
Lake	date	pН	(°C)	(Mg/l)	(mS/cm)	(Mg/l)	(NTU)	(Mg/l)
Kindai	9/12/2022	9	27.4	5.91	6868	3778	11.73	3431.33
Singidani	9/12/2022	9.3	29.4	7.26	7738	4420	16.43	3534.66
Mikuyu	9/12/2022	9.3	27.4	5.03	3450.66	1825.33	317.66	1725.66
Balangida Lalu	9/13/2022	9.6	26.5	5.6	100176.66	73266.66	112.43	50156.66
Balangida	9/13/2022	10.2	29.3	3.44	109800	99400	29.8	54710
Eyasi	9/12/2022	9.8	27.5	5.66	2843	17726.66	362	14206.66
Natron	9/12/2022	10	28	5.86	8620	4922	96.43	4306.66
Manyara	9/12/2022	9.7	30.1	5.4	6666	3686.66	597.66	3455.33
Sulunga	9/12/2022	9.2	33.7	4.53	3321.66	1750	463	1660.66

Table S2: The major ions, trace elements and heavy metal compositions of the investigated lakes, (Concentrations are in mg/l).

					Lakes				
Parameters	Kindai	Singida	Mikuyu	Balangida	Balangida	Eyasi	Natron	Manyara	Sulunga
				Lalu					
Na ⁺	1660.3	1839.67	926.33	40497	52209	9196.67	4900	2003	910.67
\mathbf{K}^{+}	25.55	20.05	9.02	1523.3	3343	22.4	215	11.04	13.8
Ca ²⁺	68.2	42.4	18.6	2.73	0.26	5.1	5.86	13.47	24.24
${\bf Mg^{2+}}$	80.48	61.99	16.92	42.91	2.78	1.98	0.65	3.77	9.42
HCO ₃ -	422.6	398.6	578.6	18439.8	45020.9	6573.6	3061.7	2653.49	534.31
CO3 ²⁻	6.1	9.8	14.1	1653.9	15618.5	992.7	2507.2	309.1	15.6
Cl-	2520.9	2682.0	1088.9	34737.9	25579.1	6858.6	2747.65	1062.1	996.4
SO ₄ ² -	83.3	120	163.3	247916.6	125000	2083.3	1750	236.7	81.7
Si	4.38	6.3	8.0	0.21	10.22	2.89	25.37	6.95	17.3
Fe	0.067	0.087	0.53	0.12	0.396	0.016	n.d.	0.144	3.29
Cu	0.097	0.065	0.072	0.21	n.d.	n.d.	n.d.	n.d.	0.067
Zn	n.d.	n.d.	n.d.	n.d.	n.d.	n.d.	n.d.	n.d.	n.d.
Se	n.d.	n.d.	n.d.	n.d.	n.d.	n.d.	n.d.	n.d.	n.d.
Sr	1.59	1.56	0.79	4.34	0.842	0.272	0.31	0.24	0.47
Mo	n.d.	n.d.	n.d.	4.21	0.265	0.218	0.235	0.08	0.022
Mn	0.023	n.d.	0.22	0.024	n.d.	n.d.	0.059	0.09	0.138
Pb	n.d.	n.d.	n.d.	n.d.	n.d.	n.d.	n.d.	n.d.	0.012
As	n.d.	n.d.	n.d.	n.d.	n.d.	n.d.	n.d.	n.d.	n.d.
Cr	n.d.	n.d.	n.d.	n.d.	n.d.	n.d.	n.d.	n.d.	n.d.
Co	n.d.	n.d.	n.d.	n.d.	n.d.	n.d.	n.d.	n.d.	n.d.
U	n.d.	n.d.	n.d.	0.354	1.168	0.085	0.042	n.d.	n.d.
Cd	n.d.	n.d.	n.d.	n.d.	n.d.	n.d.	n.d.	n.d.	n.d.
Ni	n.d.	n.d.	n.d.	n.d.	n.d.	n.d.	n.d.	n.d.	n.d.
В	n.d.	n.d.	0.042	1.215	1.786	1.996	1.165	0.412	0.11
Zr	n.d.	n.d.	n.d.	0.122	2.50	n.d.	n.d.	n.d.	n.d.
P	0.207	0.212	0.462	2.338	19.45	7.82	1.785	4.75	1.501
Rb	n.d.	n.d.	n.d.	0.274	1.078	0.018	0.09	n.d.	n.d.

Note: n.d. means not detected by the analytical measurement.

Table S3: Saturation Indices for the Investigated lakes calculated using PHREEQC

	Б. 1	Saturation indices of the studied lakes								
Minerals Phase	Formula	Kindai	Singida	Mikuyu	Balangida Lalu	Balangida	Eyasi	Natron	Manyara	Sulunga
Anhydrite	CaSO ₄	-2.45	-2.49	-2.57	-1.52	-3.42	-1.61	-3.22	-3.13	-2.68
Aragonite	CaCO ₃	0.40	0.41	0.45	0.87	-0.11	3.01	0.63	1.04	0.62
Calcite	CaCO ₃	0.54	0.55	0.60	1.01	0.03	3.15	0.77	1.18	0.75
Celestite	SrSO ₄	-2.04	-1.89	-1.88	0.67	-0.53	-0.27	-2.19	-2.52	-2.35
Chalcedony	SiO_2	-2.57	-2.39	-2.53	-6.40	-4.80	-5.55	-0.09	-3.29	-2.11
Chrysotile	$Mg_3Si_2O_5(OH)_4$	16.15	15.96	15.25	13.81	13.15	18.04	-1.42	13.41	14.81
Dolomite	CaMg (CO ₃) ₂	1.27	1.41	1.14	2.32	0.67	4.44	0.32	1.74	1.15
Goethite	FeOOH	4.86	4.97	5.55	3.59	3.96	3.43	-	4.36	6.33
Gypsum	CaSO ₄ :2H ₂ O	-2.17	-2.23	-2.30	-1.34	-3.25	-1.72	-2.96	-2.88	-2.47
Halite	NaCl	-4.07	-4.0	-4.65	-1.31	-1.50	0.56	-3.65	-4.38	-4.70
Hematite	Fe ₂ O ₃	11.74	11.97	13.12	9.25	9.98	9.07	-	10.74	14.70
Hydroxyapatit	Ca ₅ (PO ₄)3Oh	9.44	8.84	9.83	9.21	4.63	19.96	2.45	12.82	12.21
e	KFe ₃ (SO ₄)2(OH) ₆	-24.56	-23.84	-22.77	-26.75	-25.8	-32.94	-	-27.76	-20.31
Jarosite-K	MnOOH	5.80	-	7.10	7.09	-	-	-0.88	7.29	6.36
Manganite	FeSO ₄ :7H ₂ O	-23.51	-	-23.08	-27.58	-27.51	-32.86	-	-25.91	-22.32
Melanterite	Mn (OH)	1.40	0.32	-	-0.12	-	-	-4.27	1.09	0.89
Pyrochroite	MnO ₂ : H ₂ O	5.76	-	7.30	8.58	-	-	-2.91	8.40	7.28
Pyrolusite	SiO_2	-2.15	-1.97	-2.11	-5.98	-4.39	-5.13	0.33	-2.87	-1.70
Quartz	MnCO ₃	-1.34	-	-0.13	-3.0	-	-	0.42	-0.21	-0.13
Rhodochrosite	Mg ₂ Si ₃ O ₇ . 5OH:3H ₂ O	6.18	6.29	5.65	-1.85	0.30	2.05	-1.41	3.06	5.83
Sepiolite	FeCO ₃	-15.98	-15.52	-15.38	-20.14	-19.18	-22.20	-	-17.0	-14.21
Siderite	$SrCO_3$	-0.64	-0.43	-0.30	1.61	1.34	2.91	0.21	0.20	-0.49
Strontianite	KCl	-5.46	-5.55	-6.24	-2.65	-2.49	-2.09	-4.58	-6.22	-6.11
Sylvite	Mg ₃ Si ₄ O ₁₀ (OH) ₂	14.73	14.95	13.93	4.79	7.34	10.86	2.15	10.60	14.4
Talc	Fe ₃ (PO ₄) 2:8H ₂ O	-48.27	-47.26	-46.33	-63.28	-59.94	-70.82	-	10.60	-41.82
Vivianite	•									

12. REFERENCE

- Abdallah, E. A., Kasanzu, C. H., Kinabo, C. P., & Imai, A. (2023). Hydro-geochemistry and Related Processes Controlling the Composition of Thermal Waters in the Lake Natron Basin, Northern Tanzania. *Tanzania Journal of Science*, 49(3), 677–689. https://doi.org/10.4314/tjs.v49i3.11
- Ahmed, A., Rotich, B., & Czimber, K. (2024). Assessment of the environmental impacts of conflict-driven Internally Displaced Persons: A sentinel-2 satellite based analysis of land use/ cover changes in the Kas locality, Darfur, Sudan. *PLoS ONE*, 19(5 May), 1–19. https://doi.org/10.1371/journal.pone.0304034
- Alcocer, J. (1998). Saline lake ecosystems of Mexico. *Aquatic Ecosystem Health and Management*, 1(3–4), 291–315. https://doi.org/10.1016/s1463-4988(98)00011-6
- Ali, Y., Simachew, A., & Gessesse, A. (2022). Diversity of Culturable Alkaliphilic Nitrogen-Fixing Bacteria from a Soda Lake in the East African Rift Valley. *Microorganisms*, 10(9). https://doi.org/10.3390/microorganisms10091760
- Antony, C. P., Kumaresan, D., Hunger, S., Drake, H. L., Murrell, J. C., & Shouche, Y. S. (2013). Microbiology of Lonar Lake and other soda lakes. *ISME Journal*, 7(3), 468–476. https://doi.org/10.1038/ismej.2012.137
- Arad, A., & Morton, W. H. (1969). Mineral springs and saline lakes of the Western Rift Valley, Uganda. *Geochimica et Cosmochimica Acta*, 33(10), 1169–1181. https://doi.org/https://doi.org/10.1016/0016-7037(69)90039-8
- Asongwe, G. A., Yerima, B. P. K., Tening, A. S., & Bame, I. B. (2020). Pedogenic and Contemporary Issues of Fluvisol Characterization and Utilisation in the Wetlands of Bamenda Municipality, Cameroon. *Asian Soil Research Jornal*, 4(3), 8–27. https://doi.org/10.9734/ASRJ/2020/v4i330093
- Awaleh, M. O., Boschetti, T., Adaneh, A. E., Chirdon, M. A., Ahmed, M. M., Dabar, O. A., Soubaneh, Y. D., Egueh, N. M., Kawalieh, A. D., Kadieh, I. H., & Chaheire, M. (2022). Origin of nitrate and sulfate sources in volcano-sedimentary aquifers of the East Africa Rift System: An example of the Ali-Sabieh groundwater (Republic of Djibouti). Science of the Total Environment, 804, 150072. https://doi.org/10.1016/j.scitotenv.2021.150072
- Babel, M., & Schreiber, B. C. (2014). Geochemistry of Evaporites and Evolution of Seawater. In *Treatise on Geochemistry: Second Edition* (Vol. 9). https://doi.org/10.1016/B978-0-08-095975-7.00718-X
- Baesman, S. M., Stolz, J. F., Kulp, T. R., & Oremland, R. S. (2009). Enrichment and isolation of Bacillus beveridgei sp. nov., a facultative anaerobic haloalkaliphile from Mono Lake, California, that respires oxyanions of tellurium, selenium, and arsenic. *Extremophiles*, 13(4), 695–705. https://doi.org/10.1007/s00792-009-0257-z
- Beguería, S., Vicente-Serrano, S. M., Reig, F., & Latorre, B. (2014). Standardized precipitation evapotranspiration index (SPEI) revisited: Parameter fitting, evapotranspiration models, tools, datasets and drought monitoring. *International Journal of Climatology*, 34(10), 3001–3023. https://doi.org/10.1002/joc.3887
- Benvenuti, M., Bonini, M., Tassi, F., Corti, G., Sani, F., Agostini, A., Manetti, P., & Vaselli, O. (2013). Holocene lacustrine fluctuations and deep CO2 degassing in the northeastern Lake Langano basin (Main Ethiopian rift). *Journal of African Earth Sciences*, 77, 1–10. https://doi.org/10.1016/j.jafrearsci.2012.09.001
- Biggs, J., Chivers, M., & Hutchinson, M. C. (2013). Surface deformation and stress interactions during the 2007-

- 2010 sequence of earthquake, dyke intrusion and eruption in northern tanzania. *Geophysical Journal International*, 195(1), 16–26. https://doi.org/10.1093/gji/ggt226
- Borhara, K., Pokharel, B., Bean, B., Deng, L., & Wang, S. S. (2020). On Tanzania's Precipitation Climatology, Variability, and Future Projection. *Climate*, 8(34), 2–18.
- Boros, E., Horváth, Z., Wolfram, G., & Vörös, L. (2014). Salinity and ionic composition of the shallow astatic soda pans in the Carpathian Basin. *Annales de Limnologie*, 50(1), 59–69. https://doi.org/10.1051/limn/2013068
- Boros, E., Jurecska, L., Tatár, E., Vörös, L., & Kolpakova, M. (2017). Chemical composition and trophic state of shallow saline steppe lakes in central Asia (North Kazakhstan). *Environmental Monitoring and Assessment*, 189(11). https://doi.org/10.1007/s10661-017-6242-6
- Boros, E., & Kolpakova, M. (2018). A review of the defining chemical properties of soda lakes and pans: An assessment on a large geographic scale of Eurasian inland saline surface waters. *PLoS ONE*, *13*(8), 1–20. https://doi.org/10.1371/journal.pone.0202205
- Boros, E., V.-Balogh, K., Vörös, L., & Horváth, Z. (2017). Multiple extreme environmental conditions of intermittent soda pans in the Carpathian Basin (Central Europe). *Limnologica*, 62, 38–46. https://doi.org/10.1016/j.limno.2016.10.003
- Borzenko, S V. (2021). The main formation processes for different types of salt lakes: Evidence from isotopic composition with case studies of lakes in Transbaikalia, Russia. *Science of the Total Environment*, 782, 146782. https://doi.org/10.1016/j.scitotenv.2021.146782
- Borzenko, Svetlana V, & Shvartsev, S. L. (2019). Chemical composition of salt lakes in East Transbaikalia (Russia). *Applied Geochemistry*, 103(2019), 72–84. https://doi.org/10.1016/j.apgeochem.2019.02.014
- Catherine, A. M., Revocatus, M., & Hussein, S. (2015). Will Ngorongoro Conservation Area remain a world heritage site amidst increasing human footprint? *International Journal of Biodiversity and Conservation*, 7(9), 394–407. https://doi.org/10.5897/ijbc2015.0837
- Chaudhari, S., Felfelani, F., Shin, S., & Pokhrel, Y. (2018). Climate and anthropogenic contributions to the desiccation of the second largest saline lake in the twentieth century. *Journal of Hydrology*, *560*, 342–353. https://doi.org/10.1016/j.jhydrol.2018.03.034
- Chebotarev, I. I. (1955). Metamorphism of natural waters in the crust of weathering-3. *Geochimica et Cosmochimica Acta*, 8(4), 198–212. https://doi.org/10.1016/0016-7037(55)90053-3
- Chen, K., Sun, L., & Xu, J. (2021). Statistical analyses of groundwater chemistry in the Qingdong coalmine, northern Anhui province, China: implications for water rock interaction and water source identification. *Applied Water Science*, 1–12. https://doi.org/10.1007/s13201-021-01378-5
- Chernet, T., Travi, Y., & Valles, V. (2001). Mechanism of degradation of the quality of natural water in the lakes region of the Ethiopian Rift Valley. *Water Research*, 35(12), 2819–2832. https://doi.org/10.1016/S0043-1354(01)00002-1
- Congalton, R. G., & Green, K. (2019). Assessing the Accuracy of Remotely Sensed Data Principles and Practices, Third Edition. In *CRC press*.
- Dawson, J. B. (2008a). The Gregory rift valley and Neogene-recent volcanoes of northern Tanzania. Geological

- Society of London.
- Dawson, J. B. (2008b). The Gregory rift valley and Neogene-recent volcanoes of northern Tanzania. *Geological Society of London.*, 33, 33–38.
- Dawson, J. Barry. (2010). Aspects of Rift Valley faulting and volcanicity in North Tanzania: Report of a Geologists' Association Field Meeting in 2008. *Proceedings of the Geologists' Association*, 121(3), 342–349. https://doi.org/10.1016/j.pgeola.2010.06.003
- Deocampo,DM, & Jones, B. (2014). Geochemistry of Saline Lakes. In *Surface and Ground Water, Weathering and Soils* (2nd ed., Vol. 7, Issue December 2014). Elsevier Ltd. https://doi.org/10.1016/B978-0-08-095975-7.00515-5
- Deocampo, D. M., & Jones, B. F. (2014). Geochemistry of Saline Lakes. In *Treatise on Geochemistry: Second Edition* (2nd ed., Vol. 7, Issue December). Elsevier Ltd. https://doi.org/10.1016/B978-0-08-095975-7.00515-5
- Deocampo, D. M., & Renaut, R. W. (2016). Geochemistry of African soda lakes. *Soda Lakes of East Africa*, 77–93. https://doi.org/10.1007/978-3-319-28622-8
- Deocampo, Daniel M. (2004). Hydrogeochemistry in the Ngorongoro Crater, Tanzania, and implications for land use in a World Heritage Site. *Applied Geochemistry*, 19(5), 755–767. https://doi.org/10.1016/j.apgeochem.2003.10.006
- Deocampo, Daniel M., & Renaut, R. W. (2016). Geochemistry of African Soda Lakes. *Soda Lakes of East Africa*, 77–93. https://doi.org/10.1007/978-3-319-28622-8
- Deocampo, Daniel M, & Deocampo, D. M. (2005). Evaporative evolution of surface waters and the role of aqueous CO2 in magnesium silicate precipitation: Lake Eyasi and Ngorongoro Crater, northern Tanzania. 108, 493–504. https://doi.org/https://doi.org/10.2113/108.4.493
- Deocampo DM, J. B. (2014). Geochemistry of saline lakes. In Soda Lake of East Africa (Vol. 7, pp. 437–469).
- Domínguez-rodrigo, A. M., Díez-martín, F., Mabulla, A., Luque, L., Alcalá, L., Tarriño, A., López-sáez, J. A., Barba, R., Bushozi, P., Domínguez-rodrigo, M., Díez-martín, F., Mabulla, A., Luque, L., Alcalá, L., Tarriño, A., López-sáez, J. A., Barba, R., & Bushozi, P. (2007). The Archaeology of the Middle Pleistocene Deposits of Lake Eyasi, Tanzania. *Journal of African Archaeology*, *5*(1), 47–78. https://doi.org/10.3213/1612-1651-10085
- Drever, J. . (1982). The Geochemistry of Nafural Waters. Prentice-Hall, 388.
- Dunnette, D. A., Chynoweth, D. P., & Mancy, K. H. (1985). The source of hydrogen sulfide in anoxic sediment. *Water Research*, 19(7), 875–884. https://doi.org/10.1016/0043-1354(85)90146-0
- Ebinger, C. J., Yemane, T., Woldegabriel, G., Aronson, J. L., & Walter, R. C. (1993). Late Ecocene-Recent volcanism and faulting in the southern main Ethiopian rift. *Journal Geological Society (London)*, 150(1), 99–108. https://doi.org/10.1144/gsjgs.150.1.0099
- Eriksson, M. G., & Sandgren, P. (1999). Mineral magnetic analyses of sediment cores recording recent soil erosion history in central Tanzania. *Palaeogeography, Palaeoclimatology, Palaeoecology*, *152*(3–4), 365–383. https://doi.org/10.1016/S0031-0182(99)00043-7
- Eugster, H. P., & Hardie, L. A. (1978). Saline lakes. In A. Lerman (Ed.), Lakes, Chemistry, Geology, Physics

- (Issue 9781402092114, pp. 237–293). Springer-Verlag Berlin Heidelberg 1978. https://doi.org/10.1007/978-1-4020-9212-1 178
- Eugster, H. P., & Jones, B. F. (1979). Behavior of major solutes during closed basin- lakes brine evolution. In *American Journal of Science* (Vol. 279, Issue 6, pp. 609–631). https://doi.org/10.2475/ajs.279.6.609
- Eugster, Hans P. (1970). Chemistry and origin of the brines of Lake Magadi, Kenya. *Mineral. Soc. Amer. Spec. Pap.*, *3*, 213–235.
- Eugster, Hans P. (1980). Geochemistry of Evaporitic Lacustrine Deposits. *Annual Review of Earth Platenary Science*, 8(1), 35–63. https://doi.org/10.1016/0012-8252(84)90008-4
- Evans, A. E., Mateo-Sagasta, J., Qadir, M., Boelee, E., & Ippolito, A. (2019). Agricultural water pollution: key knowledge gaps and research needs. *Current Opinion in Environmental Sustainability*, *36*, 20–27. https://doi.org/10.1016/j.cosust.2018.10.003
- FAO/UNESCO. (2003). The Digital Soil Map of the World. *Food and Agriculture Organization of the United Nations*, version 3., c.30.
- Fazi, S., Amalfitano, S., Venturi, S., Pacini, N., Vazquez, E., Olaka, L. A., Tassi, F., Crognale, S., Herzsprung, P., Lechtenfeld, O. J., Cabassi, J., Capecchiacci, F., Rossetti, S., Yakimov, M. M., Vaselli, O., Harper, D. M., & Butturini, A. (2021). High concentrations of dissolved biogenic methane associated with cyanobacterial blooms in East African lake surface water. *Communications Biology*, 4(1). https://doi.org/10.1038/s42003-021-02365-x
- Fazi, S., Butturini, A., Tassi, F., Amalfitano, S., Venturi, S., Vazquez, E., Clokie, M., Wanjala, S. W., Pacini, N., & Harper, D. M. (2018). Biogeochemistry and biodiversity in a network of saline–alkaline lakes: Implications of ecohydrological connectivity in the Kenyan Rift Valley. *Ecohydrology and Hydrobiology*, 18(2), 96–106. https://doi.org/10.1016/j.ecohyd.2017.09.003
- Felföldi, T. (2020). Microbial communities of soda lakes and pans in the Carpathian Basin: a review. *Biologia Futura*, 71(4), 393–404. https://doi.org/10.1007/s42977-020-00034-4
- Foster, A., Ebinger, C., Mbede, E., & Rex, D. (1997). Tectonic development of the northern Tanzania sector of the East African Rift System Tectonic development of the northern Tanzanian sector of the East African Rift.

 *Journal of the Geological Society, 154(4), 689–700. https://doi.org/10.1144/gsjgs.154.4.0689
- Freexe, R. A., & Cherry, J. A. (1979). groundwater. Prentice-Hall. Inc., Englewood Cliffs, N.J.
- Fritz, B., Zins-Pawlas, M.-P., & Gueddari, M. (1987). Geochemistry of silica-rich brines from Lake Natron (Tanzania). Géochimie des saumures riches en silice du lac Natron (Tanzanie). *Sciences Géologiques*. *Bulletin*, 40(1), 97–110. https://doi.org/10.3406/sgeol.1987.1753
- Funk, C., Peterson, P., Landsfeld, M., Pedreros, D., Verdin, J., Shukla, S., Husak, G., Rowland, J., Harrison, L., Hoell, A., & Michaelsen, J. (2015). The climate hazards infrared precipitation with stations A new environmental record for monitoring extremes. *Scientific Data*, 2, 1–21. https://doi.org/10.1038/sdata.2015.66
- Gaciri, S. J., & Davies, T. C. (1993). The occurrence and geochemistry of fluoride in some natural waters of Kenya. *Journal of Hydrology*, 143(3–4), 395–412. https://doi.org/10.1016/0022-1694(93)90201-J
- Garrels, R. M., & Mackenzie, F. T. (1967). Origin of the Chemical Compositions of Some Springs and Lakes.

- Advances, 222–242.
- Gebremeskel, G., Tang, Q., Sun, S., Huang, Z., Zhang, X., & Liu, X. (2019). Droughts in East Africa: Causes, impacts and resilience. *Earth-Science Reviews*, 193(June 2018), 146–161. https://doi.org/10.1016/j.earscirev.2019.04.015
- Getenet, M., Garc, J. M., Getenet, M., García-ruiz, J. M., Otálora, F., & Verdugo-escamilla, C. (2022). *Mineral Precipitation from Soda Brines*, *Lake Magadi*, *Rift Valley Mineral Precipitation from Soda Brines*, *Lake Magadi*, *Rift Valley (Kenya)*. 4.
- Getenet, M., García-Ruiz, J. M., Otálora, F., Emmerling, F., Al-Sabbagh, D., & Verdugo-Escamilla, C. (2022). A Comprehensive Methodology for Monitoring Evaporitic Mineral Precipitation and Hydrochemical Evolution of Saline Lakes: The Case of Lake Magadi Soda Brine (East African Rift Valley, Kenya). *Crystal Growth and Design*, 22(4), 2307–2317. https://doi.org/10.1021/acs.cgd.1c01391
- Getenet, M., Manuel, G.-R. J., Otálora, F., Emmerling, F., Al-Sabbagh, D., & Verdugo-Escamilla, C. (2022). A Comprehensive Methodology for Monitoring Evaporitic Mineral Precipitation and Hydrochemical Evolution of Saline Lakes: The Case of Lake Magadi Soda Brine (East African Rift Valley, Kenya). *Crystal Growth and Design*, 22(4), 2307–2317. https://doi.org/10.1021/acs.cgd.1c01391
- Getenet, M., Ot´alora, F., Emmerling, F., Al-Sabbagh, D., & García-Ruiz, J. M. (2023). Mineral precipitation and hydrochemical evolution through evaporitic processes in soda brines (East African Rift Valley). *Chemical Geology*, 616(October 2022), 121222. https://doi.org/10.1016/j.chemgeo.2022.121222
- Ghiglieri, G., Pittalis, D., Cerri, G., & Oggiano, G. (2012). Hydrogeology and hydrogeochemistry of an alkaline volcanic area: The NE Mt. Meru slope (East African Rift-Northern Tanzania). *Hydrology and Earth System Sciences*, *16*(2), 529–541. https://doi.org/10.5194/hess-16-529-2012
- Giuliani, A., Soltys, A., Phillips, D., Kamenetsky, V. S., Maas, R., Goemann, K., Woodhead, J. D., Drysdale, R. N., & Griffin, W. L. (2017). The final stages of kimberlite petrogenesis: Petrography, mineral chemistry, melt inclusions and Sr-C-O isotope geochemistry of the Bultfontein kimberlite (Kimberley, South Africa).
 Chemical Geology, 455(2017), 342–356. https://doi.org/10.1016/j.chemgeo.2016.10.011
- Gizaw, B. (1996). The origin of high bicarbonate and fluoride concentrations in waters of the Main Ethiopian Rift Valley, East African Rift system. *Journal of African Earth Sciences*, 22(4), 391–402. https://doi.org/10.1016/0899-5362(96)00029-2
- Godebo, T. R., Jeuland, M. A., Paul, C. J., Belachew, D. L., & McCornick, P. G. (2021). Water quality threats, perceptions of climate change and behavioral responses among farmers in the ethiopian rift valley. *Climate*, 9(6). https://doi.org/10.3390/cli9060092
- Goshime, D. W., Absi, R., Ledésert, B., Dufour, F., & Haile, A. T. (2019). Impact of water abstraction on the water level of Lake Ziway, Ethiopia. *WIT Transactions on Ecology and the Environment*, 239, 67–78. https://doi.org/10.2495/WS190071
- Grant, W.D., & Jones, B. E. (2016). Bacteria, Archaea and Viruses of Soda Lakes. In M. Schagerl (Ed.), *Soda Lake of East Africa* (pp. 97–148). Springer International Publishing Switzerland. https://doi.org/10.1007/978-3-319-28622-8_5

- Grant, W D. (2006). Alkaline Environments and Biodiversity. In C. Gerday & N. Glansdorff (Eds.), *Extremophile Handbook: Vol. III* (pp. 21–24). Eolss Publishers, Oxford, UK. http://www.eolss.net
- Grant, William D. (2004). Introductory Chapter: Half a Lifetime in Soda Lakes. In A. Ventosa (Ed.), *Halophilic Microorganisms* (pp. 17–31). Springer-Verlag Berlin Heidelberg. https://doi.org/10.1007/978-3-662-07656-9 1
- Grant, William D, & Yu, D. (2011). Distribution and Diversity of Soda Lake Alkaliphiles. In H. K. (Ed.), *Extrimophiles Handbook* (pp. 27–54). Springer, Tokyo. https://doi.org/10.1007/978-4-431-53898-1
- Green, W. J., & Lyons, W. B. (2009). The saline lakes of the Mcmurdo Dry Valleys, Antarctica. *Aquatic Geochemistry*, 15(1–2), 321–348. https://doi.org/10.1007/s10498-008-9052-1
- Hammer, U. T. (1978). Saline lakes of Saskatchewan. *Internationale Revue Der Gesamten Hydrobiologie*, 63(3), 311–335. https://doi.org/https://doi.org/10.1002/iroh.19780630303
- Hardie, L. A., & Eugster, H. P. (1970). The Evolution of Closed-Basin Brines. *Mineral. Soc. Amer. Spec. Pap.*, 290(3), 273–290.
- Hay, W. W. (1998). Detrital sediment fluxes from continents to oceans. *Chemical Geology*, 145(3–4), 287–323. https://doi.org/10.1016/S0009-2541(97)00149-6
- Hecky, R. E., & Kilham, P. (1973). Diatoms in Alkaline, Saline Lakes: Ecology and Geochemical Implications. *Limnology and Oceanography*, 18(1), 53–71. https://doi.org/10.4319/lo.1973.18.1.0053
- ISRIC. (2014). Major soil group of the world. *International Soil Reference and Information Centre*, *Cambisols* (cm), 1–8.
- ISRIC. (2016). ANDOSOLS (AN) Summary description of Andosols.
- Janssens de Bisthoven, L., Vanhove, M. P. M., Rochette, A. J., Hugé, J., Verbesselt, S., Machunda, R., Munishi, L., Wynants, M., Steensels, A., Malan-Meerkotter, M., Henok, S., Nhiwatiwa, T., Casier, B., Kiwango, Y. A., Kaitila, R., Komakech, H., & Brendonck, L. (2020). Social-ecological assessment of Lake Manyara basin, Tanzania: A mixed method approach. *Journal of Environmental Management*, 267(September 2019). https://doi.org/10.1016/j.jenvman.2020.110594
- Jeilu, O., Gessesse, A., Simachew, A., Johansson, E., & Alexandersson, E. (2022). Prokaryotic and eukaryotic microbial diversity from three soda lakes in the East African Rift Valley determined by amplicon sequencing. Frontiers in Microbiology, 13(December), 1–14. https://doi.org/10.3389/fmicb.2022.999876
- Jiang, Y., Wu, Y., Groves, C., Yuan, D., & Kambesis, P. (2009). Natural and anthropogenic factors affecting the groundwater quality in the Nandong karst underground river system in Yunan, China. *Journal of Contaminant Hydrology*, 109(1–4), 49–61. https://doi.org/10.1016/j.jconhyd.2009.08.001
- Jirsa, F., Gruber, M., Stojanovic, A., Omondi, S. O., Mader, D., Körner, W., & Schagerl, M. (2013). Major and trace element geochemistry of Lake Bogoria and Lake Nakuru, Kenya, during extreme draught. *Chemie Der Erde*, 73(3), 275–282. https://doi.org/10.1016/j.chemer.2012.09.001
- Jobbágy, E. G., Tóth, T., Nosetto, M. D., & Earman, S. (2017). On the Fundamental Causes of High Environmental Alkalinity (pH ≥ 9): An Assessment of Its Drivers and Global Distribution. *Land Degradation and Development*, 28(7), 1973–1981. https://doi.org/10.1002/ldr.2718

- Johnson, T. C., & Odada, E. 0. (1996). The Limnology, Climatology and Paleoclimatology of the East African Lakes. In T. C. Johnson & E. 0. Odada (Eds.), *Gordon and Breach, Toronto*. Taylor & Francis. https://doi.org/10.1201/9780203748978
- Jones, B. E., Grant, W. D., Duckworth, A. W., & Owenson, G. G. (1998). Microbial diversity of soda lakes. *Extremophiles*, 2(3), 191–200. https://doi.org/10.1007/s007920050060
- Jones, B. F., & Deocampo, D. M. (2003). Geochemistry of saline lakes. *Treatise on Geochemistry*, 5–9(Figure 1), 393–424. https://doi.org/10.1016/B0-08-043751-6/05083-0
- Jones, Blair F., Eugster, H. P., & Rettig, S. L. (1977). Hydrochemistry of the Lake Magadi basin, Kenya. *Geochimica et Cosmochimica Acta*, 41(1), 53–72. https://doi.org/10.1016/0016-7037(77)90186-7
- Jones, Blair F., Naftz, D. L., Spencer, R. J., & Oviatt, C. G. (2009). Geochemical evolution of Great Salt Lake, Utah, USA. *Aquatic Geochemistry*, 15(1–2), 95–121. https://doi.org/10.1007/s10498-008-9047-y
- Jozsef Toth. (1999). Groundwater as a geologic agent: An overview of the causes, processes, and manifestations. *Hydrogeology Journal*, 7(January), 1–14.
- Kamenetsky, V. S., Belousova, E. A., Giuliani, A., Kamenetsky, M. B., Goemann, K., & Griffin, W. L. (2014). Chemical abrasion of zircon and ilmenite megacrysts in the Monastery kimberlite: Implications for the composition of kimberlite melts. *Chemical Geology*, 383, 76–85. https://doi.org/10.1016/j.chemgeo.2014.06.008
- Kamenetsky, V. S., Golovin, A. V., Maas, R., Giuliani, A., Kamenetsky, M. B., & Weiss, Y. (2014). Towards a new model for kimberlite petrogenesis: Evidence from unaltered kimberlites and mantle minerals. *Earth-Science Reviews*, 139, 145–167. https://doi.org/10.1016/j.earscirev.2014.09.004
- Kanuga, K. K. (1982). chemical composition of rains over kenya. *The Journal of Weather Modification*, 14(1), 38–42.
- Karasiak, N. (2020). Museo ToolBox: A Python library for remote sensing including a new way to handle rasters. *Journal of Open Source Software*, 5(48), 1978. https://doi.org/10.21105/joss.01978
- Kaufman, A., Margaritz, M., Paul, M., Hillaire-Marcel, C., Hollos, G., Boaretto, E., & Taieb, M. (1990). The 36C1 ages of the brines in the Magadi-Natron basin, East Africa. *Geochimica et Cosmochimica Acta*, 54(10), 2827–2833. https://doi.org/10.1016/0016-7037(90)90017-F
- Kaushal, S. S., Likens, G. E., Pace, M. L., Reimer, J. E., Maas, C. M., Galella, J. G., Utz, R. M., Duan, S., Kryger, J. R., Yaculak, A. M., Boger, W. L., Bailey, N. W., Haq, S., Wood, K. L., Wessel, B. M., Park, C. E., Collison, D. C., Aisin, B. Y. 'aaqo. I., Gedeon, T. M., ... Woglo, S. A. (2021). Freshwater salinization syndrome: from emerging global problem to managing risks. In *Biogeochemistry* (Vol. 154, Issue 2). Springer International Publishing. https://doi.org/10.1007/s10533-021-00784-w
- Kebede, E., G.-Mariam, Z., & Ahlgren, I. (1994). The Ethiopian Rift Valley lakes: chemical characteristics of a salinity-alkalinity series. *Hydrobiologia*, 288, 1–12. https://doi.org/https://doi.org/10.1007/BF00006801
- Kempe, S., & Kazmierczak, J. (2002). Biogenesis and early life on earth and Europa: Favored by an alkaline ocean? Astrobiology, 2(1), 123–130. https://doi.org/10.1089/153110702753621394
- Kempe, S., & Kazmierczak, J. (2007). SODA LAKES. 554-557.

- Kharaka, Y. K., Robinson, S. W., Law, L. M., & Carothers, W. W. (1984). Hydrogeochemistry of Big Soda Lake, Nevada: An alkaline meromictic desert lake. *Geochimica et Cosmochimica Acta*, 48(4), 823–835. https://doi.org/10.1016/0016-7037(84)90104-2
- Kijazi, A. L., & Reason, C. J. C. (2009). Analysis of the 1998 to 2005 drought over the northeastern highlands of Tanzania. *Climate Research*, 38(3), 209–223. https://doi.org/10.3354/cr00784
- Kilham, P. (1984). Sulfate in African inland waters: Sulfate to chloride ratios. *Verh. Int. Ver. Theor. Angew. Limnol.*, 22(1), 296–302. https://doi.org/10.1080/03680770.1983.11897306
- Kilham, Peter. (1990). Mechanisms controlling the chemical composition of lakes and rivers: Data from Africa. *Limnology and Oceanography*, *35*(1), 80–83. https://doi.org/10.4319/lo.1990.35.1.0080
- Kilham, Peter, & Cloke, P. L. (1990). The evolution of saline lake waters: gradual and rapid biogeochemical pathways in the Basotu Lake District, Tanzania. *Hydrobiologia*, 197(1), 35–50. https://doi.org/10.1007/BF00026937
- Kisaka, M., Fontijn, K., Shemsanga, C., Tomašek, I., Gaduputi, S., Debaille, V., Delcamp, A., & Kervyn, M. (2021). The late Quaternary eruptive history of Meru volcano, northern Tanzania. *Journal of Volcanology and Geothermal Research*, 417. https://doi.org/10.1016/j.jvolgeores.2021.107314
- Kuznetsov, V. G. (2020). Geochemical Environments of Precambrian Sedimentation. *Lithology and Mineral Resources*, 55(2), 99–110. https://doi.org/10.1134/S0024490220010034
- Lameck, A. S., Saeed, O., & Boros, E. (2024). The chemical composition, classification, and geographical distributions of soda-saline lakes in Eastern Tanzania's rift valley. *Journal of Hydrology: Regional Studies*, 51, 101668. https://doi.org/10.1016/j.ejrh.2024.101668
- Lameck, S. A., Skutai, J., & Boros, E. (2023). Review of chemical properties of inland soda and saline waters in East Africa (rift valley region). *Journal of Hydrology: Regional Studies*, 46(January), 101323. https://doi.org/10.1016/j.ejrh.2023.101323
- Landis, J. R., & Koch, G. G. (1977). The Measurement of Observer Agreement for Categorical Data Data for Categorical of Observer Agreement The Measurement. *Biometrics*, *33*(1), 159–174. https://doi.org/https://doi.org/10.2307/2529310
- Leweri, C. M., Msuha, M. J., & Treydte, A. C. (2021). Rainfall variability and socio-economic constraints on livestock production in the Ngorongoro Conservation Area, Tanzania. *SN Applied Sciences*, *3*(1), 1–10. https://doi.org/10.1007/s42452-020-04111-0
- Lewis, C. F. M. (2016). Geoscience medallist 1. Understanding the holocene closed-basin phases (Lowstands) of the laurentian great lakes and their significance. *Geoscience Canada*, 43(3), 179–197. https://doi.org/10.12789/geocanj.2016.43.102
- Lihepanyama, D. L., Ndakidemi, P. A., & Treydte, A. C. (2022). Spatio Temporal Water Quality Determines Algal Bloom Occurrence and Possibly Lesser Flamingo (Phoeniconaias. *Water*, *14*(21), 3532. https://doi.org/https://doi.org/10.3390/ w14213532
- Litchfield, C. D. (2011). Saline lakes. *Encyclopedia of Earth Sciences Series*, 9781402092114, 765–769. https://doi.org/10.1007/978-1-4020-9212-1_178

- Lyu, H., Watanabe, T., Kilasara, M., & Funakawa, S. (2018). Effects of climate on distribution of soil secondary minerals in volcanic regions of Tanzania. *Catena*, 166(December 2017), 209–219. https://doi.org/10.1016/j.catena.2018.04.005
- M. Onywere, S. (2012). Use of Remote Sensing Data in Evaluating the Extent of Anthropogenic Activities and their Impact on Lake Naivasha, Kenya. *The Open Environmental Engineering Journal*, 5(1), 9–18. https://doi.org/10.2174/1874829501205010009
- Macdonald, A. M., Davies, J., Nations, U., Programme, E., Olorunfemi, F., Rilwanu, T. Y., Inkani, A. I., Olasehinde, P. I., Journal, K., abdul, Solomon, S., Nwankwoala, H. O., Danert, K., Gesti Canuto, J., British Geological Survey, Nanbakhsh, H., Tasi ', O, I. E., Mallam I, ... Decision, M. (2000). A brief review of groundwater for rural water supply in sub-Saharan Africa. *Journal of Environment and Earth Science*, *1*(May), 1–17. http://scholar.google.com/scholar?hl=en&btnG=Search&q=intitle:REMOTE+SENSING+APPLICATIONS+t o+GROUNDWATER#5%0Ahttp://garj.org/garjas/home%0Ahttps://www.unicef.org/wash/files/Guidance_No te_005.pdf%0Ahttp://www.rural-water-supply.net/en/resources/details/130
- Mackenzie, F. T., Kump, L. R., Kovacs, J. A., Shoner, S. C., & Ellison, J. J. (1995). Reverse Weathering, Clay Mineral Formation, and Oceanic Element Cycles Metal-Carbon Bonds in Nature. *Science*, 270(5236), 586.
- Makoba, E., & Muzuka, A. N. N. (2019). Water quality and hydrogeochemical characteristics of groundwater around Mt. Meru, Northern Tanzania. *Applied Water Science*, 9(5), 1–29. https://doi.org/10.1007/s13201-019-0955-3
- Masresha, A. E., Skipperud, L., Olav, B., Zinabu, G. M., Meland, S., Teien, H., & Salbu, B. (2011). Science of the Total Environment Speciation of selected trace elements in three Ethiopian Rift Valley Lakes (Koka, Ziway, and Awassa) and their major in flows. *Science of the Total Environment, The*, 409(19), 3955–3970. https://doi.org/10.1016/j.scitotenv.2011.06.051
- Mdemu, M. V. (2021). Community's Vulnerability to Drought-Driven Water Scarcity and Food Insecurity in Central and Northern Semi-arid Areas of Tanzania. *Frontiers in Climate*, *3*(October), 1–14. https://doi.org/10.3389/fclim.2021.737655
- Melack, J. M., & Peter Kilham. (1974). *Photosynthetic rates of phytoplankton in East African alkaline, saline lake*. *19*(September).
- Mgimwa, E. F., John, J. R., & Lugomela, C. V. (2021). The influence of physical - chemical variables on phytoplankton and lesser flamingo (Phoeniconaias minor) abundances in Lake. *African Journal of Ecology*, 59(3), 667–675. https://doi.org/10.1111/aje.12863
- Mianping, Z., Jiayou, T., Junying, L., & Fasheng, Z. (1993). Chinese saline lakes. *Hydrobiologia*, 267(1–3), 23–36. https://doi.org/10.1007/BF00018789
- Ministry of Finance and Planning, N. B. of S. T. (2022). Age and Sex Distribution Report. 1–23.
- Mizota, C., Kawasaki, I., & Wakatsuki, T. (1988). Clay mineralogy and chemistry of seven pedons formed in volcanic ash, Tanzania. *Geoderma*, 43(2–3), 131–141. https://doi.org/10.1016/0016-7061(88)90039-0
- Mollel, G. F., Swisher, C. C., Feigenson, M. D., & Carr, M. J. (2008). Geochemical evolution of Ngorongoro

- Caldera, Northern Tanzania: Implications for crust-magma interaction. *Earth and Planetary Science Letters*, 271(1–4), 337–347. https://doi.org/10.1016/j.epsl.2008.04.014
- Musie, W., & Gonfa, G. (2023). Fresh water resource, scarcity, water salinity challenges and possible remedies: A review. *Heliyon*, 9(8), e18685. https://doi.org/10.1016/j.heliyon.2023.e18685
- Mwabumba, M., Yadav, B. K., Rwiza, M. J., Larbi, I., Dotse, S. Q., Limantol, A. M., Sarpong, S., & Kwawuvi, D. (2022). Rainfall and temperature changes under different climate scenarios at the watersheds surrounding the Ngorongoro Conservation Area in Tanzania. *Environmental Challenges*, 7(August 2021), 100446. https://doi.org/10.1016/j.envc.2022.100446
- Namsaraev, Z. B., Gorlenko, V. M., Buryukhaev, S. P., Barkhutova, D. D., Dambaev, V. D., Dulov, L. E., Sorokin, V. V., & Namsaraev, B. B. (2010). Water regime and variations in hydrochemical characteristics of the soda Salt Lake Khilganta (Southeastern Transbaikalia). *Water Resources*, 37(4), 513–519. https://doi.org/10.1134/S009780781004010X
- Nanyaro, J. T., Aswathanarayana, U., Mungure, J. S., & Lahermo, P. W. (1984). A geochemical model for the abnormal fluoride concentrations in waters in parts of northern Tanzania. *Journal of African Earth Sciences*, 2(2), 129–140. https://doi.org/10.1016/s0731-7247(84)80007-5
- Nicholson, K. (1993). Geothermal Fluids. In Geothermal Fluids. https://doi.org/10.1007/978-3-642-77844-5
- Nielsen, J. M. (1999). East African Magadi (trona): Fluoride concentration and mineralogical composition. *Journal of African Earth Sciences*, 29(2), 423–428. https://doi.org/10.1016/S0899-5362(99)00107-4
- Nyakeri, E. M., Mwirichia, R., & Boga, H. (2018). Isolation and characterization of enzyme producing bacteria from Lake Magadi, an extreme soda lake in Kenya. *Journal of Microbiology & Experimentation*, 6(2), 57–68. https://doi.org/10.15406/jmen.2018.06.00189
- Oduor, S. O., Schagerl, M., & Mathooko, J. M. (2003). On the limnology of Lake Baringo (Kenya): II. Pelagic primary production and algal composition of Lake Baringo, Kenya. *Hydrobiologia*, 506–509, 297–303. https://doi.org/10.1023/B:HYDR.0000008562.97458.d1
- Ogato, T., Kifle, D., Fetahi, T., & Sitotaw, B. (2014). Evaluation of growth and biomass production of Arthrospira (Spirulina) fusiformis in laboratory cultures using waters from the Ethiopian soda lakes Chitu and Shala.

 **Journal of Applied Phycology, 26(6), 2273–2282. https://doi.org/10.1007/s10811-014-0251-4
- Olaka, L. A., Odada, E. O., Trauth, M. H., & Olago, D. O. (2010). The sensitivity of East African rift lakes to climate fluctuations. *Journal of Paleolimnology*, 44(2), 629–644. https://doi.org/10.1007/s10933-010-9442-4
- Omenda, P. a. (2010). The geology and geothermal activity of the East African Rift System. *Workshop for Decision Makers on Geothermal Projects and Management*, 14–18.
- Onyango, J., Irvine, K., Bruggen, J. J. A. Van, Kitaka, N., & Kreuzinger, N. (2015). Agricultural Expansion and Water Pollution: The Yin-Yang in the Quality of Natural Water Resources. *African Centre for Technology Studies*, 9(July), 1–29.
- Orzechowski, M., Smólczyński, S., & Kalisz, B. (2020). *Physical*, water and redox properties of vertisols of the S ę popol Plain in north-eastern Poland. 71(3), 185–193.
- Owen, R. B., Renaut, R. W., & Lowenstein, T. K. (2018). Spatial and temporal geochemical variability in lacustrine

- sedimentation in the East African Rift System: Evidence from the Kenya Rift and regional analyses. *Sedimentology*, 65(5), 1697–1730. https://doi.org/10.1111/sed.12443
- Parkhurst., D. L., & Appelo, C. A. J. (1999). User's Guide to PHREEQC a Computer Program for Inverse Geochemical Calculations. *Water-Resources Investigations Report 99-4259*, *Version 2*. http://www.xs4all.nl/~appt/index.html%0ADenver,
- Parkhurst, D. L., & Appelo, C. a. J. (2013). Description of Input and Examples for PHREEQC Version 3 A Computer Program for Speciation, Batch-Reaction, One-Dimensional Transport, and Inverse Geochemical Calculations. U.S. Geological Survey Techniques and Methods, book 6, chapter A43, 497 p. *U.S. Geological Survey Techniques and Methods, Book 6, Chapter A43*, 6-43A.
- Pecoraino, G., Alessandro, W., & Inguaggiato, S. (2015). The other side of the coin: geochemistry of alkaline lakes in volcanic areas. *Volcanic Lakes*, 219–237. https://doi.org/10.1007/978-3-642-36833-2
- Pedregosa, F., Varoquaux, G., Gramfort, A., Michel, V., & Thirion, B. (2011). Scikit-learn: Machine Learning in Python. *Journal OfMachine Learning Research*, 12(9), 2825–2830. https://doi.org/10.1289/EHP4713
- Pierre, T. J., Pierre, N. J., Achile, B. M., Djakba, B. S., & Lucien, B. D. (2015). *Morphological , physico chemical , mineralogical and geochemical properties of vertisols used in bricks production in the Logone Valley (Cameroon , Central Africa*). 5(2), 20–30.
- Polong, F., Chen, H., Sun, S., & Ongoma, V. (2019). Temporal and spatial evolution of the standard precipitation evapotranspiration index (SPEI) in the Tana River Basin, Kenya. *Theoretical and Applied Climatology*, 138(1–2), 777–792. https://doi.org/10.1007/s00704-019-02858-0
- Prosser, M. V., Wood, R. B., & Baxter, R. M. (1968). Bishoftu Crater Lakes-a Bathymetric and Chemical Study Title. *Archiv Fur Hydrobiologie*, 65(3), 309.
- Pytkowicx, R. M. (1975). Activity coefficients of bicarbonates and carbonates in seawater. *Limnology and Oceanography*, 20(6), 971–975. https://doi.org/https://doi.org/10.4319/lo.1975.20.6.0971
- Renaut, R. W., & Jones, B. (2011). Hydrothermal environments, terrestrial. In T. V Reitner J (Ed.), *In Encyclopedia of geobiology*. Springer, Berlin.
- Renaut, Robin W., Owen, R. B., Jones, B., Tiercelin, J. J., Tarits, C., Ego, J. K., & Konhauser, K. O. (2013). Impact of lake-level changes on the formation of thermogene travertine in continental rifts: Evidence from Lake Bogoria, Kenya Rift Valley. *Sedimentology*, 60(2), 428–468. https://doi.org/10.1111/j.1365-3091.2012.01347.x
- Renaut, Robin W., Owen, R. B., Lowenstein, T. K., De Cort, G., Mcnulty, E., Scott, J. J., & Mbuthia, A. (2021a). The role of hydrothermal fluids in sedimentation in saline alkaline lakes: Evidence from Nasikie Engida, Kenya Rift Valley. *Sedimentology*, 68(1), 108–134. https://doi.org/10.1111/sed.12778
- Renaut, Robin W., Owen, R. B., Lowenstein, T. K., De Cort, G., Mcnulty, E., Scott, J. J., & Mbuthia, A. (2021b).

 The role of hydrothermal fluids in sedimentation in saline alkaline lakes: Evidence from Nasikie Engida,

 Kenya Rift Valley. In *Sedimentology* (Vol. 68, Issue 1). https://doi.org/10.1111/sed.12778
- Ring, U., Livingstone, D., Stanley, H. M., & Fischer, G. (2014). The East African Rift System. *Austrian Journal Of Earth Sciences*, 107/1, 132–146.

- Ringwood, A. E., Kesson, S. E., Hibberson, W., & Ware, N. (1992). Origin of kimberlites and related magmas. *Earth and Planetary Science Letters*, 113(4), 521–538. https://doi.org/10.1016/0012-821X(92)90129-J
- Robinson, J. V. (2015). The Ecology of East African Soda Lakes: Implications for lesser flamingo (Phoeniconaias minor) feeding behaviour Thesis submitted for the degree of Doctor of Philosophy at the University of Leicester By. June.
- Rodriguez-Galiano, V. F., Ghimire, B., Rogan, J., Chica-Olmo, M., & Rigol-Sanchez, J. P. (2012). An assessment of the effectiveness of a random forest classifier for land-cover classification. *ISPRS Journal of Photogrammetry and Remote Sensing*, 67(1), 93–104. https://doi.org/10.1016/j.isprsjprs.2011.11.002
- Roozitalab, M. H., Toomanian, N., Ghasemi Dehkordi, V. R., & Khormali, F. (2018). Major soils, properties, and classification. In *The soils of Iran* (pp. 93–147).
- Rosen, M. R. (1994). The importance of groundwater in playas: A review of playa classifications and the sedimentology and hydrology of playas. *Special Paper of the Geological Society of America*, 289(January 1994), 1–18. https://doi.org/10.1130/SPE289-p1
- Rounds, R. S. A. (2012). 6 . 6 Alkalinity and Acid Neutralizing Capacity. In *U.S. Geological Survey* (Vol. 4, Issue 9, pp. 1–45). https://doi.org/https://doi.org/10.3133/twri09A6.6
- Saber, E. S. A. (2020). Gold resources from clastic Cambrian rocks and their link with underlying Precambrian rocks, southern Sinai, Egypt. *Arabian Journal of Geosciences*, *13*(13). https://doi.org/10.1007/s12517-020-05526-0
- Saccò, M., White, N. E., Harrod, C., Salazar, G., Aguilar, P., Cubillos, C. F., Meredith, K., Baxter, B. K., Oren, A., Anufriieva, E., Shadrin, N., Marambio-alfaro, Y., Bravo-naranjo, V., & Allentoft, M. E. (2021). Salt to conserve: a review on the ecology and preservation of hypersaline ecosystems. 61, 2828–2850. https://doi.org/10.1111/brv.12780
- Sahajpal, R., Zimmerman, S. R. H., Datta, S., Hemming, N. G., & Hemming, S. R. (2011). Assessing Li and other leachable geochemical proxies for paleo-salinity in lake sediments from the Mono Basin, CA (USA). *Geochimica et Cosmochimica Acta*, 75(24), 7855–7863. https://doi.org/10.1016/j.gca.2011.10.001
- Schad, P. (2016). The International Soil Classification System WRB, Third Edition, 2014. In *Novel methods for monitoring and managing land and water resources in Siberia*. https://doi.org/10.1007/978-3-319-24409-9_25
- Schad, P. (2023). World Reference Base for Soil Resources—Its fourth edition and its history. *Journal of Plant Nutrition and Soil Science*, 186(2), 151–163. https://doi.org/10.1002/jpln.202200417
- Schagerl, Michael., & Robin, W. R. (2016). Dipping into the Soda Lakes of East Africa. *Soda Lakes of East Africa*, 1–408. https://doi.org/10.1007/978-3-319-28622-8
- Schagerl, Michael, & Renaut, R. W. (2016). Dipping into the Soda Lakes of East Africa. *Soda Lakes of East Africa*, 12, 1–408. https://doi.org/10.1007/978-3-319-28622-8
- Scoon, R. N. (2018). Geology of national parks of central/Southern Kenya and Northern Tanzania: Geotourism of the Gregory Rift Valley, active Volcanism and regional plateaus. In *Geology of National Parks of Central/Southern Kenya and Northern Tanzania: Geotourism of the Gregory Rift Valley, Active Volcanism and Regional Plateaus*. https://doi.org/10.1007/9783319737850

- Scoon, R. N. (2020). Geotourism, Iconic Landforms and Island-Style Speciation Patterns in National Parks of East Africa. *Geoheritage*, 12(3). https://doi.org/10.1007/s12371-020-00486-z
- Sherrod, B. D. R., Magigita, M. M., & Kwelwa, S. (2013). Geologic Map of Oldonyo Lengai Volcano and Surroundings, Arusha Region, United Republic of Tanzania. *USGS Report*, 1–61.
- Šimanský, V. (2018). Can soil properties of Fluvisols be influenced by river flow gradient? *Acta Fytotechn Zootechn*, 2018(2), 63–76.
- Singh, S. K., & P.Chandran. (2017). Soil Genesis and Classification. In soil science: an Introduction (Issue March).
- Singhal, B. B. S., & Gupta, R. P. (1999). Applied Hydrogeology of Fractured Rocks. *Kluwer Academic Publishers, Dordrecht*.
- Sisay, M. G., Tsegaye, E. A., Tolossa, A. R., Nyssen, J., Frankl, A., Van Ranst, E., & Dondeyne, S. (2024). Soil-Forming Factors of High-Elevation Mountains along the East African Rift Valley: The Case of the Mount Guna Volcano, Ethiopia. *Soil Systems*, 8(2), 38. https://doi.org/10.3390/soilsystems8020038
- Slegers, M. F. W. (2008). "If only it would rain": Farmers' perceptions of rainfall and drought in semi-arid central Tanzania. *Journal of Arid Environments*, 72(11), 2106–2123. https://doi.org/10.1016/j.jaridenv.2008.06.011
- Sorokin, D. Y., Detkova, E. N., & Muyzer, G. (2010). Propionate and butyrate dependent bacterial sulfate reduction at extremely haloalkaline conditions and description of Desulfobotulus alkaliphilus sp. nov. *Extremophiles*, 14(1), 71–77. https://doi.org/10.1007/s00792-009-0288-5
- Sorokin, Dimitry Y., Banciu, H. L., & Muyzer, G. (2015). Functional microbiology of soda lakes. *Current Opinion in Microbiology*, 25, 88–96. https://doi.org/10.1016/j.mib.2015.05.004
- Sorokin, Dimitry Y., Berben, T., Melton, E. D., Overmars, L., Vavourakis, C. D., & Muyzer, G. (2014). Microbial diversity and biogeochemical cycling in soda lakes. *Extremophiles*, *18*(5), 791–809. https://doi.org/10.1007/s00792-014-0670-9
- Sorokin, Dimitry Yu, Tourova, T. P., Henstra, A. M., Stams, A. J. M., Galinski, E. A., & Muyzer, G. (2008). Sulfidogenesis under extremely haloalkaline conditions by Desulfonatronospira thiodismutans gen. nov., sp. nov., and Desulfonatronospira delicat sp. nov. A novel lineage of Deltaproteobacteria from hypersaline soda lakes. *Microbiology*, 154(5), 1444–1453. https://doi.org/10.1099/mic.0.2007/015628-0
- Sparks, R. S. J., Brooker, R. A., Field, M., Kavanagh, J., Schumacher, J. C., Walter, M. J., & White, J. (2009). The nature of erupting kimberlite melts. *Lithos*, 112, 429–438. https://doi.org/10.1016/j.lithos.2009.05.032
- Stenger-Kovács, C., Lengyel, E., Buczkó, K., Tóth, F. M., Crossetti, L. O., Pellinger, A., Doma, Z. Z., & Padisák, J. (2014). Vanishing world: Alkaline, saline lakes in Central Europe and their diatom assemblages. *Inland Waters*, 4(4), 383–396. https://doi.org/10.5268/IW-4.4.722
- Symonds, R. B., Gerlach, T. M., & Reed, M. H. (2001). Magmatic gas scrubbing: Implications for volcano monitoring. *Journal of Volcanology and Geothermal Research*, 108(1–4), 303–341. https://doi.org/10.1016/S0377-0273(00)00292-4
- Tebbs, E. J., Remedios, J. J., Avery, S. T., & Harper, D. M. (2013). Remote sensing the hydrological variability of Tanzania 's Lake Natron, a vital Lesser Flamingo breeding site under threat. *Ecohydrology & Hydrobiology*, 13(2), 148–158. https://doi.org/10.1016/j.ecohyd.2013.02.002

- Tetiker, S., Yalçın, H., & Bozkaya, Ö. (2015). Evidence of the diagenetic history of sediment composition in Precambrian-early Paleozoic rocks: A systematic study from the Southeast Anatolian Autochthon, Mardin (Derik-Kızıltepe), Turkey. *Arabian Journal of Geosciences*, 8(12), 11261–11278. https://doi.org/10.1007/s12517-015-2006-1
- Thonfeld, F., Steinbach, S., Muro, J., & Kirimi, F. (2020). Long-term land use/land cover change assessment of the Kilombero catchment in Tanzania using random forest classification and robust change vector analysis.

 Remote Sensing, 12(7). https://doi.org/10.3390/rs12071057
- Tilahun, Z. A., Bizuneh, Y. K., & Mekonnen, A. G. (2024). A spatio-temporal analysis of the magnitude and trend of land use/land cover changes in Gilgel Gibe Catchment, Southwest Ethiopia. *Heliyon*, 10(2), e24416. https://doi.org/10.1016/j.heliyon.2024.e24416
- Timms, V. ., Hammer, U. ., & John, W. . (1986). A Study of Benthic Communities in Some Saline Lakes in Saskatchewan and Alberta, Canada. *Internationale Revue Der Gesamten Hydrobiologie Und Hydrographie*, 71(6), 759–777. https://doi.org/https://doi.org/10.1002/iroh.19860710603
- Tosca, N. J., & Tutolo, B. M. (2023). How to Make an Alkaline Lake: Fifty Years of Chemical Divides. *Elements*, 19(1), 15–21. https://doi.org/10.2138/GSELEMENTS.19.1.15
- Tóth, J. (1980). Cross-Formational Gravity-Flow of Groundwater: A Mechanism of the Transport and Accumulation of Petroleum (The Generalized Hydraulic Theory of Petroleum Migration). In I. R. J. C. W. H. Roberts (Ed.), *Problems of Petroleum Migration* (pp. 121–167). AAPG Studies in Geology. https://doi.org/10.1306/St10411C8
- Verhoeve, S. L., Keijzer, T., Kaitila, R., Wickama, J., & Sterk, G. (2021). Northern Tanzania. *Remote Sensing*, 13(22), 4592. https://doi.org/10.1007/978-94-011-7129-8_15
- Vicente-Serrano, S. M., Beguería, S., & López-Moreno, J. I. (2010). A multiscalar drought index sensitive to global warming: The standardized precipitation evapotranspiration index. *Journal of Climate*, 23(7), 1696–1718. https://doi.org/10.1175/2009JCLI2909.1
- Vye-Brown, C., Crummy, J., Smith, K., Mruma, A., & Kabelwa, H. (2014). Volcanic hazards in Tanzania. *British Geological Survey*.
- Warren, J. K. (2006). Depositional chemistry and hydrology. In *Evaporites: sediments, resources and hydrocarbons*, (pp. 59–138).
- Westberg, D. J., Stackhouse, P. W., Crawley, D. B., Hoell, J. M., Chandler, W. S., & Zhang, T. (2013). An analysis of NASA's merra meteorological data to supplement observational data for calculation of climatic design conditions. *ASHRAE Transactions*, *119*(PART 2), 210–221.
- Wood, R. B., & Talling, J. F. (1988). Chemical and algal relationships in a salinity series of Ethiopian inland waters. *Hydrobiologia*, 158(1), 29–67. https://doi.org/10.1007/BF00026266
- Wurtsbaugh, W. A., Miller, C., Null, S. E., Justin De Rose, R., Wilcock, P., Hahnenberger, M., Howe, F., & Moore, J. (2017). Decline of the world's saline lakes. *Nature Geoscience*, 10(11), 816–821. https://doi.org/10.1038/NGEO3052
- Yaiche Achour, H., & Saadi, S. A. (2023). African salt lakes: distribution, microbial biodiversity, and

- biotechnological potential. In *Lakes of Africa: Microbial Diversity and Sustainability*. INC. https://doi.org/10.1016/B978-0-323-95527-0.00009-9
- Yanda, P. Z., & Madulu, N. F. (2005). Water resource management and biodiversity conservation in the Eastern Rift Valley Lakes, Northern Tanzania. *Physics and Chemistry of the Earth*, 30(11-16 SPEC. ISS.), 717–725. https://doi.org/10.1016/j.pce.2005.08.013
- Yao, F., Livneh, B., Rajagopalan, B., Wang, J., Crétaux, J. F., Wada, Y., & Berge-Nguyen, M. (2023). Satellites reveal widespread decline in global lake water storage. *Science*, *380*(6646), 743–749. https://doi.org/10.1126/SCIENCE.ABO2812
- Yechieli, Y., & Wood, W. W. (2002). Hydrogeologic processes in saline systems: Playas, sabkhas, and saline lakes. *Earth-Science Reviews*, 58(3–4), 343–365. https://doi.org/10.1016/S0012-8252(02)00067-3
- Yona, C., Makange, M., Moshiro, E., Chengula, A., & Misinzo, G. (2022). Water pollution at Lake Natron Ramsar site in Tanzania: A threat to aquatic life. *Ecohydrology & Hydrobiology*, *xxxx*, 1–11. https://doi.org/10.1016/j.ecohyd.2022.11.001
- Yuretich, R. F., & Cerling, T. E. (1983). Hydrogeochemistry of Lake Turkana, Kenya: Mass balance and mineral reactions in an alkaline lake. *Geochimica et Cosmochimica Acta*, 47(6), 1099–1109. https://doi.org/10.1016/0016-7037(83)90240-5
- Zahoor, I., & Mushtaq, A. (2023). Water Pollution from Agricultural Activities: A Critical Global Review. International Journal of Chemical and Biochemical Sciences, 23(1), 164–176.
- Zaitsev, A. N., & Keller, J. (2006). Mineralogical and chemical transformation of Oldoinyo Lengai natrocarbonatites, Tanzania. *Lithos*, *91*(1–4), 191–207. https://doi.org/10.1016/j.lithos.2006.03.018
- Zango, Sm. S., Sunkari, E. D., Abu, M., & Lermi, A. (2019). Hydrogeochemical controls and human health risk assessment of groundwater fl uoride and boron in the semi-arid North East region of Ghana. *Journal of Geochemical Exploration*, 207(August), 106363. https://doi.org/10.1016/j.gexplo.2019.106363
- Zebire, D. A., Ayele, T., & Ayana, M. (2019). Characterizing soils and the enduring nature of land uses around the Lake Chamo Basin in South-West Ethiopia. *Journal of Ecology and Environment*, 43(1), 1–32. https://doi.org/10.1186/s41610-019-0104-9
- Zhao, Z., Yao, X., Ding, Q., Gong, X., Wang, J., Tahir, S., Aaron, I., & Zhang, L. (2022). A comprehensive evaluation of organic micropollutants (OMPs) pollution and prioritization in equatorial lakes from mainland Tanzania, East Africa. *Water Research*, 217(March), 118400. https://doi.org/10.1016/j.watres.2022.118400
- Zheng, M., & Liu, X. (2009). Hydrochemistry of Salt Lakes of the Qinghai-Tibet Plateau, China. *Aquatic Geochemistry*, 15(1–2), 293–320. https://doi.org/10.1007/s10498-008-9055-y